

**Proceedings of
The 7th Asian Symposium on Advanced Materials:
Chemistry, Physics & Biomedicine of Functional and
Novel Materials
(ASAM-7)**



September 4-7, 2019

Beijing Institute of Petrochemical Technology,
Beijing, China

Welcome Message

The first Asian Symposium on Advanced Materials: Chemistry, Physics & Biomedicine of Functional and Novel Materials (ASAM-1), which was held at Far Eastern National University, Vladivostok, Russia on Oct.1-4, 2007, was very successful, with active participation of scientists from several Asian countries as well as Russia and Korea. The symposium showcased a number of research topics such as fundamental science of materials, materials on energy science, materials on environmental science, materials on biomedical science and multidisciplinary materials, and also offered a forum for interdisciplinary discussion between scientists and engineers from Asian universities, academic institutes and industry. From the success of the event, the participants expressed great desire to organize this symposium on a regular basis.

In keeping with the spirit of the first symposium in 2007, the second symposium was held on October 11-14, 2009 at Fudan University, China. The third symposium was held on September 19-22, 2011 at Kyushu University, Japan. The fourth symposium was held on October 22-25, 2013 at National Taiwan University of Science and Technology, Chinese Taiwan. The fifth symposium was held on November 1-4, 2015 at the Sangnam International House, Busan, Korea. The Sixth symposium was held on September 27-30, 2017 at HoaBinh Hotel, Hanoi, Vietnam. Now, we are happy to have the seventh symposium (ASAM-7) at the Beijing Institute of Petrochemical Technology, Beijing, China in 2019.

It is our sincere hope that we will be able to welcome your active participation in this symposium. We are looking forward to the meeting with you at Beijing, China.

September1, 2019

DongyuanZhao

Chairperson of the ASAM-7
Fudan University, China

Yijian Jiang

Co-chairperson of the ASAM-7
Beijing Institute of Petrochemical Technology, China

Xiuguo Cui

Co-chairperson of the ASAM-7
Beijing Institute of Petrochemical Technology, China

交通指南/Transport Guide

本次会议场地为北京石油化工学院。地址：北京市大兴区清源北路 19 号。

This conference will be held at **Beijing Institute of Petrochemical Technology (BIPT)**.

Address: No. 19, Qingyuan North Road, Daxing District, Beijing

1. 首都机场出发/Beijing Capital International Airport Depart

由 T3 航站楼站乘机场线至东直门下车，由东直门站换乘地铁 2 号线(内环)至宣武门站，由宣武门站换乘地铁 4 号线大兴线(天宫院方向)至清源路站(A 出口)下车，向北步行 330 米后左转进入清源北路，沿路向西直行 550 米至北京石油化工学院。

出租车出行：车费约 200 元。

By Metro: Take Metro Airport Line at Terminal T3 to Dongzhimen Station, and change for Line 2 (inner ring) to Xuanwumen Station, then change for Line 4 (Tiangongyuan direction) to Qingyuan Road Station. Get off from Exit A, and walk 330 m to the north, and turn left on Qingyuan North Road for 550 m. BIPT is on right.

By Taxi: The fare is about CNY 200.

2. 北京南苑机场出发/Beijing Nanyuan Airport

由南苑机场站乘南苑机场大巴北京西站专线(或南苑机场大巴公主坟专线)至新宫站下车，由新宫站乘地铁 4 号线大兴线(天宫院方向)至清源路站(A 出口)下车，向北步行 330 米后左转进入清源北路，沿路向西直行 550 米至北京石油化工学院。

出租车出行：车费约 60 元。

By Metro: Take Airport Shuttle Bus (Beijing West Railway Station, or Gongzhufen direction), get off at Xingong Stop. Take Metro Line 4 (Tiangongyuan direction) to Qingyuan Road Station. Get off from Exit A and walk 330 m to the north, and turn left on Qingyuan North Road for 550 m. BIPT is on right.

By Taxi: The fare is about CNY 60.

3. 北京火车站出发/Beijing Railway Station

地铁出行：乘坐地铁 2 号线(内环)由北京站至宣武门站；由宣武门站换乘地铁 4 号线大兴线(天宫院方向)至清源路站(A 出口)下车，向西步行 330 米后左转进入清源北路，沿路向西直行 550 米至北京石油化工学院。

出租车出行：车费约 100 元。

By Metro: Take Metro Line 2 (inner ring) to Xuanwumen, and change for Line 4 (Tiangongyuan direction) to Qingyuan Road Station. Get off from Exit A and walk 330 m to the north, and turn left on Qingyuan North Road for 550 m. BIPT is on right.

By Taxi: The fare is about CNY 100.

4. 北京南站出发/Beijing South Railway Station

地铁出行：由北京南站乘坐地铁 4 号线大兴线（天宫院方向）至清源路站（A 出口）下车，向西步行 330 米后左转进入清源北路，沿路向西直行 550 米至北京石油化工学院。

出租车出行：出租车约 60 元。

By Metro: Take Metro Line 4 (Tiangongyuan direction) to Qingyuan Road Station. Get off from Exit A and walk walk 330 m to the north, and turn left on Qingyuan North Road for 550 m. BIPT is on right.

By Taxi: The fare is about CNY 60.

5. 北京西站出发/Beijing West Railway Station

地铁出行：由北京西站乘坐地铁 7 号线（焦化厂方向）至菜市口站下车，由菜市口站换乘地铁 4 号线大兴线（天宫院方向）至清源路站（A 出口）下车，向西步行 330 米后左转进入清源北路，沿路向西直行 550 米至北京石油化工学院。

出租车出行：出租车约 80 元。

By Metro: Take Metro Line 7 (Jiaohuachang direction) to Caishikou, and change for Line 4 (Tiangongyuan direction) to Qingyuan Road Station. Get off from Exit A and walk walk 330 m to the north, and turn left on Qingyuan North Road for 550 m. BIPT is on right.

By Taxi: The fare is about CNY 80.



The 7th Asian Symposium on Advanced Materials (ASAM-7)

Date September 4-7, 2019

VENUE Beijing Institute of Petrochemical Technology, Beijing, China

LOCAL ORGANIZING COMMITTEE

Chairman

Prof. Dongyuan Zhao (Fudan University, CHINA)

Co-Chairman

Prof. Yijian Jiang (Beijing Institute of Petrochemical Technology, CHINA)

Prof. Xiuguo Cui (Beijing Institute of Petrochemical Technology, CHINA)

Members

Huiqinlian (Beijing Institute of Petrochemical Technology, CHINA)

YangLiu (Beijing Institute of Petrochemical Technology, CHINA)

YushunJin (Beijing Institute of Petrochemical Technology, CHINA)

YanyanWang (Beijing Institute of Petrochemical Technology, CHINA)

YanLi (Beijing Institute of Petrochemical Technology, CHINA)

LeiZu (Beijing Institute of Petrochemical Technology, CHINA)

INTERNATIONAL ADVISORY COMMITTEE

Li-Jen Chen (National Taiwan Univ., CHINESE TAIWAN)

Jianping Gong (Hokkaido University, JAPAN)

Chang-Sik Ha (Pusan National University, KOREA)

Toyoko Imae (National Taiwan University of Science & Technology, CHINESE TAIWAN)

Jung-II Jin (Korea Univ. and Korean Academy of Science and Technology, KOREA)

Alexei Khokhlov (Lomonosov Moscow State Univ., RUSSIA)

Junghyun Kim (Yonsei Univ., KOREA)

YuryKulchin (Russian Academy of Sciences, RUSSIA)

Nguyen Quang Liem (Vietnam Academy of Science and Technology, VIETNAM)

Valentin Parmon (Russian Academy of Sciences, RUSSIA)

YuryShchipunov (Russian Academy of Science, RUSSIA)

Atsushi Takahara (Kyushu Univ., JAPAN)

Supason Wanichwecharungruang (Chulalongkorn Univ., THAILAND)

Limin Wu (Fudan Univ., CHINA)

Dongyuan Zhao (Fudan Univ., CHINA)

Organized by

- College of Materials Science and Technology Beijing Institute of Petrochemical Technology, China
- Beijing Key Lab of Special Elastomeric Composite Materials, China

Language

The working language of the conference is English for all activities, papers and presentations.

Oral Presentation

Plenary Lectures; 40 minutes including discussion
Keynote Lectures; 30 minutes including discussion
Invited talks; 25 minutes including discussion

The plenary lectures will be held at Zhiyuan Lecture Hall, while keynote lecture, invited lecture and oral session will be held at Library 401 and Library 602. The session room is equipped with an LCD projector and personal computer as well as microphone and laser pointer. Please up-load your presentation file at least 30 minutes before your presentation. Also, please contact the chairperson you present for detail information.

Poster Presentation

Poster presentation will be at Library 7th floor on September 5 (16:30 – 18:00 p.m.) Posters should be in place before the exposure time indicated in the program, and be removed immediately after the presentation. The space available for each poster is 80 cm width and 120 cm height.

Registration

The registration fee includes conference bag with an abstract book, tea/coffee at the venue, lunch, welcome reception, dinner, and short excursion.

	Before July 1, 2019	After July 1, 2019
Active Participant	300\$(2100 CNY)	350\$(2500 CNY)
Student	100\$(700 CNY)	150\$(1000 CNY)
Accompanying Person	150\$(1000 CNY)	200\$(1400 CNY)

Registration Desk

Registration Desk is available in the Library Lobby.

Social Events and Others

Dinner: September 6, 18:30 at Xiaozhang Hotel

Post Symposium Tour

Payment (cash-only) at the registration desk

Route 1: Half-day Tour: The Imperial Palace (¥120/ person)

Departure from Beijing Institute of Petrochemical Technology BIPT (September 7 at 7:00)
→ Beijing XingguangMeidiya Hotel (7:15) → The Imperial Palace (8:30 - 10:30) →
Restaurant → Back to BIPT

Route 2:

One-day Tour: The Great Wall (¥100/ person) (cable car at one's own expense)

Departure from Beijing Institute of Petrochemical Technology BIPT (September 7 at 6:00)
→ Beijing XingguangMeidiya Hotel (6:15) → The Great Wall (9:30 - 13:30) →
Restaurant → Beijing International Airport → Back to BIPT

*The tour course may be changed without pre-announcement depending on the circumstances of that day.

Restaurants and International House

Participants can have their lunchmeals at Tong Le Yuan of Beijing Institute of Petrochemical Technology (The fee was included in registration fee) However, you can also enjoy Chinese food at many restaurants near Beijing XingguangMeidiya Hotel and Beijing Institute of Petrochemical Technology campus. (The fee has to be paid by yourself.)

Accommodation

Rooms at Beijing XingguangMeidiya Hotel are reserved for on request only.

Internet Service

We provide work computers at the venue with internet service. Internet can be accessed in each guest room of the Beijing XingguangMeidiya Hotel.

Introduction for Conference Hall

-Conference Office and Preview Room:

September 5

- Plenary Lecture: Zhiyuan Lecture Hall
- Keynote Lecture: Library 401 and Library 602
- Invited Lecture: Library 401 and Library 602
- Oral Presentation: Library 401 and Library 602

September 6

- Plenary Lecture: Zhiyuan Lecture Hall
- Keynote Lecture: Library 401 and Library 602
- Invited Lecture: Library 401 and Library 602
- Oral Presentation: Library 401 and Library 602
- Poster Session: Library 7th Floor
- Dinner: Xiaozhang Hotel

- Closing ceremony: Library 602

November 7

- Plenary Lecture: Zhiyuan Lecture Hall
- Keynote Lecture: Zhiyuan Lecture Hall

Sept. 4 (Wednesday)		
07:30-18:30	Registration (Library Lobby)	
Sept. 5 (Thursday)		
	Zhiyuan Lecture Hall	
07:30-08:50	Registration	
	(Opening Session)	(Chair: Huiqin Lian)
09:00-09:10	Opening Remark	Yijian Jiang (President of the BIPT)
09:10-09:20	Welcome Address	Chang-Sik Ha (Pusan National University, Korea)
09:20-10:00	PL1-Ulich Wiesner (Cornell Univ., USA) (Chair: Dongyuan Zhao)	
10:00-10:50	GROUP PHOTO COFFEE BREAK (Library 401 and 602)	
	Library 602	Library 401
	(Porous Nanomaterials) (Chair: Hyuk-Sang Yoo)	(Functional Nanomaterials) (Chair: Xiaodong Wang)
10:50- 11:20	KL1- Dongyuan Zhao (Fudan University, China)	KL3 Hatsuo Ishida (Case Western Reserve University, USA)
11:20-11:45	IL1- Chongchen Wang (Beijing University of Civil Engineering and Architecture, China)	IL5- Weizhong Qian (Tsinghua University, China)
11:45-12:00	OL1- Sung-Soo Park (Pusan National University, Korea)	OL-3 Chen Wang (Boreskov Institute of Catalysis, Russia)
12:00-13:30	Buffet Lunch	
	Zhiyuan Lecture Hall	
13:30-14:10	PL2- Jian Ping Gong (Hokkaido Univ., Japan) (Chair: Chang-Sik Ha)	
14:10-14:30	COFFEE BREAK (Library 401 and 602)	
	Library 602	Library 401
	(Biomedical Materials) (Chair: Hyuk Sang Yoo and Ildoo Chung)	(Functional Nanomaterials) (Chair : Dong Gi Seong and Kiyoshi Kanie)
14:30-15: 00	KL2-Thai Hoang (VAST, Vietnam)	KL4-Xiaodong Wang(Beijing University of Chemical Technology, China)
15:00-15:25	IL2 –Ildoo Chung (Pusan National University, Korea)	IL4 – Kiyoshi Kanie (Tohoku University, Japan)
15:25-15:50	IL3- Hyuk Sang Yoo (Kangwon National University, Korea)	IL6- Dong Gi Seong (Pusan National University, Korea)
15:50-16:05	OL2-Riyasudheen Nechikkattu (Pusan National University, Korea)	OL4- Xin Jia (Shihezi University, China)
16:05-16:25	COFFEE BREAK (Library 401 and 602)	

16:30-18:00	POSTER SESSION (Room: Library 7 th Floor)	
Sept. 6 (Friday)		
08:00-09:00	Registration (Library Lobby)	
	Zhiyuan Lecture Hall	
09:00-09:40	PL3- Sang-Young Lee (Ulsan National Institute of Science and Technology, Korea) (Chair: Xiuguo Cui)	
09:40-10:00	COFFEE BREAK	
	Library 602	Library 401
	(Materials for Energy) (Chair: Hideyuki Otsuka)	(Materials for Optoelectronics) (Chair: Dongpeng Yan)
10:20-10:50	KL5- Toyoko Imae (National Taiwan University of Science and Technology, Chinese Taiwan)	KL8-Yury Shchipunov (Russian Academy of Science, Russia)
10:50-11:20	KL6-Xuefeng Yu (Shenzhen Institute of Advanced Technology CAS, China)	KL9-Li-Jen Chen (National Taiwan University, Chinese Taiwan)
11:20-11:35	OL5- Xiaohua Zhang (Soochow University, China)	IL-12 Yuxi Liu ((Beijing University of Technology, China)
11:35-11:50	OL-6 Xusheng Wang (Technical Institute of Physics and Chemistry, CAS, China)	OL-9 Hao Wang, ((BIPT, China)
11:50- 13:30	Buffet Lunch	
	Library 602	Library 401
	(Functional Nanomaterials) (Chair: Yinzhou Yan)	(Materials with Specific Functions) (Chair: Yury Shchipunov)
13:30-14:00	KL7-Hideyuki Otsuka (Tokyo Institute of Technology, Japan)	KL-10 Xiuguo Cui (BIPT, China)
14:00-14:25	IL7- Dongpeng Yan (Beijing Normal University, China)	IL13 Aleksey Vedyagin (Russian Academy of Science, Russia)
14:25-14:50	IL8 Huiqin Lian (BIPT, China)	OL10-Lanchao Ma (BIPT,China)
14:50-15:05	OL-7 Yan Li (BIPT, China)	OL11- Dahai Gao (BIPT, China)
15:05-15:30	COFFEE BREAK	
	Functional Nanomaterials (Chair: Toyoko Imae)	Functional Nanomaterials (Chair: Li-Jen Chen)
15:30-16:00	KL11-Chang-Sik Ha (Pusan National University, Korea)	KL12 -Yin Zhou Yan (Beijing University of Technology, China)

16:00-16:25	IL9 Yongri Liang (BIPT, China)	IL14 Zhanpeng Wu, (Beijing University of Chemical Technology, China)
16:25-16:50	IL10-Vladimir Egorkin (Russian Academy of Sciences, Russia)	IL15- Xu Xiang (Beijing University of Chemical Technology, China)
16:50-17:15	IL11 Yang Liu (BIPT, China)	IL16 Yibo Wu (BIPT, China)
17:15-17:30	OL8 Shengfu Ji, (Beijing University of Chemical Technology, China)	OL12- Fuping Dong (Guizhou University, China)
Library 602 (Chair: Xiuguo Cui)		
17:50-18:00	CLOSING REMARK / Introduction of the ASAM-8	
18:30-20:30	Buffet (Xiaozhang Hotel)	
Sept. 7 (Saturday)		
Zhiyuan Lecture Hall		
Special Symposium on Black Phosphorus Materials (in Chinese, Chair; Xuefeng Yu)*		
09:00-09:40	PL-a, Han Zhang , Shenzhen University	
09:40-10:20	PL-b, Xuefeng Yu, Shenzhen Institute of Advanced Technology, CAS	
10:20-10:40	COFFEE BREAK	
10:40-11:20	PL-c, Xiuguo Cui, Beijing Institute of Petrochemical Technology	
11:20-11:40	KL-a, Xu Jiang, Nanjing Xianfeng Nano Tech. Co. Ltd	
Post Symposium Tour *		
07:30-12:00	Half-day Tour : The Imperial Palace (¥120/ person) Charge Items: Entrance ticket + Transportation +Lunch Payment (cash-only) at the registration desk	
05:30-17:00	One-day Tour : The Great Wall (¥100/ person) Charge Items: Entrance ticket + Transportation +Lunch (cable car at one's own expense) Payment (cash-only) at the registration desk	

* Though the official language of the ASAM-7 is English, the special symposium on phosphorous materials are provided in Chinese only. Who do not attend the special symposium on phosphorous materials are invited to join half-day or one-day tour with personal payment.

Note: It is better to get tickets in advance in case of the total number limitation for the tourist spot.

Please send the form to asam7th@163.com before August 30, 2019.

Type of Tour	passport number	Choice
1 The Imperial Palace (Bipt-spot-Bipt)		
2 The Great Wall (Bipt-spot-airport-Bipt)		

Program

Wednesday, Sept. 4

07:30-18:30 Registration (Library Lobby)

Thursday, Sept. 5

Zhiyuan Lecture Hall

07:30-08:50 Registration
(Chair: Huiqin Lian)

09:00-09:10 Opening Remark Yijian Jiang (President of the BIPT)

09:10-09:20 Welcome Address Chang-Sik Ha (Pusan National University, Korea)

(Chair: Dongyuan Zhao)

09:20-10:00 (PL-1) **Ulich Wiesner** (Cornell Univ., USA)
Advanced Functional Nanomaterials for Applications in Oncology

(Chair: Chang-Sik Ha)

13:30-14:10 (PL-2) **Jian Ping Gong** (Hokkaido Univ., Japan)
Self-Growing Hydrogels by Mechanical Training

Library 602

Porous Nanomaterials (Chair: Hyuk-Sang Yoo)

10:50- 11:20 (KL-1) **Dongyuan Zhao** (Fudan University, China)

11:20-11:45 (IL-1) **Chongchen Wang** (Beijing University of Civil Engineering and Architecture, China)
Metal-Organic Frameworks and Their Composites: Potential Applications in Wastewater Treatment

11:45-12:00 (OL-1) **Sung-Soo Park** (Pusan National University, Korea)
Functionalized Mesoporous Silica Nanoparticles for Anticancer Chemotherapy

12:00-13:30 **LUNCH**

Biomedical Materials (Chair: Hyuk Sang Yoo and Ildoo Chung)

14:30-15: 00 (KL-2) **Thai Hoang**(VAST, Vietnam)
Chitosan/Alginate Bionanoparticles Loading Lovastatin and Ginsenoside Rb1 (Extracted from Panax Ginseng): Preparation, Characterization and in Vitro Drug Release Control

15:00-15:25 (IL-2) **Ildoo Chung** (Pusan National University, Korea)
Biodegradable Polyester Based Porous Microspheres by RAFT Polymerization and UV Irradiation

15:25-15:50 (IL-3) **Hyuk Sang Yoo** (Kangwon National University, Korea)
Biomimetic Nanofibrils for Controlling and Stimulating Cellular Functions

15:50-16:05 (OL-2) **Riyasudheen Nechikkattu** (Pusan National University) Korea)
Phosphorylcholine Functionalised MCM-41 Nanoparticles for

16:05-16:25 Controlled Drug Release
COFFEE BREAK

Library 401

Functional Nanomaterials (Chair: Xiaodong Wang)

10:50- 11:20 (KL-3) **Hatsuo Ishida** (Case Western Reserve University, USA)

11:20-11:45 (IL-5) **Weizhong Qian** (Tsinghua University, China)
3D Porous Al Current Collector-Enhanced Graphene Supercapacitor
11:45-12:00 (OL-3) **Chen Wang** (Boreskov Institute of Catalysis, Russia)
New Approaches to the Functionalization of CNF
12:00-13:30 **LUNCH**

Functional Nanomaterials(Chair: Kiyoshi Kanie)

14:30-15:00 (KL-4) **Xiaodong Wang** (Beijing University of Chemical Technology, China)
A High Reliable Reversible Thermochromic Phase Change Microcapsule System for Durable Indication of Thermal Energy Storage and Management
15:00-15:25 (IL-4) **Kiyoshi Kanie (Tohoku University, Japan)**
Self-organizing Liquid-Crystalline Hybrid Nanoparticles
15:25-15:50 (IL-6) **Dong Gi Seong** (Pusan National University, Korea)
High Speed Manufacturing Process of Carbon Fiber Reinforced Polymer Composites for Automotive Lightweight Applications
15:50-16:05 (OL-4) **Xin Jia** (Shihezi University, China)
Tunable Sub-Micrometer N-Doped Carbon Spheres from Phenol-Amine Building Blocks by Competitive Self-Assembly
16:05-16:25 **COFFEE BREAK**

16:30-18:00 **POSTER SESSION (Room: Library 7th Floor)**

Friday, Sept. 6

08:00-09:00		Registration (Library Lobby)
Zhiyuan Lecture Hall		
(Chair: Xiuguo Cui)		
09:00-09:40	(PL-3)	Sang-Young Lee (Ulsan National Institute of Science and Technology, Korea) Form Factor-Free, Monolithic Printed Power Sources
09:40-10:00		COFFEE BREAK (Library 401 and Library 602)
Library 602		
Materials for Energy (Chair: Hideyuki Otsuka)		
10:20-10:50	(KL-5)	Toyoko Imae (National Taiwan University of Science and Technology, Chinese Taiwan) Carbon Quantum Dot-Enhanced Energy Devices
10:50-11:20	(KL-6)	Xuefeng Yu (Shenzhen Institute of Advanced Technology CAS, China)
11:20-11:35	(OL-5)	Xiaohua Zhang (Soochow University, China) Enhanced Ion Transport in Densified CNT Arrays
11:35-11:50	(OL-6)	Xusheng Wang (Technical Institute of Physics and Chemistry, CAS, China) Novel Metal Chalcogenides as High-Performance Anodes for Sodium-Ion Battery
11:50-13:30		LUNCH
Functional Nanomaterials (Chair: Yinzhou Yan)		
13:30-14:00	(KL-7)	Hideyuki Otsuka (Tokyo Institute of Technology, Japan) Dynamic Covalent Chemistry Approaches toward Self-Healing and Mechanochromic Polymers
14:00-14:25	(IL-7)	Dongpeng Yan (Beijing Normal University, China) The Long-Lasting Luminescence in Hybrid Materials
14:25-14:50	(IL-8)	Huiqin Lian (BIPT, China) Black Phosphorus Enhanced Actuation in Nafion Based IPMC
14:50-15:05	(OL-7)	Yan Li (BIPT, China) Cobalt-based Oxide Materials for Cathode of IT-SOFC
15:05-15:30		COFFEE BREAK
Functional Nanomaterials (Chair: Toyoko Imae)		
15:30-16:00	(KL-11)	Chang-Sik Ha (Pusan National University, Korea) Graphene Reinforced Polymer Nanocomposites
16:00-16:25	(IL-9)	Yongri Liang (BIPT, China) Positive and Negative Electrostriction Effect of Dielectric Polyurethane Elastomers
16:25-16:50	(IL-10)	Vladimir Egorkin (Russian Academy of Sciences, Russia) Protection of Metals by Multifunctional Coatings on the Basis of PEO-Layers
16:50-17:15	(IL-11)	Yang Liu (BIPT, China) Tough Hydrogels Based on a Facile Strategy: Micellar Polymerization Followed by Solution Polymerization

17:15-17:30	(OL-8)	Shengfu Ji (Beijing University of Chemical Technology, China)
17:50-18:00		CLOSING REMARK / Introduction of the ASAM-8 (Chair: Xiuguo Cui)

Library 401

Materials for Optoelectronics (Chair: **Dongpeng Yan**)

10:20-10:50	(KL-8)	Yury Shchipunov (Russian Academy of Science, Russia) Sol-Gel-Derived Photonic Nanocomposites
10:50-11:20	(KL-9)	Li-Jen Chen (National Taiwan University, Chinese Taiwan) Effect of Surface Hydrophobicity on the Pretilt Angle Control of Nematic Liquid Crystal Alignment
11:20-11:35	(IL-12)	Yuxi Liu (Beijing University of Technology, China) Transition Metal Oxide-Supported Bimetallic Catalysts with High Performance for VOCs Oxidation
11:35-11:50	(OL-9)	Hao Wang (BIPT, China) Rapid and facile Ratiometric Luminescent Detection of an Anthrax Biomarker in a Bimetallic Tb/Eu-MOFs
11:50-13:30		LUNCH

Materials with Specific Functions (Chair: **Yury Shchipunov**)

13:30-14:00	(KL-10)	Xiuguo Cui (BIPT, China) Enhanced Cycle Stability and Energy Density of Zinc Ionic Battery using Phosphorene/Polyaniline Composite Cathode
14:00-14:25	(IL-13)	Aleksey Vedyagin (Russian Academy of Science, Russia) From Binary to Ternary Systems of Partly Miscible Metals: in Search of an Optimal Ratio
14:25-14:50	(OL-10)	Lanchao Ma (BIPT, China) Organic and Polymeric Functional Field Effect Transistors
14:50-15:05	(OL-11)	Dahai Gao (BIPT, China) Thermal Conductive Epoxy Adhesive with Synergy of Hexagonal Boron Nitride and α -Aluminum Oxide Fillers
15:05-15:30		COFFEE BREAK

Functional Nanomaterials (Chair: **Li-Jen Chen**)

15:30-16:00	(KL-12)	Yinzhou Yan (Beijing University of Technology, China) Tailored Wide-Bandgap Semiconductor Microcavity in Nanophotonics
16:00-16:25	(IL-14)	Zhanpeng Wu (Beijing University of Chemical Technology, China) Poly(dichlorophosphazene) as a Precursor for Polyphosphazenes: Synthesis and Stabilization
16:25-16:50	(IL-15)	Xu Xiang (Beijing University of Chemical Technology, China) Efficient Separation of Magnesium and Lithium from Salt Lake Brine via Ion Imprinted Layered Double Hydroxide Materials
16:50-17:15	(IL-16)	Yibo Wu (BIPT, China) Characteristics and Mechanism of Cationic Polymerization in Aqueous Media Initiated by Cumyl Alcohol/B(C ₆ F ₅) ₃
17:15-17:30	(OL-12)	Fuping Dong (Guizhou University, China) Controllable Fabrication of Raspberry-Like Porous Polysilsesquioxane Particles

Saturday, Sept. 7

Zhiyuan Lecture Hall (Chair: Xiuguo Cui)

Special Symposium on Black Phosphorus Materials (in Chinese)*

- 09:00-09:40 (PL-a) **Han Zhang** (Shenzhen University)
- 09:40-10:20 (PL-b) **Xuefeng Yu** (Shenzhen Institute of Advanced Technology, CAS)
- 10:20-10:40 **COFFEE BREAK**
- 10:40-11:20 (KL-a) **Xiuguo Cui** (Beijing Institute of Petrochemical Tehnology)
- 11:20-11:40 **Xu Jiang** (Nanjing Xianfeng Nano Tech. Co. Ltd)

Post Symposium Tour *

- 07:30-12:00 Half-day Tour : The Imperial Palace (¥120/ person)
 Charge Items:
 Entrance ticket + Transportation +Lunch
 Payment (cash-only) at the registration desk
- 05:30-17:00 One-day Tour : The Great Wall (¥100/ person)
 Charge Items:
 Entrance ticket + Transportation +Lunch (cable car at one's own expense)
 Payment (cash-only) at the registration desk

* Though the official language of the ASAM-7 is English, the special symposium on phosphorous materials are provided in Chinese only. Who do not attend the special symposium on phosphorous materials are invited to join half-day or one-day tour with personal payment.

Note: It is better to get tickets in advance in case of the total number limitation for the tourist spot. Please send the form to asam7th@163.com before August 30, 2019.

Type of Tour	Passport number	Choice
1 The Imperial Palace (Bipt-spot-Bipt)		
2 The Great Wall (Bipt-spot-airport-Bipt)		

Poster Presentation

(Sept. 5, 16:30-18:00, Room: Library 7th Floor)

- (P-01) Jungwon Kong, Sung-Soo Park, Chang-Sik Ha
(Pusan National University, Korea)
Fabrication of pH-Responsive Poly(Acrylic Acid)/MCM-41 and Incorporation of Guest Molecules for Sustained Drug Release
- (P-02) Anju Maria Thomas, Chang-Sik Ha
(Pusan National University, Korea)
Dual Stimuli-Responsive PDMAEMA Functionalized SBA-15 with Pd Nanoparticles Incorporated Hybrid System for Catalytic Application
- (P-03) Yanqi Liu, Yan Zhao
(Beijing University of Technology, China)
Controllable Plasmon-induced Catalytic Reaction by Tip Enhanced Raman Spectroscopy
- (P-04) Xu Jinghan, Zhao Yan
(Beijing University of Technology, China)
Application of Ag-Loaded TiO₂ Nanocolumn Array in Photocatalysis
- (P-05) Jintong Du, Piyue Gong, Aifang Geng, Haiying Huang
(Changchun Institute of Applied Chemistry, Chinese Academy of Sciences, China)
Complexation Behavior of Fulvic Acid with Heavy Metal Ions
- (P-06) Yong-Zhu Yan, Saravanan Nagappan, Sung Soo Park and Chang-Sik Ha
(Pusan National University, Korea)
Designed Synthesis of Monodisperse Hollow Polysilsesquioxane@PEI Spheres for Dye Removal
- (P-07) Jian Hao
(Beijing Institute of Petrochemical Technology, China)
Enhanced Thermal Conductivity of Epoxidized Natural Rubber with Poly(dopamine) Modified Boron Nitride
- (P-08) Qiaoyu Han
(Beijing Institute of Petrochemical Technology, China)
Improved Thermal Conductivity of Nitrile Butadiene Rubber by Incorporating Modified Alumina/Boron Nitride Using Dopamine Chemistry
- (P-09) Qungui Wei, Dan Yang
(Beijing Institute of Petrochemical Technology, China)
Improved Thermal Conductivity of XNBR Dielectric Composites by Using Multilayered Core-Shell Structure Dielectric Particles as High Dielectric Constant Filler
- (P-10) Xinxin Kong
(Beijing Institute of Petrochemical Technology, China)
Improved Electromechanical Properties of Acrylonitrile-Butadiene Rubber Composites by Modification of TiO₂ Nanoparticles via Non-Covalent Poly(catechol/polyamine) Deposition and Covalent Grafting with Silane

- (P-11) Shan Gao
(Beijing institute of Petrochemical Technology, China)
Preparation of Thermal Conductive Composite with Tannic Acid Modified Boron Nitride
- (P-12) Tingting Hu
(Beijing institute of Petrochemical Technology, China)
Preparation of High Thermal Conductive Composites with Tannic Acid Modified Carbon Nanotubes
- (P-13) Jia Ai
(Beijing institute of Petrochemical Technology, China)
High Thermal Conductivity Dielectric Elastomer Composites Prepared by Modifying Alumina Particles with Catechol and Tetraethylenepentamine
- (P-14) Liyuan Yu, Dan Yang
(Beijing institute of Petrochemical Technology, China)
Preparation of High Thermal Conductivity Elastomer Composites with Novel Core/Shell-Structured Thermal Conductive Nanoparticles
- (P-15) Qiang Wang, Yinzhou Yan, Yijian Jiang
(Beijing institute of Petrochemical Technology, China)
Growth and Optoelectronic Properties of Acceptor-rich ZnO Single-crystal Microtubes
- (P-16) Qingyang Gu, Jinyan Li
(Beijing institute of Petrochemical Technology, China)
The Preparation and Properties Investigation of 5-Aminolevulinic Acid Intercalated Composites
- (P-17) Jae-Choon Lee, Myeon-Cheon Choi, Dong-Hee Choi, Chang-Sik H
(Pusan National University, Korea)
Toughness Enhancement of Poly(Lactic Acid) through Hybridisation with Epoxide-Functionalized Silane via Reactive Extrusion
- (P-18) Yubin Jeon, Saravanan Nagappan, Chang-Sik Ha
(Pusan National University, Korea)
Design and Fabrication of Robust and Transparent Amphiphilic Metallopolymer Coatings
- (P-19) Yong-Hyeok Lee, Sang-Young Lee
(Ulsan National institute of Science and Technology, Korea)
Anion Exchangeable Separator Mimicking Spiderweb for Lithium Sulfur Battery
- (P-20) Jintong Du, Piyue Gong, Aifang Geng, Haiying Huang
(Changchun institute of Applied Chemistry, Chinese Academy of Sciences, China)
Complexation Behavior of Fulvic Acid with Heavy Metal Ions
- (P-21) Tianlu Li, You Zhang, Li Li, Kang Wang, Fei Chen
(Beijing institute of Petrochemical Technology, China)
Sealing of PEO Layers on Ti Alloy with Zirconia-Filled Sol-Gel Coatings and its Tribocorrosion Performance
- (P-22) Shangzhou Liu, Ziqian Yu, Xiaorui Wang, Huiqin Lian
(Beijing institute of Petrochemical Technology, China)

-
- Preparation and Characterization of Black Phosphorus-Carbon Nanotubes Composites**
(P-23) Qing Xu Wen, Yong Wang, Ying Dan Liu
(Yanshan University, China)
- Preparation of P(Nipam-Co-Amim[X]) Microgel and Rheological Properties of Aqueous Solution**
(P-24) Lei Zu, Huiqin Lian, Xing Gao, Ce Li and Xiuguo Cui
(Beijing institute of Petrochemical Technology, China)
- High Performance of Supercapacitor Based on Simultaneous Redox of Polyaniline and Bromide Ions**
(P-25) Kihun Jeong, Ju-Myung Kim, and Sang-Young Lee
(Ulsan National institute of Science and Technology, Korea)
- One-Dimensional Nanohybrid Based on Cobalt Porphyrin and Carbon Nanotube for Lithium-Ion Battery Anodes**
(P-26) Wu Xia, Yue Wang, Yinzhou Yan, Yijian Jian
(Beijing University of Technology, China)
- Fabrication of Acceptor-Rich ZnO Microtube/n-ZnS Heterojunctions for Highly Efficient Photodegradation of Organic Dyes**
(P-27) Cheng Xing, Yinzhou Yan, Qiang Wang, Yijian Jiang
(Beijing University of Technology, China)
- The Electroluminescence of Ga: ZnO Microrod Grown by Optical Vapor Supersaturated Precipitation**
(P-28) Lixue Yang, Lin Li, Yinzhou Yan, Yijian Jiang
(Beijing University of Technology, China)
- Giant Enhancement of Unidirectional Photoluminescence by a Microsphere Cavity-array Capping on QDs/PDMS Composite Film for Flexible Lighting and Displays**
(P-29) Lingling Liang, Yan Zhao and Chao Feng
(Beijing University of Technology, China)
- Preparation of Aluminum-Based Silver Nanoarrays and the Ultraviolet-Visible-near Infrared Absorption Properties**
(P-30) Donggue Lee, Sang-Young Lee
(Ulsan National institute of Science and Technology, Korea)
- Monolithic Heteronanomat Paper Air Cathodes toward Origami-Foldable/Rechargeable Zn-Air Batteries**
(P-31) Kwon-Hyung Lee, Sang-Young Lee
(Ulsan National institute of Science and Technology, Korea)
- Ultrahigh Areal-Number-Density Printable on-Chip Microsupercapacitor**
(P-32) Ju-Myung Kim, Sang-Young Lee
(Ulsan National institute of Science and Technology, Korea)
- 1D Elementals-Interconnected Nanomat Electrode for High-Capacity Li-Ion Battery Cathodes**
(P-33) Sodam Park, Sang-Young Lee
(Ulsan National institute of Science and Technology, Korea)
- Single Lithium-Ion Conducting Covalent Organic Framework**
(P-34) Ahn David byungsun, Sang-Young Lee

-
- (P-35) Seok-Kyu Cho, Sang-Young Lee
(Ulsan National institute of Science and Technology, Korea)
Direct Ink Writing Based Solid-State Supercapacitors for Smart Contact Lenses
- (P-36) Seung Hyeok Kim, Sang Young Lee
(Ulsan National institute of Science and Technology, Korea)
Antioxidative Lithium Storage Based on Nanoconfinement of Carbon Nanotube Bundles
- (P-37) Yijian Jiang, Haoqi Tan, Yan Zhao
(Beijing institute of Petrochemical Technology, China)
Improving Optical and Electrical Properties of Gan Epitaxial Wafers and Enhancing Luminescent Properties of Gan-Based Light-Emitting-Diode with Excimer Laser Irradiation
- (P-38) Chunnuan Du, XiaohuiLv , Yang Liu, Zikang Jia, Jianxiang Yu
(Beijing institute of Petrochemical Technology, China)
Synthesis of Silver Nanofiber Transparent Electrodes by Silver Mirror Reaction with Electrospun Nanofiber Template
- (P-39) Xueping Chen, Guangjian Xing, Linfeng Xu, Huiqin Lian, Yanyan Wang
(Beijing Institute of Petrochemical Technology, China)
Vertically Aligned MoS₂ Thin Films Prepared by Rf-Magnetron Sputtering Method as Electrocatalysts For Hydrogen Evolution Reactions
- (P-40) Hongyu Feng, Tong Zhao, Yuhua Dai
(Beijing Institute of Petrochemical Technology, China)
Preparation of Polyurethane Solid Electrolytes Adding Nanocarbon Material For Dye-sensitized Solar Cells
- (P-41) Minyoung Lee, WanheeJeong, Ildoo Chung
(Pusan National University, Korea)
Preparation and Characterization of Polybenzimidazole Based 3D Printable Photocurable Dental Resin
- (P-42) Minyoung Lee, WanheeJeong, Ildoo Chung
(Pusan National University, Korea)
Preparation and Characterization of Poly(Ether Ether Ketone) Based 3D Printable Photocurable Dental Resin
- (P-43) MijinJeong, Injun Song and Ildoo Chung
(Pusan National University, Korea)
Synthesis and Characterization of Carboxylic β -Cyclodextrin with Vitamin E/C
- (P-44) MijinJeong, Injun Song and Ildoo Chung
(Pusan National University, Korea)
Synthesis and Characterization of β -Cyclodextrin- L-Ascorbic Acid Conjugates
- (P-45) Weijin Zhang, Yushun Jin, Dan Yu
(Beijing Institute of Petrochemical Technology, China)

-
- Preparation and Characterization of Environmentally Sensitive Microcapsules**
- (P-46) Minji Kwon, Daehwi Lim, Inchul Choi, Hae-Won Kwon, and Chang-Sik Ha
(Pusan National University, Korea)
- Preparation and Properties of Ethylene-Vinyl Acetate Copolymer Based Blend Foams**
- (P-47) Inho Shin, Yury Shchipunov, Chang-Sik Ha
(Pusan National University, Korea)
- Fabrication and Characterization of Cellulose/Montmorillonite Intercalated by Polyhedral Oligomeric Silsesquioxane Nanocomposites**
- (P-48) Seong-Sun Lee, Keun-Ho Choi, Se-Hee Kim and Sang-Young Lee
(Ulsan National Institute of Science and Technology, Korea)
- Flexible Solid-State Supercapacitors Printed on Textiles for Smart Garments**
- (P-49) Yong-Zhu Yan, Saravanan Nagappan, Sung Soo Park and Chang-Sik Ha
(Pusan National University, Korea)
- Designed Synthesis of Monodisperse Hollow Polysilsesquioxane@PEI Spheres for Dye Removal**
- (P-50) Haoyuan An
(Beijing Institute of Petrochemical Technology, China)
- The Research of Low Temperature Curing Epoxy Resin for Winding Composites**
- (P-51) Yifan Meng, Shi Sun, Yingying Li, Yixin Yang, Mingsheng Luo
(Beijing Institute of Petrochemical Technology, China)
- Modification of Titanium Dioxide by Doping with Zn for the Catalytic Ozonation of *p*-Chlorobenzoic Acid**
- (P-52) Yingying Li, Yifan Meng, Dan Song, Jingchao Yang, Yixin Yang, Mingsheng Luo
(Beijing Institute of Petrochemical Technology, China)
- Application of Graphene in the Catalytic Ozonation of *p*-Chlorobenzoic Acid in Aqueous Solution**
- (P-53) Linlin Li, Wei Ma, Akihiko Takada, Yuji Higaki, Maiko Okajima, Tatsuto Kaneko, Atsushi Takahara
(Kyushu University, Japan)
- Hybrid Film Fabricated by Layer by Layer Assembly of Sacran and Imogolite Nanotubes**
- (P-54) Dan Song, Yingying Li, Yifan Meng, Yixin Yang, Mingsheng Luo
(Beijing Institute of Petrochemical Technology, China)
- Degradation of Ibuprofen by Nano-TiO₂ Catalyzed Ozonation**
- (P-55) Zengzeng Xue, Xu An, Mingshan Yang
(Beijing Institute of Petrochemical Technology, China)
- Analysis of Modification Effect of Peroxide Masterbatch on Homo-polypropylene from Crystallization Behavior**
- (P-56) Bao Zhu, Mingshan Yang
(Beijing Institute of Petrochemical Technology, China)
- Curing Resin for 3D Printing**

-
- (P-57) Ce Li, Xing Gao
(Beijing Institute of Petrochemical Technology, China)
The Flame Retardant Properties of Black Phosphorene in Epoxy Resin
- (P-58) Jingjing He, Yongri Liang
(Beijing Institute of Petrochemical Technology, China)
Improved Dielectric and Mechanical Properties of Thermoplastic Polyurethanes Elastomer Achieved by Blending with Small Molecules
- (P-59) Ou Shen, Guang-Xiang He
(Beijing Institute of Petrochemical Technology, China)
Simulation of Liquid Seepage in Medical Dry Chemical Diagnostic Reagent Materials
- (P-60) Shanglei Ning, Haibo Jin, Suohe Yang, Gaungxiang He, Xiaoyan Guo (Beijing Institute of Petrochemical Technology, China)
Hydrodynamic Characteristics of p-Xylene Oxidation Reactors with an Acetic Acid System
- (P-61) Qianqian Zhu, Haibo Jin, Gaungxiang He, Xiaoyan Guo
(Beijing Institute of Petrochemical Technology, China)
Synthesis of ϵ -Caprolactone by Cyclohexanone Baeyer-Villiger Green Oxidation
- (P-62) Jiaqi Liu, Xiaoyan Guo, Haibo Jin, Gaungxiang He
(Beijing Institute of Petrochemical Technology, China)
Preparation and Application of Barium Sulfate Multifunctional Layer
- (P-63) Fangfang Tao, Haibo Jin
(Beijing Institute of Petrochemical Technology, China)
Gas-Liquid Two-Phase Flow Characteristics in Microchannels Based on Electrical Resistance Tomograph
- (P-64) Yunlong Zhang, Haibo Jin
(Beijing Institute of Petrochemical Technology, China)
The CWPO Degradation of m-Cresol on Activated Carbon-Based Catalysts: Surface Chemical Characteristics
- (P-65) Wenlong Zhang, Haibo Jin
(Beijing Institute of Petrochemical Technology, China)
Simulation Study on Fluid Dynamics Behavior in a Bubble Column by CFD-PBM Coupled Model
- (P-66) Li Li, Jia Qi, Tianlu Li, Tengyan Zhang, Kang Wang, Fei Chen
(Beijing Institute of Petrochemical Technology, China)
A Hierarchical Graphene Oxide Hydrophobic Coating for Improved Wear Resistance and Corrosion Resistance
- (P-67) Xiaogang Liu, Yu Zhao, Jinru Sun, Yu Tian, Cuiqing Li, Yongji Song, Hong Wang
(Beijing Institute of Petrochemical Technology, China)
Simultaneous Removal of NO and Soot Catalytic Performance of $\text{La}_{1-x}\text{Na}_x\text{MnO}_3$ Perovskite Catalysts
- (P-68) Jinru Sun, Xiaogang Liu, Yu Zhao, Yu Tian, Hong Wang*, Cuiqing Li, Yongji Song
(Beijing Institute of Petrochemical Technology, China)

**Effect of Crystallization Temperature on the Performance of Catalytic
Decomposition of N₂O over Co₃O₄ Catalysts**

(P-69) Piyue Gong, Jintong Du, Haiying Huang
(Beijing Institute of Petrochemical Technology, China)

Extraction and Characterization of Humic Acid from Lignite

(P-70) He Nan Yuan, Bin Zhang, Guang Xiang He
(Beijing Institute of Petrochemical Technology, China)

**Preparation of polystyrene microspheres and its application in the
diffusion of dry chemical reagent slides**

Plenary Lecture

PL 1 ~ PL 3

PL1

Advanced Functional Nanomaterials for Applications in Oncology

Ulrich Wiesner

Materials Science and Engineering, Cornell University, Ithaca, NY 14853, USA
E-mail: ubw1@cornell.edu

Despite significant promise of nanomaterials in medicine, few colloidal materials make the transition into the realm of human clinical applications. In this presentation a class of ultras-small fluorescent core-shell silica nanoparticles will be introduced referred to as “Cornell dots” or simply “C dots”. These particles have diameters below 10 nm, *i.e.* below the cut-off for renal clearance, leading to favorable biodistribution and pharmacokinetics. These smaller than 10 nm sized PEGylated probes for nanomedicine are the first dual-modality (optical/PET) hybrid nanoparticles of their class and properties receiving investigational new drug (IND) food and drug administration (FDA) approval for first in-human clinical trials with melanoma patients in the US.¹ In this presentation, results on C dot synthesis and characterization will be reported with focus on materials properties that facilitate translation into clinical applications, including the synthesis of ultras-small antibody fragment-C dot conjugates and the introduction of high performance liquid chromatography (HPLC) for the characterization of surface chemical heterogeneities of such inorganic nanoparticles.^{2,3} It will include the use of C dots in unconventional therapeutic strategies against cancer as well as the discovery of novel silica nanoparticle structures.^{4,5} The talk will finally discuss novel generations of C dots as advanced amorphous quantum nanomaterials for applications in optical super-resolution microscopy (SRM) and photodynamic therapy.⁶

References:

1. E. Phillips, O. Penate-Medina, P. B. Zanzonico, R. D. Carvajal, P. Mohan, Y. Ye, J. Humm, M. Gönen, H. Kaliagian, H. Schöder, H. W. Strauss, S. M. Larson, U. Wiesner, M. S. Bradbury, *Sci. Transl. Med.* 2014, **6**, 260.
2. F. Chen, K. Ma, B. Madajewski, L. Zhuang, L. Zhang, K. Rickert, M. Marelli, B. Yoo, M. Turker, M. Overholtzer, T. Quinn, M. Gonen, P. Zanzonico, A. Tiesca, M. Bowen, L. Norton, J. Subramony, U. Wiesner, M. Bradbury, *Nat. Commun.* 2018, **9**, 4141.
3. T. C. Gardinier, F. F. E. Kohle, J. S. Peerless, K. Ma, M. Z. Turker, J. A. Hinckley, Y. G. Yingling, U. Wiesner, *ACS Nano* 2019, **13**, 1795-1804.
4. S. Eun Kim, L. Zhang, K. Ma, M. Riegman, F. Chen, I. Ingold, M. Conrad, M. Z. Turker, M. Gao, X. Jiang, S. Monette, M. Pauliah, M. Gonen, P. Zanzonico, T. Quinn, U. Wiesner, M. S. Bradbury, M. Overholtzer, *Nat. Nanotech.* 2016, **11**, 977.
5. K. Ma, Y. Gong, T. Aubert, M. Z. Turker, T. Kao, P. C. Doerschuk, U. Wiesner, *Nature* 2018, **558**, 577.
6. F. F. E. Kohle, J. A. Hinckley, S. Li, N. Dhawan, W. P. Katt, J. A. Erstling, U. Werner-Zwanziger, J. Zwanziger, R. A. Cerione, U. B. Wiesner, *Adv. Mater.* 2019, **31**, 1806993.

PL2

Self-Growing Hydrogels by Mechanical Training

Takahiro Matsuda¹, Tasuku Nakajima^{2,3,4}, Jian Ping Gong^{2,3,4,*}

¹Graduate School of Life Science, Hokkaido University; ²Faculty of Advanced Life Science, ³Soft Matter GI-CoRE, ⁴WPI-ICReDD, Hokkaido University, Japan

E-mail: gong@sci.hokudai.ac.jp

Living tissues, such as muscle, autonomously grow and remodel themselves to adapt to their surrounding mechanical environment through metabolic processes. By contrast, typical synthetic materials cannot grow and reconstruct their structures once formed. We present a strategy for developing “self-growing” polymeric materials that respond to repetitive mechanical stress through an effective mechanochemical transduction in the robust double network hydrogels ^[1,2]. We show that the double-network hydrogels, with supply of monomers, self-grow and significantly strengthen under repetitive loading. Such sustained self-growing is through a repetitive structural destruction and reconstruction process, in analogy to the metabolic processes of biological system. This strategy also endows to impart the hydrogels with tailored functions at desired positions by mechanical stimuli. This work may pave the way for the development of self-growing gel materials for applications such as soft robots and intelligent devices.

References:

1. Jian Ping Gong, *Soft Matter*, 2010, **6**, 2583.
2. Takahiro Matsuda, Runa Kawakami, Ryo Namba, Tasuku Nakajima, Jian Ping Gong, *Science*, 2019, **363**, 504.

PL3

Form Factor-Free, Monolithic Printed Power Sources

Sang-Young Lee

Department of Energy Engineering, UNIST, Ulsan, 44919, Korea
E-mail: syleek@unist.ac.kr

Upcoming wearable/flexible electronics with shape diversity and mobile usability have garnered significant attention as a kind of disruptive technology to drastically change our daily lives, which inspires the relentless pursuit of advanced power sources with high energy density, electrochemical sustainability, design diversity and mechanical flexibility. From the viewpoint of cell design and architecture, the conventional assembly and materials have pushed the power sources to lack of variety in form factors, thus imposing formidable challenges on their integration into versatile-shaped electronic devices. Here, my talk describes a new class of form factor-free, printed power sources with aesthetic versatility that lie far beyond those achievable with conventional technologies. The printed power sources are fabricated directly on arbitrary objects of complex geometries through a variety of simple, low-cost and scalable printing processes. Their salient features include various form factors, shape conformability and monolithic integration with devices of interest. A key-enabling technology for the printed power source systems is to design battery inks (specifically, electrode and electrolyte inks), with a focus on their rheology and electrochemistry. Our particular attention is devoted to discussing effects of the battery inks on printing processability, microstructure (focusing on bicontinuous ion/electron transport channels) and electrochemical performance of the resultant printed power sources. We envision that the printed power sources open a new avenue towards form factor-free/monolithic integrated power sources with object-tailored design versatility, which play a vital role in the upcoming flexible/wearable electronics, the internet of things and ubiquitous energy applications.

References:

1. Keun-Ho Choi, David B. Ahn and Sang-Young Lee*, *ACS Energy Lett.* 2018, **3**, 220.
2. Se-Hee Kim, Keun-Ho Choi, Sung-Ju Cho, JongTaeYoo, Seong-Sun Lee and Sang-Young Lee*, *Energy & Environ. Sci.* 2018, **11**, 321 (highlighted as a front cover image).

3. Han-Don Um, Keun-Ho Choi, Inchan Hwang, Se-Hee Kim, Kwanyong Seo and Sang-Young Lee*, *Energy & Environ. Sci.* 2017, **10**, 931 (highlighted as a front cover image).
4. Keun-Ho Choi, JongTaeYoo, Chang Kee Lee and Sang-Young Lee*, *Energy & Environ. Sci.* 2016, **9**, 2812 (highlighted as a back cover image).

Keynote Lecture

KL 1 ~ KL 12

KL2

Chitosan/Alginate Bionanoparticles Loading Lovastatin and Ginsenoside Rb1 (Extracted from Panax Ginseng): Preparation, Characterization and in Vitro Drug Release Control

Thai Hoang^{1,2}, Nguyen Thuy Chinh¹, Tran Dai Lam^{1,2}*

¹Institute for Tropical Technology, Vietnam Academy of Science and Technology, 18, Hoang Quoc Viet, Cau Giay, Ha Noi, 100000, Vietnam

²Graduate University of Science and Technology, Vietnam Academy of Science and Technology, 18 Hoang Quoc Viet, Cau Giay, Ha Noi, 100000, Vietnam

Corresponding author: hoangth@itt.vast.vn

Currently, biopolymers are commonly used for lovastatin delivery to enhance the bioavailability of lovastatin in the treatment of obesity (due to cholesterol in the blood exceeded the prescribed limit) and cardiovascular disease. It is found that the published papers only have focused preparation of polymer composites in micro- and nano-size based on alginate and chitosan containing some drugs and in vitro drug release and drug release kinetics in different solution pH¹⁻³. The polymer nanoparticles of alginate/chitosan carrying drug have advantages like non-toxic, drug loading ability, good adhesion, biodegradability, and biocompatibility. However, there is no report so far on the fabrication and characterizations of alginate (AG)/chitosan (CS) bionanoparticles loading lovastatin and ginsenoside Rb1 (extracted from panax ginseng) by ionic gelation method. Therefore, this work researches the effect of ginsenoside Rb1 on characterizations and properties of the alginate/chitosan/lovastatin/Rb1 nanoparticles by using some methods such as infrared spectroscopy (IR), scanning field emission scanning electron microscopy (FESEM), differential scanning calorimetry (DSC), dynamic light scattering (DLS). In addition, the in vitro lovastatin and ginsenoside Rb1 releases from the alginate/chitosan/lovastatin/Rb1 (ACLR) nanoparticles in different simulated body fluids are considered and discussed. The suitable AG/CS ratio of 1/1 (w/w), the ginsenoside Rb1 and lovastatin content of 3 wt.% and 10 wt.% (in comparison with total weight of AG and CS), respectively are best for the preparation of ACLR nanoparticles by ionic gelation method. AG, CS, lovastatin and Rb1 in the bionanoparticles can interact together through

hydrogen bond, electrical interaction, and dipolar-dipolar interaction. The ACLR bionanoparticles are formed successfully in the size range of 54 - 400 nm. The drug loading capacity of ACLR nanoparticles reached from 61 – 78 %. Drug release from the ACLR nanoparticles followed 2 stages: fast release at the first 10 hours and then, slow and stable release. After 32 hours of testing, the drug release content is above 99 % in both pH 2 and pH 7.4 solutions.

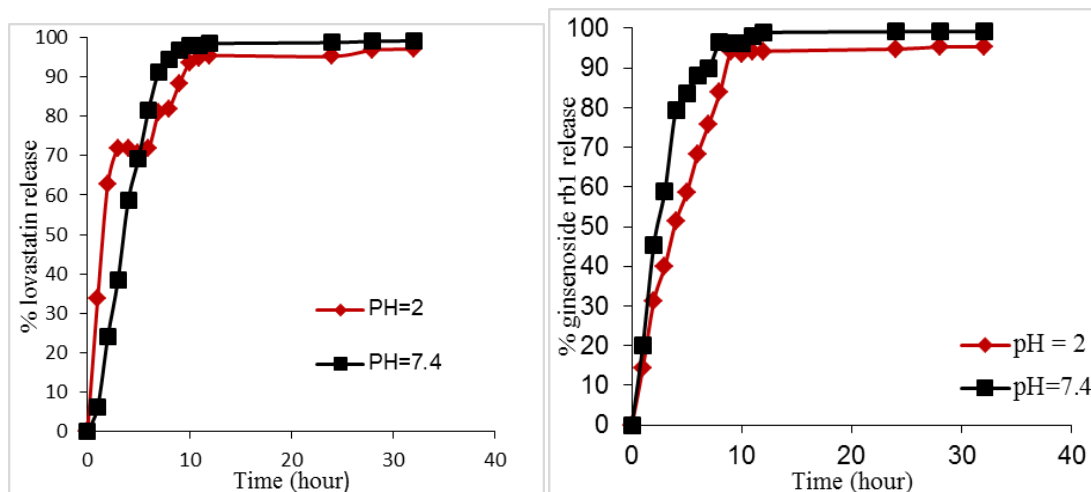


Fig.1. Drug release content from ACLR nanoparticles in pH 2 and pH 7.4 solutions.

Keywords: alginate, chitosan, lovastatin, ginsenoside Rb1, *in vitro* drug release, bionanoparticles.

Acknowledgments

The authors would like to thank the National Foundation for Science and Technology Development in Vietnam for financial support (subject code 104.02-2017.17, period of 2017–2020).

References:

1. S. Bernal, C. Edward, M. Patrick, B. Ramiz, M. B. Roy, A. S. Alejandro, E. Marianelly, P. Jennifer, D. L. F. Leonardo, L. A. Maria, Preparation of alginate-chitosan fibers with potential biomedical applications, *Carbohydrate Polymers*, 134, 598-608 (2015).
2. Loreana Lacerda, Alexandre Luis Parize, Valfredo Fávere, Mauro Cesar Marghetti Laranjeira, Hellen Karine Stulzer. Development and evaluation of pH-sensitive sodium alginate/chitosan microparticles containing the antituberculosis drug rifampicin, *Materials Science and Engineering C*, 39, 161–167 (2014).
3. R. Giovanna, S. Andrea, P. P. Elena, G. Paolo, R. Marta, G. Elisabetta, Composite chitosan/alginate hydrogel for controlled release of deferoxamine: A system to potentially treat iron deregulation diseases, *Carbohydrate Polymers*, 136, 1338-1347 (2016).

KL4

A High Reliable Reversible Thermochromic Phase Change Microcapsule System for Durable Indication of Thermal Energy Storage and Management

Ya Zhang, Huan Liu, Jinfei Niu, Xiaodong Wang, Dezhen Wu*

State Key Laboratory of Organic-Inorganic Composites, Beijing University of
Chemical Technology, Beijing 100029, China

E-mail: wangxdf@aliyun.com

We reported a novel design of sandwich-structured shell configuration for a high reliable reversible thermochromic phase change microcapsule (TCM) system. This configuration was constructed by fabricating a silica base shell onto the *n*-docosane core and then self-assembling a thermochromic indication layer onto the surface of base shell, followed by formation of a polymeric protective layer. Two types of TCMs with red and blue color thermochromic indicators were successfully synthesized according to the design scheme and construction methodology, and their multilayered configuration and well-defined core-shell structure were confirmed by microstructural investigation and chemical composition analysis. These two types of TCMs not only showed an outstanding latent heat-storage/release capability with a high capacity over 150 J/g, but also exhibited a good shape stability, high thermal stability and excellent phase change reliability and durability. The optimum operation conditions for thermal energy storage/release were also determined by nonisothermal and isothermal programmed DSC thermal analyses. Most of all, the two TCMs presented an entirely reversible thermochromic behavior individually with high-contrast red and blue color indications for the phase change state of *n*-docosane core. Both types of TCMs exhibited the highly reliability and long-term durability in thermochromic indication, which meets the design requirements for durable indication of latent heat storage and thermal management. In the light of an innovative configuration of sandwich-structured shell and a smart combination of latent heat-storage and thermochromic functions, the TCM system designed by this study has a great potential for applications in smart fibers and textiles, wearable electric devices, energy-saving buildings, temperature-sensitive medical system, safety clothing, smart windows, aerospace engineering and many more.

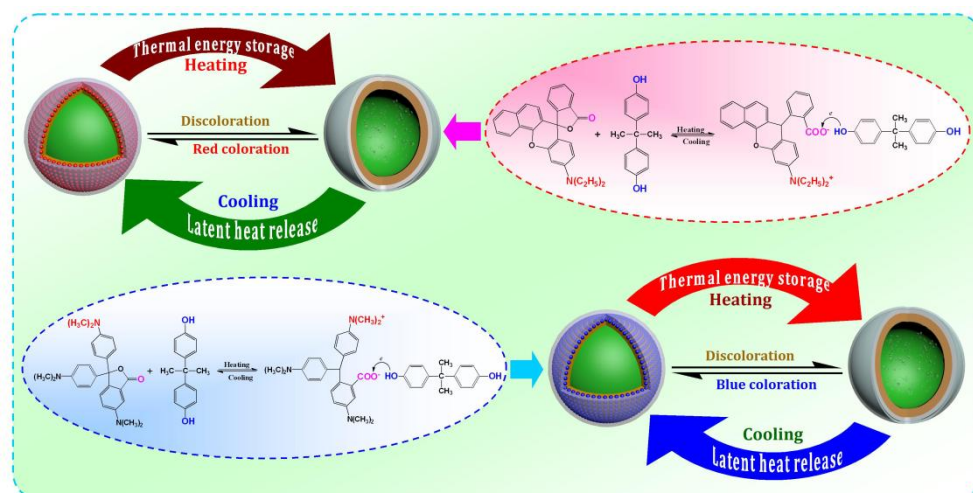


Fig. 1 The synthetic strategy and reaction mechanisms of two types of TCMs.

KL5

Carbon Quantum Dot-Enhanced Energy Devices

Toyoko Imae

Graduate Institute of Applied Science and Technology, National Taiwan University of Science and Technology, Keelung Road, Taipei 10607, Taiwan ROC

Department of Chemical Engineering, National Taiwan University of Science and Technology, Keelung Road, Taipei 10607, Taiwan ROC

E-mail: imae@mail.ntust.edu.tw

Carbon quantum dots (Cdots) are the fluorescent nanosized carbon particles developed in 2004. Since the Cdots possess the sp^2 graphitic core structure and the oxidized functionalities, they provide semiconducting properties and water dispersibility. Thus, they can replace these semiconducting quantum dots and help the fast charge tunneling on electronic devices. In addition, the intensive interaction of Cdots with other semiconducting materials enhances the electron transport and ionic motion and stimulates fast redox reactions in the nanocomposites. Thus, the Cdots-based hybrid materials are applicable to the electron-relating devices. In this talk, the Cdots are applied to electrochemical devices such as supercapacitor and photovoltaic devices.

On the application to supercapacitors, the composites were synthesized by the in situ chemical oxidative polymerization method of semiconducting monomers in the presence of Cdots. The specific capacitance values of polyaniline and polypyrrole increased up to double or more by adding an adequate amount of Cdots. Moreover, as the most important result, the contribution of Cdots approved the durability of the polymer pseudocapacitor, which was the serious disadvantage. Thus, the polymer/Cdots hybrid is the ultimate choice as an electrode material for application to supercapacitors.

The investigations to improve the performance of dye-sensitized solar cells (DSSCs) were performed by the addition of Cdots on semiconducting ZnO. The addition of Cdots to ZnO enhanced the photovoltaic performance. The potency of Cdots is the contribution to the electron-hole pair separation in semiconducting nanoparticles in the different ways from photosensitizer (N719), although the maximum performance of Cdots was at the confined content (10 wt%), since the excess adsorption of Cdots reduced the performance of photosensitizer because of the reduction of its adsorption on ZnO. The present investigation confirmed that the conversion efficiency of DSSC fabricated with ZnO/Cdots/N719 was 5.9% at 2:1 mol ratio of ethylenediamine/citric acid in

Cdots. This investigation demonstrates the performance on DSSCs by adding low-cost additives (Cdots) with high-effective contribution.

KL 7

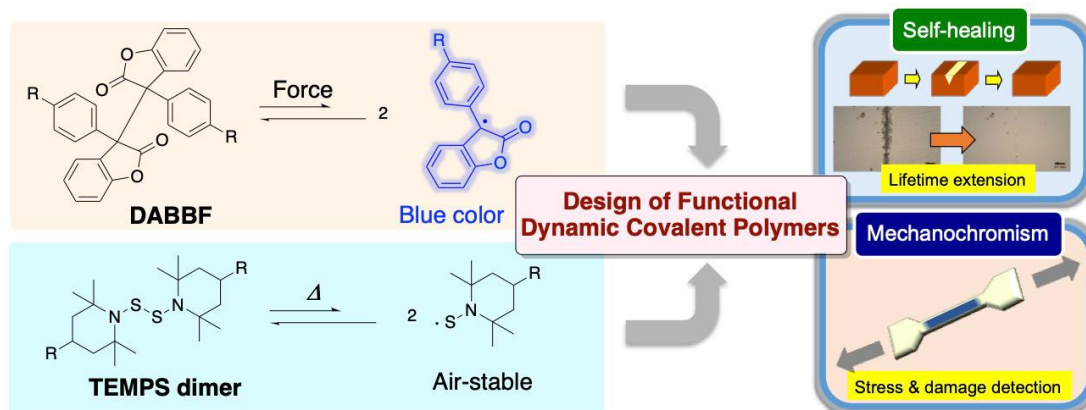
Dynamic Covalent Chemistry Approaches toward Self-Healing and Mechanochromic Polymers

Hideyuki Otsuka

Department of Chemical Science and Engineering, Tokyo Institute of
Technology,
Ookayama, Meguro-ku, Tokyo 152-8550, Japan
E-mail: otsuka@polymer.titech.ac.jp

Carbon–carbon bonds are one of the most important covalent bonds in organic and polymeric materials. Although the bond dissociation energy of carbon–carbon bond in ethane is relatively high, that of the central carbon–carbon bond in tetraarylethane is much lower. Here, we report self-healing and mechano-responsive behavior of polymeric materials with tetraarylethane derivatives. Self-healing of cross-linked polymeric materials with diarylbibenzofuranone (DABBF)-based dynamic covalent linkages at ambient temperature was demonstrated, and their healing behavior from both macroscopic and microscopic viewpoints was investigated.¹⁻³ In addition, we report self-healing polymers based on the dynamic covalent chemistry of 2,2,6,6-tetramethylpiperidine-1-sulfanyl (TEMPS) dimers derived from thermally reversible homolytic dissociation of the disulfide linkages.^{4,5}

Furthermore, mechano-responsive behavior of polymers with tetraarylethane derivatives was also investigated. Linear, star-shaped, and cross-linked polymeric samples showed mechano-responsive behavior by grinding, stretching, and freezing.⁶⁻¹⁶ In particular, the central carbon–carbon bonds of DABBF units embedded in polymer skeletons can afford the corresponding arylbenzofuranone radicals with blue color by homolytic cleavage of the covalent bonds by the mechanical stress, and the regeneration of the carbon–carbon bonds was also confirmed. The mechano-responsive behavior was also investigated by EPR measurements.



References:

1. Otsuka, H. et al. *Angew. Chem. Int. Ed.* 2012, **51**, 1138.
2. Otsuka, H. et al. *J. Am. Chem. Soc.* 2014, **136**, 11839.
3. Otsuka, H. et al. *Macromolecules* 2015, **48**, 5632.
4. Otsuka, H. et al. *Angew. Chem. Int. Ed.* 2017, **56**, 2016.
5. Otsuka, H. et al. *ACS Macro Lett.*, 2017, **5**, 1280.
6. Otsuka, H. et al. *Angew. Chem. Int. Ed.* 2015, **54**, 6168.
7. Otsuka, H. et al. *ACS Macro Lett.* 2015, **4**, 1307.
8. Otsuka, H. et al. *Chem. Commun.*, 2016, **52**, 10482.
9. Otsuka, H. et al. *ACS Macro Lett.*, 2016, **5**, 1124.
10. Otsuka, H. et al. *Macromolecules*, 2016, **49**, 5903.
11. Otsuka, H. et al. *Chem. Commun.*, 2017, **53**, 11885.
12. Otsuka, H. et al. *Chem. Euro. J.*, 2018, **24**, 3170.
13. Otsuka, H. et al. *ACS Macro Lett.*, 2018, **7**, 556.
14. Otsuka, H. et al. *ACS Macro Lett.*, 2018, **7**, 1087.
15. Otsuka, H. et al. *ACS Macro Lett.*, 2018, **7**, 1359.
16. Moore, J. S.; Otsuka, H. et al. *J. Am. Chem. Soc.* 2019, **141**, 1898.

KL8

Sol-Gel-Derived Photonic Nanocomposites

Yury Shchipunov

Institute of Chemistry, Far East Department, Russian Academy of Sciences,
690022 Vladivostok, Russia
E-mail: YAS@ich.dvo.ru

Silica's transparency makes it very appropriate for optical materials and devices. Furthermore, it is mechanically strong, stable in various solvents, nonswelling and nonshrinkable in water. Silica syntheses are performed by the sol-gel method at mild conditions that can be suitable to immobilize even unstable organic substances. Here, this technique is used to develop photonic materials. As optically active components, quantum dots and gold nanoparticles are entrapped.

CdS and ZnS were synthesized in aqueous solutions by exchange reactions after mixing corresponding metal salt with sodium sulfide in the presence of mercaptosuccinic acid, glutathione or cysteine, which serves as stabilizing ligands against merging. They were entrapped into a silica matrix at appropriate conditions by using completely water-soluble compatible tetrakis(2-hydroxyethyl)orthosilica with ethylene glycol residues. Green sol-gel synthesis was carried out in aqueous solutions without the addition of an organic solvent and acid/alkali at ambient temperature. Nanocomposites thus synthesized were optically transparent with bright luminescence. Their properties and structure were well characterized by various physico-chemical techniques. A new phenomenon was found that consisted in a change of the optical properties under laser lightening at $\lambda = 405$ nm. Furthermore, red-shifting about 50 nm was observed for the emission maxima. When the lightening was ceased, the initial optical state was restored, evidencing the reversibility of photonic effects.

Gold nanoparticles were stabilized by capping with hyaluronic acid or dendrimer-like (hyperbranched polyglycidol) macromolecules. The nonlinear refractive index of these nanocomposites was three orders of magnitude greater than that of fused silica. This high optical nonlinearity was responsible for the generation of supercontinuum. The optical phenomenon consisted in the broadening of initial spectra that resulted in a filamentous intense white lightening when ultra-short laser pulses of 40 fs duration propagated through silica. To have an insight into a possible mechanism of high nonlinearity, the

properties and structure were examined by various physico-chemical techniques, including high resolution transmission and scanning electron microscopy, NMR, FTIR and UV-vis spectroscopy, dynamic rheology. These type of photonic materials are very promising for applications in planar optical devices for optical computers, real-time holography, optical correlators and femtosecond Kerr shutter.

Acknowledgements. The financial support of the Presidium of Far East Department, Russian Academy of Sciences (Program “Dalnii Vostok”) is appreciated.

KL9

Effect of Surface Hydrophobicity on the Pretilt Angle Control of Nematic Liquid Crystal Alignment

Li-Jen Chen, Da-Ren Chiou, Bang-Yan Liu, Kuan-Yu Yeh, Ching-Hsuan Meng

Department of Chemical Engineering, National Taiwan University, Taiwan
10617, Taiwan
E-mail: ljchen@ntu.edu.tw

Liquid crystal alignment strongly depends on the interface properties. The uniform alignment of liquid crystals is essential for the electro-optical performance in the liquid crystal display industry. Particularly, an appropriate pretilt angle of liquid crystals is necessary for the twisted nematic liquid crystal display to prevent reverse tilted disclinations upon exerting an external electric field. The surface hydrophobicity of the substrate is found to adjust the pretilt angle of liquid crystal alignment both experimentally and theoretically.

The periodical micro-grooved silica surfaces are fabricated by soft embossing silica sol-gel precursor on glass substrates with an elastomeric polydimethylsiloxane mold. The patterned silica surface could induce the planar alignment of liquid crystal 5CB along the direction of micro-grooves but with no pretilt angle. The pretilt angle of 5CBs is adjusted from 0° to 90° by the further deposition of organosilane self-assembled monolayers with different functional end-groups on the patterned silica surfaces^{1,2}. It is found that the pretilt angle of liquid crystals increases along with increasing the surface hydrophobicity under the condition of a fixed surface topography, consistent with the results of the polyimide surfaces³. The Oseen-Frank equation is applied to model the bulk energy of liquid crystal and Rapini-Papoular form for surface energy of liquid crystal molecules. Finite difference method is used to calculate the pretilt angle of liquid crystals. It is found that the results of these theoretical calculations are consistent with our experimental observation. Using the surface hydrophobicity to control the pretilt angle of liquid crystal in the polymer-stabilized liquid crystal alignment system is also discussed^{4,5}.

References:

1. D.R. Chiou, L.J. Chen, C.D. Lee, *Langmuir* 2006, **22**, 9403.
2. D.R. Chiou, K.Y. Yeh, L.J. Chen, *Applied Physics Letters* 2006, **88**, 133123.
3. D.R. Chiou, L.J. Chen, *J. Phys. Chem. C* 2009, **113**, 9797.
4. B.Y. Liu, L.J. Chen, *J. Phys. Chem. C* 2013, **117**, 13474.
5. B.Y. Liu, C.H. Meng, L.J. Chen, *J. Phys. Chem. C* 2017, **121**, 21037.

KL10

Enhanced Cycle Stability and Energy Density of Zinc Ionic Battery Using Phosphorene/Polyaniline Composite Cathode

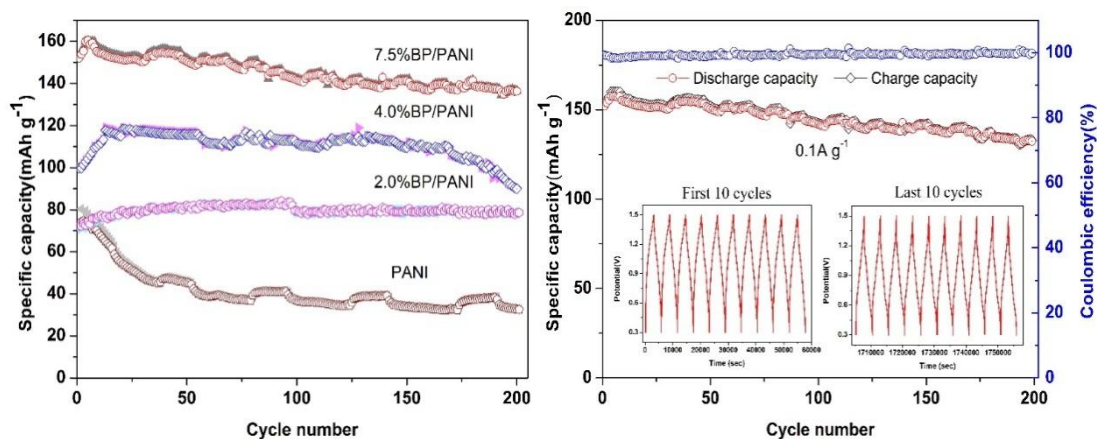
Xing Gao, Ce Li, Lei Zu, Xuemei Cui, Huiqin Lian, Yang Liu, Xiuguo Cui*

Beijing Key Lab of Special Elastomer Composite Materials, College of Materials Science and Engineering, Beijing Institute of Petrochemical Technology, Beijing 102617, China

E-mail: cuxiuguo@bipt.edu.cn

Safety and cost are key factors for the battery design. Although lithium-based batteries have shown very promising results including energy density, cycle stability, there are still difficulties in their practical application owing to high cost of lithium and lithium salts and easy burning or explosion of the organic electrolytes¹. Due to its earth-abundance, low cost, non-toxic, and low sensitivity to moisture, zinc is an attractive anode candidate to replace lithium for aqueous rechargeable batteries². In recent years, many researchers have investigated the aqueous Zn-polyaniline rechargeable batteries [3]. These systems consist of a polyaniline cathode, an aqueous electrolyte solution containing a mixture of ZnCl₂ and NH₄Cl, and a zinc metal foil anode. However, low energy density and poor cycle stability have always been an insurmountable technical defect of zinc polymeric batteries.

In this presentation, we prepared phosphorene/polyaniline composite electrodes with various phosphorene additions, and investigated effects of phosphorene on performances of zinc phosphorene/polyaniline battery.



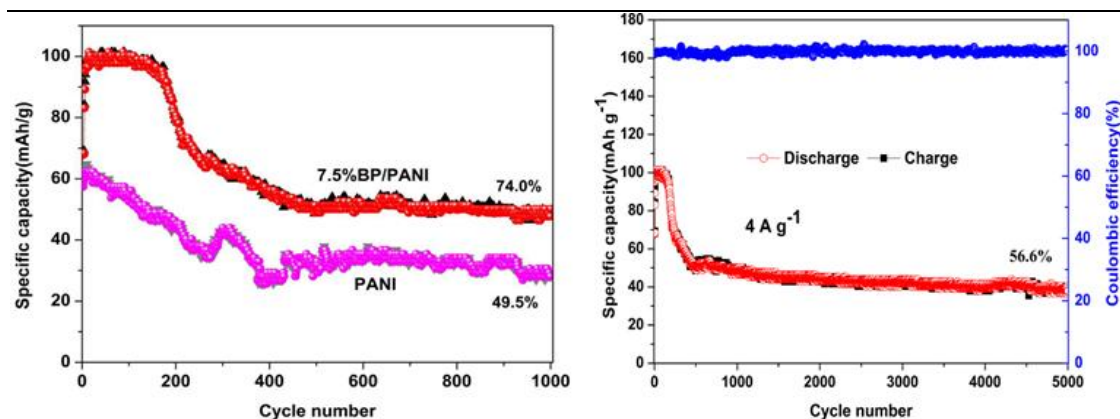


Fig. 1 Comparison of electrochemical performance of zinc polyaniline battery with various phosphorene additions

References:

1. K. Xu, Nonaqueous liquid electrolytes for lithium-based rechargeable batteries, *Chemical Reviews* 2004, **104**, 4303.
2. A. Guerfi, J. Trottier, I. Boyano, I. De Meatza, J.A. Blazquez, S. Brewer, K.S. Ryder, A. Vijn, K. Zaghib, High cycling stability of zinc-anode/conducting polymer rechargeable battery with non-aqueous electrolyte, *Journal of Power Sources*, 2014, **248**, 1099.
3. Y.F. Zhao, S.H. Si, C. Liao, A single flow zinc/polyaniline suspension rechargeable battery, *Journal of Power Sources*, 2013, **241**, 449.

KL11

Graphene Reinforced Polymer Nanocomposites

Chang-Sik Ha

Dept. of Polymer Science and Engineering, Pusan National University, Busan
46241, Korea
E-mail: cscha@pnu.edu

Graphene has extraordinary high electrical conductivity, thermal conductivity, and mechanical properties because of its two-dimensional honeycomb lattice structure. Graphene-based nanofillers are widely used to improve the mechanical and thermal properties of polymers because of the excellent physical properties and large surface area of graphene. In this presentation, therefore, I will talk on some examples of the graphene reinforced polymer nanocomposites that have been done in my laboratory for years.

For instance, aromatic polyimides (PIs) are important super-engineering plastics that have advanced technological applications in microelectronics, automobiles, and aircraft. They feature good inherent thermal stability, physical properties, flexibility, chemical resistance, and electronic properties. However, more enhancement of the properties of PIs is, however, frequently needed for further advanced applications. In this sense, recently, PI-based hybrid composites have attracted extensive research interest because of their excellent electronic and mechanical properties, such as high thermal stability, low dielectric constant, and good optical properties. In this talk, thus graphene reinforced PI nanocomposites will be introduced.

References:

1. D.G. Yoo, S.S. Park, C.W. Noh, I. Shin, K.H. Lim, J. Son, S. Ahn and C.S. Ha, *Polym. Int'l.*, 2019, DOI: 10.1002/pi.5836
2. K. M. Jeong, Y. Li, D.G. Yoo, N.K. Lee, H.G. Lee, S. Ando, and C.S. Ha, *Polym. Int'l.*, 2018, **67**, 588.

KL12

Tailored Wide-Bandgap Semiconductor Microcavity in Nanophotonics

Yinzhou Yan^{1,2,3}, Yijian Jiang^{1,2,3}

¹ Institute of Laser Engineering, Beijing University of Technology, Beijing 100124, China

² Beijing Engineering Research Center of Laser Technology, Beijing University of Technology, Beijing 100124, China

³ Key Laboratory of Trans-scale Laser Manufacturing, Ministry of Education, Beijing University of Technology, Beijing 100124, China

E-mail: yyan@bjut.edu.cn

Semiconductor microcavities have shown great promise as potential core component structures for micro-lasers, light-emitting diodes and photonic sensors due to their outstanding optoelectronic properties. Here the tailored wide-bandgap semiconductor, *i.e.* ultrathin-walled ZnO (UTW-ZnO) hexagonal microtube, are achieved by new-developed optical vapor supersaturated precipitation (OVSP). The growth mechanism is interpreted and the process parameters are optimized for time-saving fabrication. The dimensions of the UTW-ZnO microtube are >5 mm in length and ~50-200 μm in diameter with the wall thickness down to 500 nm. The UTW-ZnO microtube cavity supports multiple types of optical modes, demonstrating several applications, *i.e.* temperature-sensitive multicolor luminescence in the visible band from near-white to bluish-violet, ultralow-threshold UV WGM-lasing, and enhanced photocatalyst for on-chip degradation of organic dyes. Moreover, several techniques, *e.g.* the in-situ ion-doping, solid state reaction and UV laser nano-patterning, are employed in order to manipulate the electrical and optical properties of the microtube for improvement of performance. The present work provides new opportunities to design novel tailored wide-bandgap semiconductor devices for a variety of optoelectronic applications in nanophotonics.

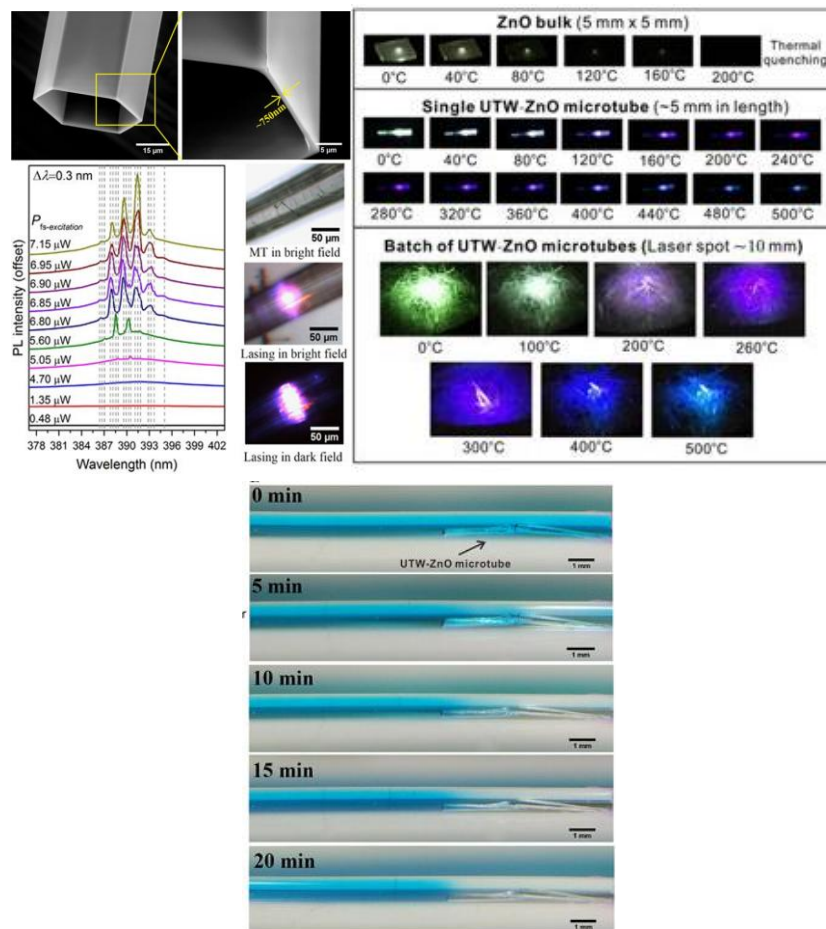


Figure 1. UTW-ZnO microtube cavity for UV micro-lasering, temperature-dependent multicolor luminescence and on-chip photodegradation.

References:

1. Q. Wang, Y. Yan*, *et al. NPG Asia Mater.*, 2017, **9**, 442.
2. Z. Huang, Y. Yan*, *et al. J. Alloys Compd.*, 2019, **789**, 841-851.
3. Q. Wang, Y. Yan*, *et al. J. Lumin.*, 2019, **208**, 238-244.
4. S. Hu, Y. Yan*, *et al. J. Cryst. Growth*, 2018, **498**, 25-34.

Invited Lecture

IL 1 ~ IL 17

IL1

**Metal-Organic Frameworks and Their Composites: Potential
Applications in Wastewater Treatment**

Chongchen Wang

Beijing University of Civil Engineering and Architecture, Beijing 102612, China

IL2

Biodegradable Polyester Based Porous Microspheres by RAFT Polymerization and UV Irradiation

Taeyoon Kim², Sorim Lee¹, Ildoo Chung¹

¹Department of Polymer Science and Engineering,
Pusan National University, Busan 46241, Korea

²Advanced Convergent Chemistry Division,
Advanced Industrial Chemical Research Center, Ulsan 44412, Korea

E-mail: idchung@pusan.ac.kr

Porous biodegradable microspheres were fabricated by successful RAFT polymerization of methyl vinyl ketone (MVK) onto polycaprolactone (PCL) and polylactide (PLA), which was first synthesized by ring opening polymerization of lactide followed by an oil/water emulsion-evaporation method, then finally photodegradation of PMVK blocks by UV irradiation. Macro-CTA (chain transfer agent) was synthesized by reacting carboxylic acid terminated CTA, S-1-dodecyl-S'-(α, α' -dimethyl- α'' -acetic acid) trithiocarbonate (DDMAT) with hydroxyl terminated polycaprolactone, which was then used for the synthesis of triblock copolymer with methyl vinyl ketone (MVK).

The synthesized block copolymers were characterized by FT-IR, ¹H NMR spectroscopies. Gel permeation chromatography (GPC) was used to evaluate the molecular weight and molecular weight distribution and monitored the photodegradability of the block copolymers. Although molecular weights of triblock copolymers decreased with UV irradiation time under two different conditions, solution and solid states, their degradation behaviors were slightly different depending on each condition.

For photodegradation by UV light under dried condition, the molecular weight of triblock copolymer was decreased gradually with UV irradiation time, reaching close to that of macro-CTA, meaning that 90% of PMVK block was photodegraded after 24 h of UV irradiation. On the other hand, photodegradation in THF solution showed slightly different behavior from that under dried condition. The molecular weight of triblock copolymer decreased even faster than that under dried conditions. More than 60% of PMVK block was photodegraded after 4 h of UV irradiation together with the production of low molecular weight degraded residues.

The morphology of microspheres was spherical with smooth surfaces before UV irradiation. However, those from PCL-PMVK and PCL-PLA-PMVK block

copolymers had rough surfaces and porous structures after UV irradiation due to the photodegradation of PMVK blocks as a porous template. The porosity and shape of the microspheres and shape of microspheres were dependent on the PMVK contents and size of microspheres.

IL3

Biomimetic Nanofibrils for Controlling and Stimulating Cellular Functions

*Wei Mao, Ji Un Shin, Ju Won Lee, Jae Keun Park, Vu Nguyen Oanh
Pham, Hyuk Sang Yoo*

Department of Biomedical Materials Engineering, College of Biomedical
Science

Kangwon National University, Chuncheon, Republic of Korea, 24341

E-mail: hsyoo@kangwon.ac.kr

Biomedical applications of electrospun nanofibrous meshes have been receive tremendous attentions because of their unique structures and versatilities as novel biomaterials. In the previous studies, we showed that neo-collagen and cytokeratin accumulation were significantly increased as well as the expression of the keratinocyte-specific markers at the re-epithelized tissue treated with therapeutic gene incorporated nanofibrous meshes, which consequently assisted wound recovery without phenotypic changes of the re-epithelized tissues. For the cell-directed association of nanofibrils, polymeric nanofibrils (NF) were fabricated by fragmentation of electrospun nanofibers and subsequent surface-decoration with poly (methacrylate) derivatives via ATRP. The decorated NFs showed higher degrees of protein sequestration and enhanced cell proliferation with free infiltration of cells, which leads to hydrogel-like behavior.

IL4

Self-Organizing Liquid-Crystalline Hybrid Nanoparticles

Kiyoshi Kanie

Institute of Multidisciplinary Research for Advanced Materials, Tohoku University, 2-1-1, Katahira, Aoba-ku, Sendai, 980-8577, Japan
E-mail: kanie@tohoku.ac.jp

Nanoparticle (NP)-based periodic structure formation has attracted a considerable attention in material science, because new synergistic functions could be derived from the periodic structure.¹ Among organic soft materials, liquid-crystalline (LC) organic dendron is one of the most representatives to form spherical dendrimer-like structures by the self-assembling property. Such spherical assembly spontaneously forms a self-organized periodical structure. Thus, we focused our attention on introduction of such self-organization ability into inorganic NPs. As dendrons, we synthesized phenetyl ether-type dendrons with an amino-group at the apex. These dendrons themselves show thermotropic LC phases. The dendrons are attached as the outer corona, through amidation, to the carboxylic groups at the surface of the inner aliphatic corona encapsulating the NP. Purpose-designed CO₂H-modified monodisperse gold and CdS NPs were synthesized in the presence of 12-dodecanethiol (DT) and 16-mercaptohexadecanoic acid (MHA). The dendron-modified gold NP showed an LC hexagonal columnar phase at 130 °C and formed a simple cubic (SC) LC phase at 150 °C. The result indicated that the dendron-modified gold NPs can be regarded as organic-inorganic hybrid dendrimers with thermotropic LC behaviour.² On the other hand, the dendron-modified CdS NPs also formed a thermotropic cubic LC phase with a novel, low-symmetry structure, space group P213 by annealing at 150 °C for 15 h. The cubic structure was retained at room temperature after cooling. In contrast, unannealed dendron-modified CdS NPs on glass substrate formed a disordered structure. In such a state, it showed strong photoluminescence (PL) when UV irradiated at 365 nm. However, PL was quenched when the dendron-modified CdS NPs formed the cubic phase after annealing at 150 °C followed by cooling. Such PL quenching behavior was totally reversible, and appears to be associated with the periodic structure of the dendron-modified CdS NPs (Figure 1).³ Such unusual PL behavior might be a powerful tool to develop future functional devices.

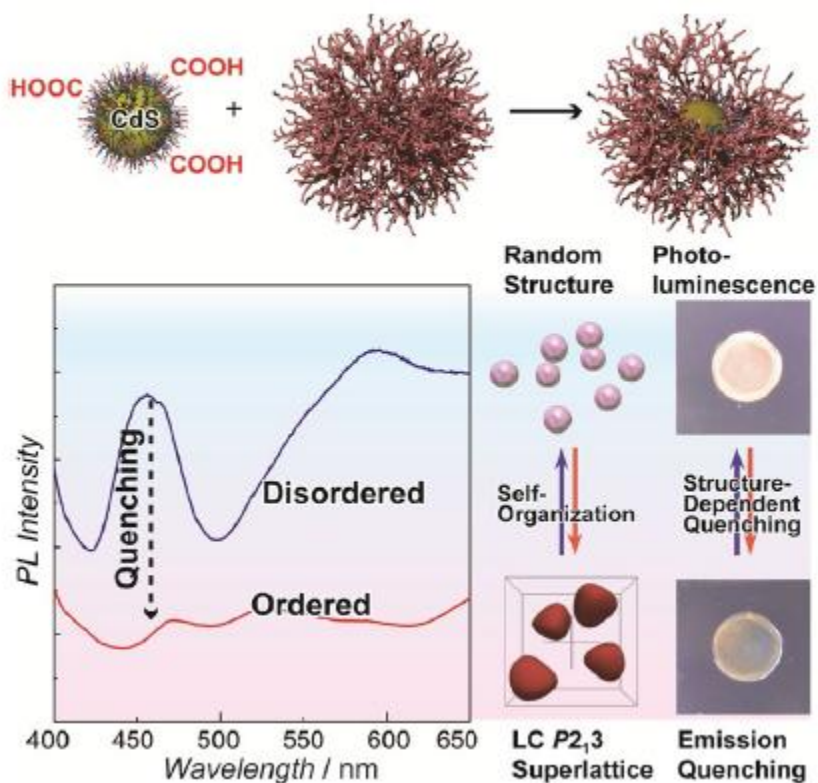


Figure 1. A schematic illustration of structure-dependent PL emission-quenching behavior of dendronized CdS NPs.

References:

1. K. Kanie, T. Sugimoto, *J. Am. Chem. Soc.*, 2003, **125**, 10518; K. Kanie, A. Muramatsu, *J. Am. Chem. Soc.*, 2005, **127**, 11578.
2. K. Kanie, M. Matsubara, X. Zeng, F. Liu, G. Ungar, H. Nakamura, A. Muramatsu, *J. Am. Chem. Soc.*, 2012, **134**, 808.
3. M. Matsubara, W. Stevenson, J. Yabuki, X. Zeng, H. Dong, K. Kojima, S. F. Chichibu, K. Tamada, A. Muramatsu, G. Ungar, K. Kanie, *Chem*, 2017, **2**, 860.

IL5

3D Porous Al Current Collector-Enhanced Graphene Supercapacitor

Zhoufei Yang, Jiarui Tian, Chaojie Cui, Weizhong Qian*

Department of Chemical Engineering, Tsinghua University, Beijing, 100084, China

E-mail: qianwz@tsinghua.edu.cn

Graphene, with high electrical conductivity, high surface area, exohedral surface and sufficient mesopore and high chemical stability, was proposed as an electrode of next generation EDLC supercapacitor with high energy density. Chemical vapour deposition method now offered graphene with high surface area, high yield, and high purity, making the fabrication of graphene-based supercapacitor more and more promising. However, low bulk density and large liquid intake of graphene bring unexpected great difficulties in fabricating an electrode sheet of graphene, with comparable property and performance to the conventional sheet of activated carbon with conventional processing method. This belongs to the important engineering of graphene, but is always neglected by scientists.

3D porous Al current collector was very light, highly conductive, highly chemical stable and, in theory, was very suitable for the use in supercapacitor. However, the fabrication of 3D porous Al current collector with high porosity and high tensile strength remained a great challenge for scientists and engineers in most of countries in the world. Here, we reported such a new progress as fabricating 3D porous Al current collector in large scale and reported the fabrication of graphene supercapacitor (100F-500F soft pack) with volumetric energy density 3-4 times that of AC-based device with similar weight. The result suggested the use of 3D porous Al collector would be a new direction in developing high performance supercapacitor.

Reference:

1. Cui CJ, Qian WZ*, et al. J. Am. Chem. Soc. 2014, 136, 2256–2259.
2. Tian JR, Qian WZ, et al. J. Mater. Chem. A, 2018, 6, 3593–3601.



Weizhong Qian
Professor
Dept. Chem. Eng.
Tsinghua University
Beijing, 100084, China

Research field: (1) Carbon nanomaterials and energy storage; (2) zeolite catalyst and reaction engineering. (3) Microgrid metal materials

IL6

High Speed Manufacturing Process of Carbon Fiber Reinforced Polymer Composites for Automotive Lightweight Applications

Dong Gi Seong

Department of Polymer Science and Engineering, Pusan National University,
63-2 Busandaehang-ro, Geumjeong-Gu, Busan 46241, Korea
E-mail: dgseong@pusan.ac.kr

As fuel economy regulations in the automotive industry become tighter, carbon fiber reinforced polymer composite parts and their processing are more attractive because the parts have lighter weight with better mechanical properties than steel parts while still maintain the durability and safety as the automotive parts. Automotive industry requires the mass production system of composite parts, for which cost reduction and high speed of manufacturing process are inevitable. The ideal cycle time for a production line would be between 3 and 7 min per part.

There are two kinds of approaches for high speed process of fiber reinforced composite products, which are liquid molding based process and compression molding based one¹⁻³. Even though some companies have already produced the composite carbody parts, there are still remained problems for applying to the mass production system of automotive parts. Engineering issues, formation of defects in the manufacturing processes, are described and the possible approaches for predicting and solving them are discussed in the study.

References:

1. R. Chaudhari, M. Karcher, P. Elsner, F. Henning, *Proceedings of ECCM-15*, Venice, Italy, 24-28 June 2012.
2. M. Baskarana, I. Ortiz de Mendibila, M. Sarrionandia, J. Aurrekoetxea, J. Acosta, U. Argarateb, D. Chicoc, *Proceedings of ECCM-16*, Seville, Spain, 22-26 June 2014.
3. J.A. Sherwood, K.A. Fetfatsidis, J.L. Gorczyca, L. Berger, Elsevier: New York, NY, USA, 2012; pp. 139–179.

The Long-Lasting Luminescence in Hybrid Materials

Dongpeng Yan*

Affiliation, Address, Country

College of Chemistry, Beijing Normal University, Beijing, China

E-mail: yandp@bnu.edu.cn

Long-lasting phosphorescence systems usually feature much prolonged lifetimes, and therefore the development of phosphorescent materials can not only supply new understanding on the relationship between structure and long-lived excitation-state, but also construct new types of long-afterglow (also known as long-lasting phosphorescence or persistent luminescence) materials. In this work, recent long-afterglow phosphorescent hybrid systems will be introduced, and their further applications in logic gate and smart materials will be discussed.¹⁻⁷

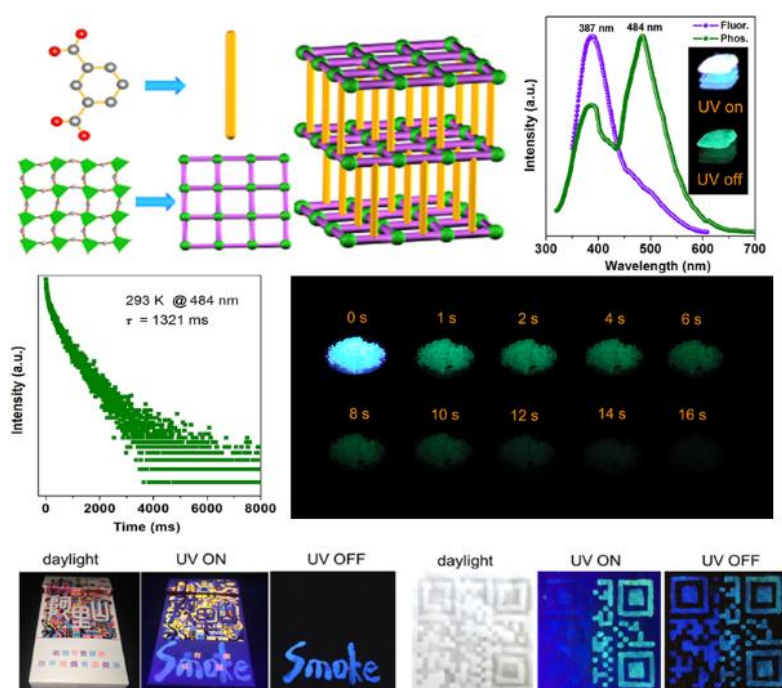


Fig. 1 The inorganic-organic hybrids with long-lasting phosphorescence.

References:

1. X. Yang and D. Yan, *Chem. Sci.* 2016, **7**, 4519; *Adv. Opt. Mater.* 2016, **4**, 897; *Chem. Commun.* 2017, **53**, 1801; *J. Mater. Chem. C* 2017, **5**, 7898.
2. R. Gao and D. Yan, *Chem. Sci.* 2017, **8**, 590; *Chem. Commun.* 2017, **53**, 5408; *Nano Res.*, 2017, **10**, 3606.
3. Y. Yang, K. Z. Wang, D. P. Yan. *ACS Appl. Mater. Interfaces* 2016, **8**, 15489; *ACS Appl. Mater. Interfaces* 2017, **9**, 17399; *Chem. Commun.* 2017, **53**, 7752.
4. X. Yang, X. Lin, Y. Zhao, Y. S. Zhao, D. Yan, *Angew. Chem. Int. Ed.* 2017, **56**, 7853.
5. X. Yang, X. Lin, Y. S. Zhao, D. Yan, *Chem. Eur. J.* 2018, **24**, 6484.
6. R. Gao, X. Mei, D. Yan, R. Liang, M. Wei, *Nat. Commun.* 2018, **9**, 2798.
7. B. Zhou and D. Yan, *Adv. Funct. Mater.* 2019, **29**, 1807599.

IL8

Black Phosphorus Enhanced Actuation in Nafion Based IPMC

*Shangzhou Liu, Ziqian YU, XiaoRui Wang, Huiqin Lian**

Beijing Key Lab of Special Elastomer Composite Materials, College of Materials Science and Engineering, Beijing Institute of Petrochemical Technology, Beijing 102617, China.

Abstract

Ionic polymer-Carbon nanotube composite (IPCC) actuators based on black phosphorus (BP)-Nafion composite membranes were fabricated. BP-Nafion composite was used as the ionic matrix and functional carbon nanotube (FCNT) as electrodes. The IPCC actuator exhibited a blocking force of 33.6 gfg^{-1} for 30s under an electrical field of 2 V, and the same behavior could be repeatedly played or hundreds of cycles. The introduction of BP into Nafion improved the mechanical properties, more importantly, the BP provides a wide range of channels for lithium insertion and extraction which restricts the back diffusion of cationic during action and thus enhanced the deformation of actuator without back-relaxation. In addition, layer crystal structure of BP protects the inter-lamellar liquid from evaporation thus ensured the durability.

Keywords: black phosphorus; back-relaxation; composite; durability

1. Introduction

Ionic polymer-metal composites (IPMC) based artificial muscles have attracted much attention in the field of robotic actuators, and dynamic sensors^[1-2] due to its characteristics of flexibility, lighter weight, biocompatibility, and a large displacement under low potential stimuli.^[3-6] IPMC is usually composed of ionic matrix and electrodes forming sandwich structure. The electromechanical response mechanism is that under an electric field, the hydrated metal cations in the ionic matrix membrane are driven toward the cathode, resulting in bending deformation of the membrane.^[7] However, several drawbacks limit its wide application in the fields of actuator and sensor. Firstly, IPMC shows poor durability due to evaporation of solvent in open air under electric field;^[8] second is the back relaxation under long-term actuation because of the back-diffusion of cationic clusters. In our group, it is found that layer structure of materials can protect the inter-lamellar liquid from evaporation because of its barrier property.^[8,9]

Black phosphorus (BP) is a layered material composed of individual stacking

*Corresponding author, Professor, E-mail; lianhuiqin@bipt.edu.cn

atomic layers by van der Waals interactions.^[10] It has attracted increasing interest because of its high carrier mobility, excellent current saturation characteristics and planar anisotropy, so it has a good application prospect in the fields of electronics and optoelectronics.^[11-15]

It is well known that BP has a large interlayer spacing which benefits its lithium intercalation properties. BP provides a wide range of channels for lithium insertion and extraction. The channel between the phosphors (0.52 nm) provides large space for storing Lithium ions.^[16] During the lithiated process, Lithium ions are inserted into the BP interlayer and react with BP to form new phases, leading to anisotropic lattice expansion and morphological evolution. The interaction between P and Li ions can be roughly described by the following formula: $x\text{Li}^+ + x\text{e}^{-1} + y\text{P} \rightarrow \text{Li}_x\text{P}_y \rightarrow \text{Li}_3\text{P}$. The mesophase Li_xP_y was detected as LiP_5 , Li_3P_7 , and LiP . With the process of lithium intercalation, the mesophase Li_xP_y finally turned into Li_3P . The special pleated layered structure of the BP along the (0k0) crystal plane provides a two-dimensional deintercalation channel for lithium ions. It has the largest lithium ion deintercalation channel along the a axis in the (020) crystal plane, and has the optimal lithium ion deintercalation channel in the (040) crystal plane a, c axis, so the lithium ion migration in BP is easier.^[17] Therefore, it is suitable using BP to attract lithium ion in IPCC to solve back relaxation problem.

In this paper, ionic polymer-carbon nanotube composite (IPCC) is fabricated. BP-Nafion composite is ionic matrix with FCNT as the electrodes. The layer structure of BP prevents solvent evaporation and BP attracts lithium ion in such a sandwich structure, thus provides the merit of low liquid evaporation and fixing lithium ion to restrict the back diffusion. Above mentioned drawbacks in conventional actuator could be overcome simultaneously. To the best of our knowledge, no similar work had reported on this aspect.

2. Experimental Section

2.1 Materials

Nafion suspension (5 wt% in alcohol) was purchased from DuPont. N,N-Dimethylformamide (DMF) were obtained from Aladin. BP was prepared according to the literature.^[18] BP powder was prepared by grinding BP in ethanol using a ball mill for 24 hours.

2.3. Preparation of BP-Nafion film

A certain amount of BP powder was dispersed in 20 g Nafion suspension with 20 mL DMF. The content of BP was 0.5, 1.0, 2.0, and 5.0 wt% based on neat Nafion, labeled 0.5, 1.0, 2.0, and 5.0% BP-Nafion composite, respectively. The dispersion was first sonicated for 30 minutes, then mechanically stirred at 70° C for 24 h. The obtained mixture was poured into a Teflon mold in an oven at 80° C for 24 h forming a film with a thickness about 0.2 mm.

2.4 Fabrication of Carbon Nanotube (CNT) electrodes

The CNTs were esterified according to references.^[19,20] The mixture of a weight ratio of esterified carbon nanotubes (FCNT): Nafion membrane with weight ratio of

1:2, and quantitative DMF was added to form FCNT-Nafion dispersions. The prepared BP-Nafion membrane was immersed in the above-mentioned proportioned FCNT-Nafion dispersion for 1 minute and then taken out and dried at 70°C for 5 minutes. The immersing and drying process was repeated 3 times to ensure that the FCNT-Nafion layer covered the surface of the film to form a sandwich structure, and pure Nafion was used as the substrate plating electrode as the control group. Finally, the sandwich membrane was soaked with 0.1 mol/L LiCl solution for 24 hours at room temperature. Thus prepared sandwich film was composed of a BP-Nafion matrix and a pair of CNT-Nafion electrodes and was denoted as BP-Nafion IPCC.

2.5. Physical/chemical characterization

X-ray diffraction (XRD) patterns were obtained on a Scintag PAD X diffractometer equipped with Cu K_{α} source, operated at 45 kV and 40 mA. Samples were scanned at 5°/min between 2θ of 2-30°.

Scanning electron microscopy (SEM) was performed with Tecnai T12 at 100 kV.

Water uptake ($W\%$) was calculated using Equation (1)

$$W\% = \frac{(W_1 - W_0)}{W_0} \quad (1)$$

W_1 and W_0 were the weights of the swollen and the dried samples, respectively. Anionic matrix film was first vacuum-dried at 80 °C for 24 h. Then the film was immersed in deionized water at ambient temperature for 24 h. Wiping off its surface water with, it was immediately weighed. The film was then dried at 60 °C under vacuum until the weight was constant.

The ion exchange capacity (IEC) was determined by placing the film in 1mol/L NaCl solution at 25°C for 24 h followed by titration using a 0.01 mol/L NaOH solution with phenolphthalein as an indicator. The ion exchange capacity (IEC, meq g^{-1}) was calculated based on the dry weight of the film.

Characterization of the actuation performance was carried out using a Labview-based system device. The IPCC was stimulated by programmable power, and the blocking force was measured using a balance.

3. Results and Discussion

3.1 Raman spectrum

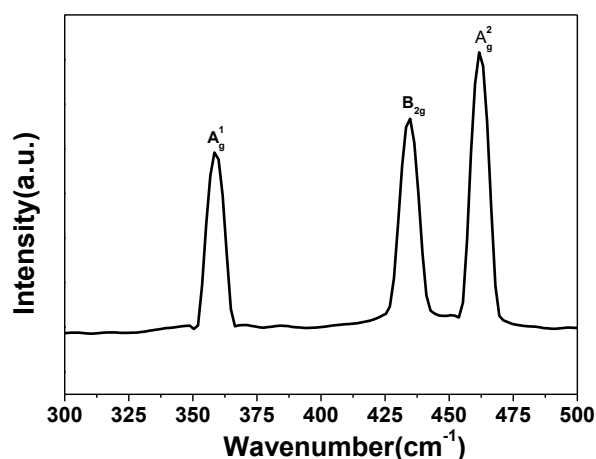


Figure. 1 Raman spectra of BP

The Raman spectroscopy of BP is shown in Fig.1. It presents three prominent peaks at 361, 436 and 463 cm⁻¹, which are attributed to the vibrations of the crystalline lattice of BP: A_g¹ (out-of-plane mode), B_{2g} (in-plane mode), and A_g² (in-plane mode) phonon modes, respectively, which agrees well with the earlier experiment.^[21-23]

3.2 SEM Observation

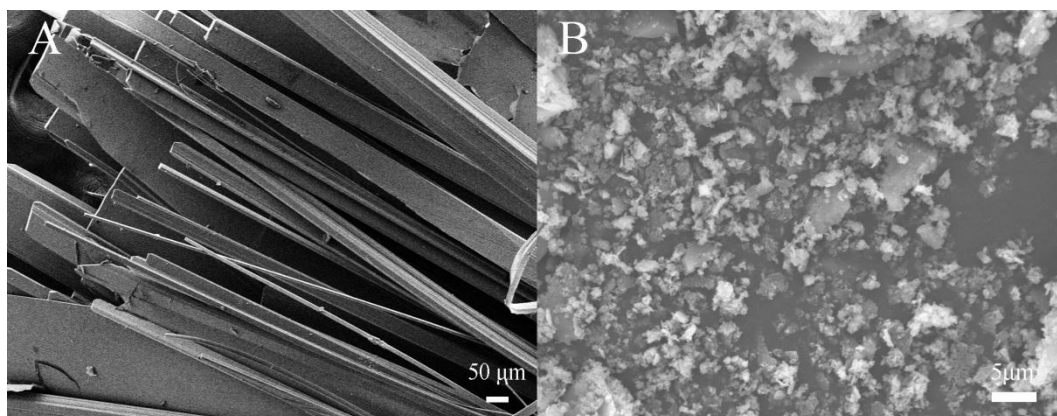


Figure 2 SEM images of (A) BP ribbons; (B) BP powder

Figure 2 shows SEM images of BP. The SEM image of BP ribbons (Fig.2A) indicate that these crystalline BPs have amicroribbon morphology with layered structure. Fig.2B shows the BP powder image, it can be seen that after the process of ball milling, the BP crystals are fully ground with size about 2 μm.

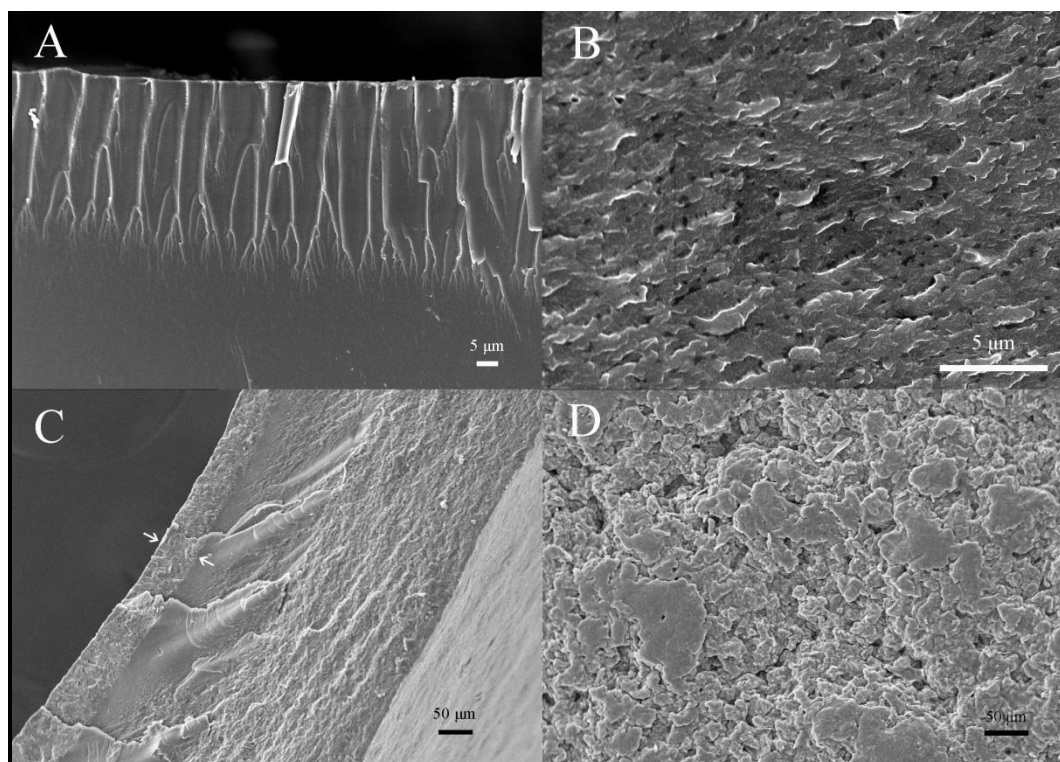


Figure 3 Cross-section SEM images of (A) neat Nafion; (B) 5% BP-Nafion composite film; (C) 5% BP-Nafion film with FCNT electrodes; (D) electrodes horizontal surface of neat Nafion;

Figure 3 shows SEM images of neat Nafion and 5% BP-Nafion composites. From Fig. 3A, the cross-sectional surface of neat Nafion is smooth, while that of 5% BP-Nafion composites was rather rough (Fig. 3B), indicating a rather strong intercalating force between BP and Nafion. From Fig. 3C it can be seen that the electrode layer and the matrix are completely combined to form a sandwich structure, and the thickness of the electrode layer is about 56 μm (as marked by the arrow). From Fig. 3D it is seen that the electrodes of FCNT uniformly covered in the matrix.

3.3 XRD Characterization

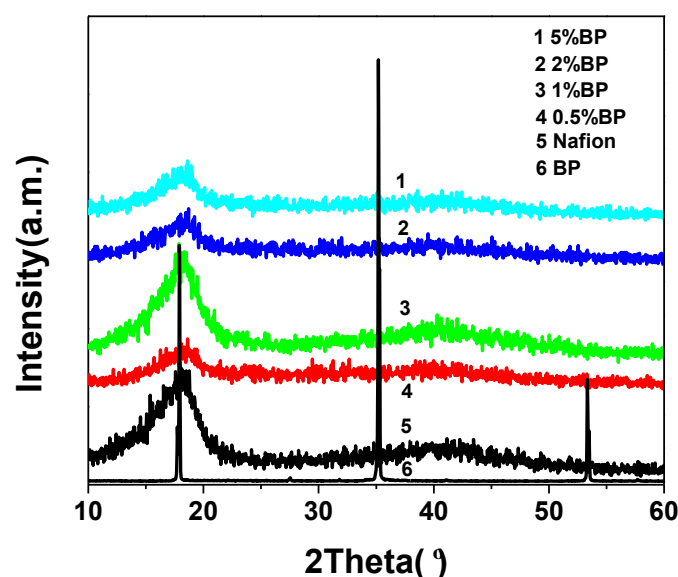


Figure 4 XRD patterns of BP-Nafion films, Nafion, and BP

Fig. 4 shows the XRD patterns of Nafion, BP, and BP-Nafion composite films with different doping levels of BP. From the curve of BP, only characteristic diffraction peaks can be observed on the (020), (040) and (060) planes, indicating that these BP crystals belong to an orthogonal system (space), which is similar to that reported in the literature.^[24,25] From the XRD patterns of different doping levels of the BP-Nafion membrane, it can be seen that the diffraction peaks assigned to the BP do not appear in all XRD patterns, indicating that the BP completely separates in the Nafion.

3.4 Physical properties

Table 1 Physical Properties of the neat Nafion and the BP-Nafion composite films

Film	Water uptake (%)	Swelling (%)	IEC (meq/g)	kt (s^{-1})
Pure Nafion	30.69	7.42	0.86	0.009
0.5%BP	29.63	6.76	0.80	0.005
1.0%BP	29.03	6.69	0.80	0.003
2.0%BP	28.90	6.27	0.79	0.003
5.0%BP	28.67	6.05	0.76	0.003

Table 1 shows the physical properties of the neat Nafion and BP-Nafion composite films in terms of water absorption, swelling property, and ion exchange capacity (IEC) for pure Nafion and BP-Nafion composite membranes. With the BP content increase, the water absorption of composite films decreases, the water uptake amount is from 30.69% of pure Nafion to 28.67% of 5% BP-Nafion composite film. It is noticed that the swelling property of BP-Nafion membrane shows a similar trend with that of water uptake, from a swelling rate of 7.42% of neat Nafion to 6.05% of 5%

BP-Nafion composite film. While the IEC value of BP-Nafion composite film decreases slightly with BP content increase, from 0.86 of neat Nafion to 0.76 of 5% BP-Nafion composite film. It properly due to the BP has no water absorption, which decrease the physical properties discussed above.

3.5 Actuation

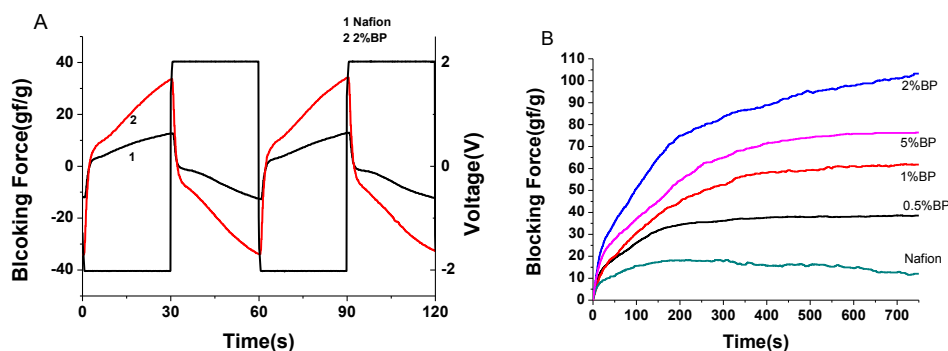


Figure 5 A) Generated blocking force under voltage 2 V with a period 30s and B) Blocking force relaxation as a function of BP content of the films

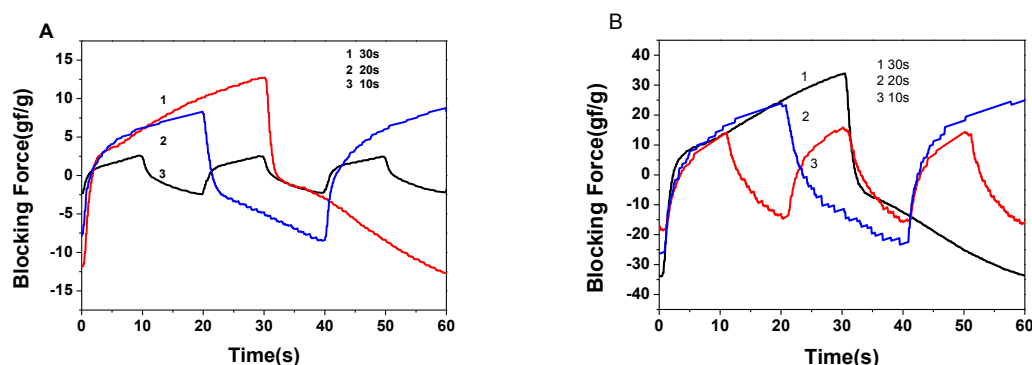


Figure 6 Generated blocking force of A) Nafion and B) 2%BP films under 2 V with periods of 10 s, 20 s, 30 s

The actuator performance of the Nafion and 2% BP-Nafion sandwich films was measured by a cantilevered actuation system.^[26] The blocking force was defined as the force produced by one gram of IPCC actuator under a certain electric field. Evaluated by attaching one end of the IPCC to the device and the other end to the balance. Figure 5A shows a pure Nafion and 2% BP-Nafion IPCC actuator at 2 V voltage with a period of 30 s. It can be seen that the highest value of 2% BP-Nafion IPCC is 33.6 gf g⁻¹, which is about 2.6 times that of pure Nafion, 12.6 gf g⁻¹. Obviously adding BP to the IPCC matrix can increase the motivation of IPCC.

According to the mechanism of IPMC actuation, the blocking force is generated by the migration of cation.^[8] However at a certain voltage, the hydrated cations in Nafion show reverse diffusion due to repulsion between ions and water permeation on the cathode side of the membrane. Fig. 5B shows the function of blocking force and time, for pure Nafion based IPCC, the blocking force first increases with time

increase, arrives the highest point at 208 s with value of 18 gf g^{-1} , then decreases with the time going on. This is because the reverse diffusion of cation in Nafion based IPCC. Amazingly, the phenomenon does not appear in BP-Nafion composite based IPCC. The blocking force of composite IPCC increase with time increase, the value does not decrease during test time. At the same time, it is noticed that the value of the blocking force of composite based IPCC increase with the content of BP increase, to the highest value with BP doping level of 2%. Liu^[16] reported that BP can attract Lithium ions. We propose that BP attracts the Lithium ion in this IPCC system, which restricts cation diffusion, thus an increasing blocking force without back-relaxation. However, when BP doping level is 5%, the blocking force of IPCC decreases comparing with that of BP doping level of 2%. We propose that rigid BP does not show the deformation, relative high BP doping level limits the deformation of composite based IPCC thus decrease of blocking force.

Figure 6 shows the tendency of the blocking force and time of the IPMC at different periods when the driving voltage is 2 V. The blocking force of pure Nafion increase with the period time increase, from 2.5 gf g^{-1} to 12.4 gf g^{-1} (Fig.6A). From Fig. 6B, the blocking force of 2% BP-Nafion film has the similar tendency with that of pure Nafion. Moreover, the blocking force value of composite is much larger than that of pure Nafion. The highest value is 33.6 gf g^{-1} of 2% BP-Nafion, 2.7 times of that of pure Nafion.

Based on the curve of the blocking force vs. stimulated time (Fig.6B), the relationship between $\log[(B_H - B_0)/(B_H - B_t)]$ and t could be obtained, as shown in Figure 7A. It is found that at the initial stage, the response performance coincided with first-order kinetics equation, i.e. $\log[(B_H - B_0)/(B_H - B_t)] = k_t \cdot t$. Where B_H is the highest value of blocking force under the test condition, B_0 is the initial value and B_t is the value at time t . k_t is defined as the actuation rate constant.^[27] The values for various BP content are listed in Table 1. The fastest one ($k_t = 0.009 \text{ s}^{-1}$) is provided by neat Nafion. While, BP-Nafion composite films give the lower k_t . It maybe that BP blocked the movement of ions, thus delays the response of composite film.

Figure.7B shows the durability of a pure Nafion membrane and a BP-Nafion membrane. It can be seen that as time increases, the difference between the highest and lowest blocking forces of the BP-Nafion film is not significantly reduced. However, the barrier force difference of the pure Nafion membrane gradually decreases with time. We purpose that BP protects the inter-lamellar liquid from evaporation thus ensured the durability.

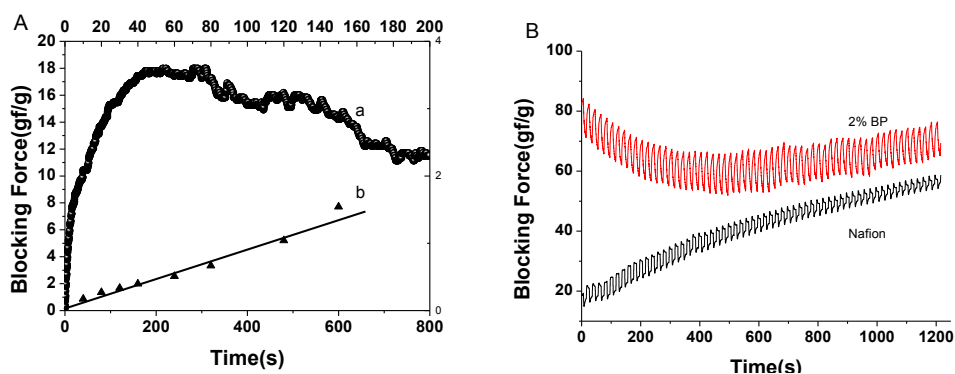


Figure 7(A) Variation of the blocking force with time (curve a) and the first-order plot (curve b) of Nafion under 2 V field; (B) Durability of Nafion and 2% BP sandwich film.

4. Conclusions

In this paper, a novel IPCC actuator is fabricated. BP is added as a filler to Nafion forming a composite matrix with CNT as electrode. The BP-Nafion based IPCC shows excellent actuation performance in terms of blocking force, durability and back relaxation. The improvement of properties could be attributed to the barrier property as well as the attracting ability of BP to lithium ion.

Acknowledgements

This work was supported by the Natural Science Foundation of China (NSFC, Nos. 51063009, 21271031, 51203012), the Beijing Natural Science Foundation of China (Nos. 2132009, 2122015) and the project about the promotion of innovation in Beijing universities funded by Beijing Municipal commission of education of China.

Undergraduate Research Training Program of Beijing Institute of Petrochemical Technology (No. 2018J00022, 2018J00023)

References

- [1] Shahinpoor M (2003) Ionic polymer-conductor composites as biomimetic sensors, robotic actuators and artificial muscles—a review. *Electrochim Acta* 48(14–16):2343–2353
- [2] Akle BJ, Bennett MD, Leo DJ (2006) High-strain ionomeric–ionic liquid electroactive actuators. *Sens Actuators A* 126(1):173–181
- [3] M. Shahinpoor, K.J. Kim, Ionic polymer-metal composites I. Fundamentals, *Smart Mater. Struct.* 10 (2001) 819–833.
- [4] S.N. Nasser, J.Y. Li, Electromechanical response of ionic polymer–metal composites, *J. Appl. Phys.* 87 (2000) 3321–3331.
- [5] B.J. Akle, M.D. Bennett, D.J. Leo, High-strain ionomeric-ionic liquid electroactive actuators, *Sens. Actuator A: Phys.* 126 (2006) 173–181.
- [6] J.H. Jung, S. Vadahanambi, I.K. Oh, Electro-active nano-composite actuator based on Nafion, *Compos. Sci. Technol.* 70 (2010) 584–592.
- [7] Lian H, Qian W, Estevez L, et al. Enhanced actuation in functionalized carbon nanotube–Nafion composites[J]. *Sensors & Actuators B Chemical*, 2011, 156(1):187-193.
- [8] Hu Y, Lian H, Zu L, et al. Durable electromechanical actuator based on graphene oxide with in situ reduced graphene oxide electrodes[J]. *Journal of Materials Science*, 2016, 51(3):1376-1381.
- [9] Lian Y, Liu Y, Jiang T, et al. Enhanced Electromechanical Performance of Graphite Oxide-Nafion Nanocomposite Actuator[J]. *Journal of Physical Chemistry C*, 2010, 114(21):9659-9663.
- [10] Zhao Y, Chen Y, Zhang Y H, et al. Recent advance in black phosphorus: Properties and applications[J]. *Materials Chemistry & Physics*, 2017, 189:215-229.

- [11] ZHANG X, XIE H M, LIU Z D, et al. Black phosphorus quantum dots[J]. *Angewandte Chemie international edition*, 2015, 54 (12) :3653-3657.
- [12] ENGEL M, STEINER M, AVOURIS P. Black phosphorus photodetector for multispectral, high-resolution imaging[J]. *Nano letters*, 2014, 14 (11) :6414-6417.
- [13] VITI L, HU J, COQUILLAT D, et al. Black phosphorus terahertz photodetectors[J]. *Advanced materials*, 2015, 27 (37) :5567-5572.
- [14] DAI J, ZENG XC. Bilayer phosphorene: effect of stacking order on bandgap and its potential applications in thin-film solar cells[J]. *The journal of physical chemistry letters*, 2014, 5 (7) : 1289-1293.
- [15] KANG J, WOOD J D, WELLS S A, et al. Solvent exfoliation of electronic-grade, two-dimensional black phosphorus[J]. *ACS Nano*, 2015, 9 (4) : 3596-3604.
- [16] H. Liu, L. Tao, Y. Zhang, C. Xie, P. Zhou, H. Liu, R. Chen, S. Wang, *ACS Appl. Mater. Interfaces* 2017, 9, 36849.
- [17] Sun L Q, Li M J, Sun K, et al. Electrochemical Activity of Black Phosphorus as an Anode Material for Lithium-Ion Batteries[J]. *Journal of Physical Chemistry C*, 2012, 116(28):14772–14779.
- [18] Li S, Liu X, Fan X, et al. New strategy for black phosphorus crystal growth through ternary clathrate[J]. *Crystal Growth & Design*, 2017, 17(12).
- [19] G.W. Lee, S. Kumar, Dispersion of nitric acid-treated SWNTs in organic solvents and solvent mixtures, *J. Phys. Chem. B* 109 (2005) 17128–17133.
- [20] J.W. Lee, E.J. Park, J. Choi, J.H. Hong, S.E. Shim, Polyurethane/PEG-modified MWCNT composite film for the chemical vapor sensor application, *Synth. Met.* 160 (2010) 566–574.
- [21] Sugai S, Shirovani I. Raman and infrared reflection spectroscopy in black phosphorus. *Solid State Commun*, 1985, 53: 753-755
- [22] Fei R, Yang L. Lattice vibrational modes and Raman scattering spectra of strained phosphorene. *Appl Phys Lett*, 2014, 105: 083120
- [23] Castellanos-Gomez A, Vicarelli L, Prada E, et al. Isolation and characterization of few-layer black phosphorus. *2D Mater*, 2014, 1:025001
- [24] Lange S, Schmidt P, Nilges T. Au₃SnP₇@black phosphorus: an easy access to black phosphorus. *Inorg Chem*, 2007, 46: 4028-4035
- [25] Zhang CD, Lian JC, Yi W, et al. Surface structures of black phosphorus investigated with scanning tunneling microscopy. *J Phys Chem C*, 2009, 113: 18823-18826
- [26] Y. Lian, Y. Liu, T. Jiang, J. Shu, H. Lian and M. Cao, *J. Phys. Chem. C*, 2010, 114, 9659–9663
- [27] Zu L, Li Y, Lian H, et al. The Enhancement Effect of Mesoporous Graphene on Actuation of Nafion - Based IPCC[J]. *Macromolecular Materials & Engineering*, 2016, 301(9):1076-1083.

IL9

Positive and Negative Electrostriction Effect of Dielectric Polyurethane Elastomers

*Yongri Liang**, Dong Xiang, and Jingjing He

College of Materials Science and Engineering, Beijing Institute of Petrochemical Technology, Beijing 102617, P. R. China
E-mail: liangyr@bipt.edu.cn

Dielectric elastomers (DEs) which is one of electroactive polymer (EAP) have attracted much interest due to their applications as fast, lightweight, and large-displacement actuators. Polyurethane elastomer (PUE) is one kind of promising DE materials due to their great breakdown strength, easy processability, recyclability, larger force output and good mechanical properties. In the DEs, external electric field generated Maxwell stress and electrostriction effect can act as driving forces to actuate DE. The Maxwell stress is generated by the columbic force from dielectric inhomogeneity. The Maxwell stress can account for voltage-induced deformation only for a very special type of materials, the ideal dielectric elastomers, where the permittivity is deformation-independent. Whereas, the electrostriction effect is known as direct coupling between the polarization and mechanical response in the material. Since the PUEs have microphase separated structure, the electric field induced actuation forces are contributed from both Maxwell stress and electrostriction¹⁻⁴. In this work, we will report the microstructure dependent electrostriction effect of PUEs and poly(urethane-urea) elastomers (PUUEs) in detail. We found that the electrostriction effect can take the important role in the final actuation strain of dielectric PUEs and PUUEs and the direction of electrostriction effect are strongly related to the microdomains orientation of dielectric PUEs and PUUEs along the electric field direction.

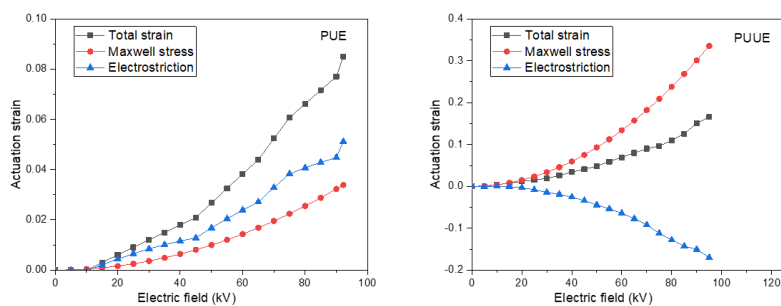


Fig. 1 Maxwell stress and electrostriction of PDCP

References:

1. Chen, G.; Liang, Y.; Xiang, D.; Wen, S.; Liu, L., *J Mater Sci* **2017**, *52* (17), 10321-10330
2. Xiang, D.; Liu, L.; Liang, Y., *Polymer* **2017**, *132*, 180-187
3. Xiang, D.; Liu, M.; Chen, G.; Zhang, T.; Liu, L.; Liang, Y., *RSC Advances* **2017**, *7* (88), 55610-55619
4. Xiang, D.; He, J.; Cui, T.; Liu, L.; Shi, Q. S.; Ma, L. C.; Liang, Y., *Macromolecules* **2018**, *51* (16), 6369-6379

IL10

Protection of Metals by Multifunctional Coatings on the Basis of PEO-Layers

*Vladimir Egorkin, Igor Vyaliy, Andrey Gnedenkov, Dmitry Mashtalyar,
Sergey Sinebryukhov, Sergey Gnedenkov*

Institute of Chemistry Far Eastern Branch of the Russian Academy of
Sciences,
159 Pr. 100-letiya Vladivostoku, Vladivostok, Russia
E-mail: egorkin@ich.dvo.ru

Operation of light metals under heavy loads, high speeds, in hostile environments and extreme service conditions leads to a tightening of the requirements for the structural materials. In this regard, the development of surface modification technologies of metallic parts – is an actual and prospective challenge. One of the rapidly developing technologies in the field of surface modification – is the plasma electrolytic oxidation (PEO).

PEO method allows achieving a high level of the insulating, anti-friction, anti-corrosion properties, magnetic activity, heat and wear resistances of the surface of the processed metals. Nanoscale materials might be added to the composition of the surface layers, which can significantly extend the range of practical applications due to the appearance of additional properties: antiscale, hydrophobic, superhydrophobic etc.

In this regard, superdispersed polytetrafluoroethylene and its low-molecular fractions are of considerable interest that is caused primarily by the variety of properties of these fluoropolymers and their practical significance.

Nanostructured powders of aluminum, silicon, zirconium and cobalt oxides were used as inorganic materials in the synthesis of new composite layers.

Incorporation of the metal oxide nanoparticles into the coating's composition provides formation of the defect-free coatings having better protective properties than the initial PEO layer. Developed approaches open up broad prospects for the formation of nanostructured protective coatings on the contacting surfaces of critical parts, components, mechanisms and machines.

Such nanomodified layers provide the required functional and operational characteristics to the general and special-purpose components operated in extreme conditions.

Acknowledgements: The work was supported by FEB RAS Program “Far East” (project No.18-3-002). XRD data were collected within the frames of the State Order of the Institute of Chemistry FEB RAS, project no. 265-2019-0001.

IL11

Tough Hydrogels Based on a Facile Strategy: Micellar Polymerization Followed by Solution Polymerization

Yang Liu, Yu Zhao, Bing Hu Xia, Run Jun Wang*

Beijing Key Lab of Special Elastomer Composite Materials
College of Materials Science and Engineering
Beijing Institute of Petrochemical Technology
Beijing 102617, P. R. China
E-mail: yang.liu@bipt.edu.cn

How to prepare a hydrogel with high strength and excellent tearing fracture energy is a problem faced by researchers. Here, tough and tear-resistant double-network hydrogels (Cx-SMy gels) are successfully prepared via a facile strategy: micellar polymerization followed by solution polymerization.

The strength and fracture energy of these hydrogels are up to 13 MPa and 26500 J/m², respectively, which are attributed to the synergy of quatra-crosslinking interactions inside the double-network. The quatra-crosslinking interactions include hydrophobic interaction, crystallization, electrostatic attraction, and hydrogen bonding. Moreover, it is confirmed that the facile strategy is a general way to prepare tough hydrogels by using electrolytic monomers and hydrophobic acrylates.

References:

1. Yu Zhao, Bing Hu Xia, Lei Wang, *Macromol. Mater. Eng.* 2018, 1700527
2. J. P. Gong, Y. Katsuyama, T. Kurokawa, Y. Osada, *Adv. Mater.* 2003, 15, 1155.
3. U. Gulyuz, O. Okay, *Macromolecules* 2014, 47, 6889.

IL12

Transition Metal Oxide-Supported Bimetallic Catalysts with High Performance for VOCs Oxidation

YuxiLiu*

College of Environmental and Energy Engineering, Beijing University of Technology, Beijing, China
E-mail: yxliu@bjut.edu.cn

Catalytic oxidation is one of the most effective pathways to eliminate volatile organic compounds, in which the key issue is the availability of high-performance catalysts. In this work, we report the preparation of PdGa/Al₂O₃¹, AuPdCo_x/3DOM Co₃O₄², and AuPdFe_x/3DOM Mn₂O₃³ and their catalytic performance for methane or *o*-xylene oxidation.

TEM results reveal that all of the samples possessed a high-quality 3DOM and 3D ordered mesoporous architecture, and their average pore sizes were 120-190 and 3-7 nm, respectively. The metal alloy nanoparticles (NPs) with a size of 2-5 nm were highly dispersed on the surface of the porous support. The Pd-GaO_x/Al₂O₃ sample performed the best for methane oxidation, showing the $T_{50\%}$ and $T_{90\%}$ of 336 and 372 °C at a space velocity of 80,000 mL/(g h). The 1.94Au-Pd-0.21Co/3DOM Mn₂O₃ and 1.94Au-Pd-0.22Fe/3DOM Mn₂O₃ samples performed the best for methane and *o*-xylene oxidation, respectively. Methane oxidation rate at 340 °C (339.0×10^{-6} mol/(g_{Pd} s)) over 1.94Au-Pd-0.21Co/3DOM Mn₂O₃ was three times higher than that (93.8×10^{-6} mol/(g_{Pd} s)) over 1.97Au-Pd/3DOM Mn₂O₃, and *o*-xylene reaction rate at 140 °C ($2.59 \mu\text{mol}/(\text{g}_{\text{Noble metal}} \text{ s})$) over 1.94Au-Pd-0.22Fe/3DOM Mn₂O₃ was two times higher than that ($0.93 \mu\text{mol}/(\text{g}_{\text{Noble metal}} \text{ s})$) over 1.97Au-Pd/3DOM Mn₂O₃.

It is concluded that excellent performance of the catalysts is associated with their high surface areas, high adsorbed oxygen species, low-temperature reducibility, strong interaction between noble metal alloy and support as well as highly dispersed noble metal NPs and unique porous structures.

References:

1. Z. Q. Hou, Y. X. Liu, J. G. Deng, Y. Lu, S. H. Xie, X. Z. Fang, and H. X. Dai, *ChemCatChem*, 2018, **10**, 5637.
2. S. H. Xie, Y. X. Liu, J. G. Deng, S. M. Zang, Z. H. Zhang, H. Arandiyani, and H. X. Dai, *Environ. Sci. Tech.*, 2017, **51**, 2271.
3. S. H. Xie, Y. X. Liu, J. G. Deng, X. T. Zhao, J. Yang, K. F. Zhang, Z. Han, H. Arandiyani, and H. X. Dai, *Appl. Catal. B*, 2017, **206**, 221.

IL13

From Binary to Ternary Systems of Partly Miscible Metals: in Search of an Optimal Ratio

*Aleksey Vedyagin¹, Yury Shubin², Pavel Plyusnin²,
Roman Kenzhin¹, and Vladimir Stoyanovskii¹*

¹Boriskov Institute of Catalysis SB RAS, pr. Lavrentieva 5,
630090 Novosibirsk, Russian Federation

²Nikolaev Institute of Inorganic Chemistry SB RAS, pr. Lavrentieva 3,
630090 Novosibirsk, Russian Federation

E-mail: vedyagin@catalysis.ru

In the modern materials science and nanotechnology, partly miscible and immiscible metals attract a special interest due to a wide range of novel unique properties. Such metals being alloyed together represent thermodynamically unfavorable state that complicates the preparation technique. In order to bring them together, a “single-source precursor” concept looks more promising. As we have reported recently¹⁻³, this approach can be efficiently applied for obtaining the Au-Pt, Pd-Ru and Pd-Rh binary systems.

Depending on the nature of metals and the phase diagram of their miscibility, the resulting bulk alloys can be metastable or instable. In terms of practical interest, these systems are more attractive being supported on various carriers. All this additionally complicates the situation. The thermal behavior of the supported alloyed nanoparticles can differ significantly from that for the bulk ones. Thus, the most of the bulk systems consisting of immiscible (partly miscible) metals being annealed at elevated temperatures undergo delamination or decomposition with formation of the individual metallic phases or thermodynamically favorable alloys, according to the corresponding phase diagram. When the alloyed nanoparticles of the same composition are distributed over the support's surface, an interaction with the support starts to contribute to the overall stability of the system. For example, as it was found for alumina-supported Au-Pt system, platinum can be strongly anchored to the support's surface, thus preventing the surface migration of the nanoparticles followed by their agglomeration and segregation. At the same time, high-temperature aging of such system at 600 °C and above results in redistribution of metals within each nanoparticle and formation of quite stable structures of core-shell type. Appositely, the Pd-Rh binary system was proven to be stable up to 1000 °C showing no segregation or redistribution of the

components². So, it was chosen for further studies, which were aimed as a step forward towards the ternary Pt-Pd-Rh composition. The effects of the metal ratio within this system will be discussed in detail.

This study was supported by the Russian Science Foundation (grant number 16-13-10192).

References:

1. Y.V. Shubin, A.A. Vedyagin, P.E. Plyusnin, A.K. Kirilovich, R.M. Kenzhin, V.O. Stoyanovskii, S.V. Korenev, *J. Alloys and Compounds*, 2018, **740**, 935.
2. A.A. Vedyagin, Y.V. Shubin, R.M. Kenzhin, P.E. Plyusnin, V.O. Stoyanovskii, A.M. Volodin, *Topics in Catalysis*, 2019, **62**, 305.
3. G.A. Kostin, P.E. Plyusnin, E.Y. Filatov, N.V. Kuratieva, A.A. Vedyagin, D.B. Kal'nyi, *Polyhedron*, 2019, **159**, 217.

IL14

Poly(dichlorophosphazene) as a Precursor for Polyphosphazenes: Synthesis and Stabilization

*Shuangkun Zhang, Wei Liu, Hanlin Ma, Zhanpeng Wu**

Key Laboratory of Carbon Fiber and Functional Polymers (Beijing University of Chemical Technology), Ministry of Education, Beijing 100029, China.

E-mail: wuzp@mail.buct.edu.cn

The polyphosphazenes, with a backbone of alternating phosphorus and nitrogen atoms and two substituents at each phosphorus, are the most versatile class of inorganic polymers. Polyphosphazene materials possess various physical and chemical properties for many potential applications due to their diverse substituent side groups. And some linear polyphosphazenes are commercially available and the development of the polymers with unique performance will surely continue. The chemical and physical properties of polyphosphazenes are greatly influenced by the nature of the side groups. And most of linear polyphosphazenes are derived from a precursor, namely poly(dichlorophosphazene), PDCP, through substitution reactions. The conventional synthesis of PDCP has been carried out via ring-opening polymerization (ROP) of hexachlorocyclophosphazene (HCCP) in the presence of catalysts. However, the ROP is rather complicated and somewhat unpredictable due to the lack of complete understanding and easy control during the polymerization processes. Herein, recent progress of controlling synthesis of PDCP and several derived polyphosphazenes containing various reactive side groups such as amino, hydroxyl or carboxyl groups will be introduced¹⁻⁶.

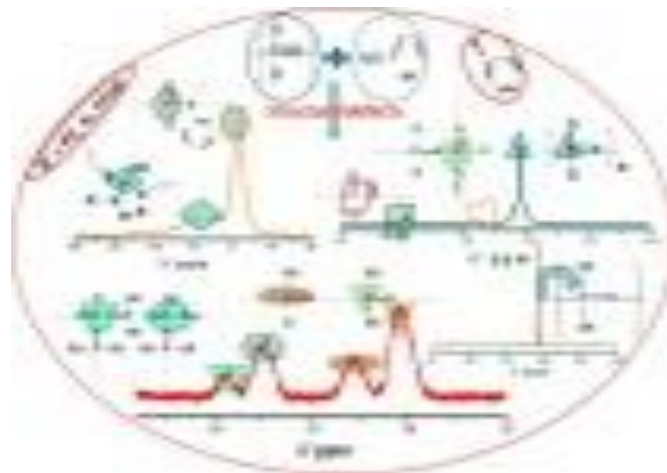


Fig. 1 Proposed reaction mechanism of the polymerization of PDCP

References:

1. S. Zhang, S. Ali, Z. Wu, et al. *J. Mol. Liq.* 2017, 225, 536.
2. S. Zhang, S. Ali, Z. Wu, et al. *J. Phys. Chem. B* 2016, 120, 11307.
3. W. Zou, S. Zhang, Z. Wu, et al. *Compos. Part A-Appl. S* 2019, 119, 145.
4. W. Liu, S. Zhang, Z. Wu, et al. *Carbon* 2018, 129, 420.
5. S. Zhang, J. Wang, Z. Wu, et al. *High Perform. Polym.* 2017, 29, 450.
6. W. Liu, S. Zhang, Z. Qiao, et al. *Colloid Surface A* 2018, 541, 17.

IL15

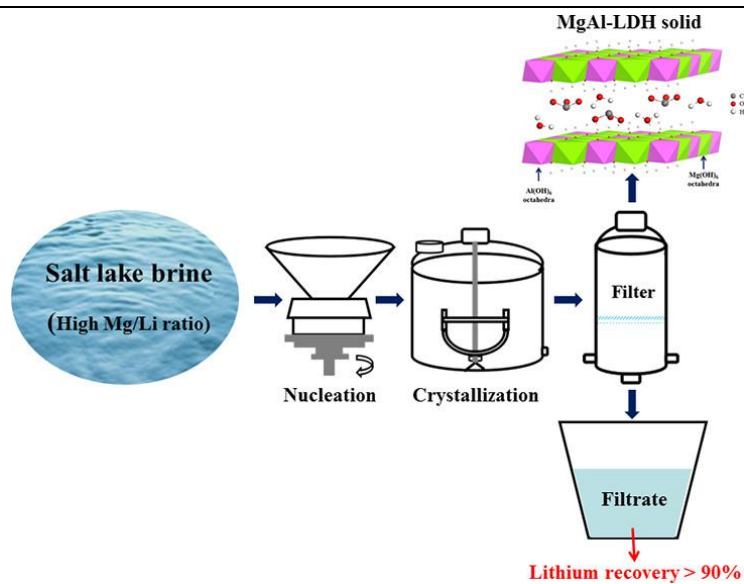
Efficient Separation of Magnesium and Lithium from Salt Lake Brine via Ion Imprinted Layered Double Hydroxide Materials

Ying Sun, Xu Xiang, Xue Duan

State Key Laboratory of Chemical Resource Engineering, Beijing University of Chemical Technology, Beijing 100029, China

E-mail: xiangxu@mail.buct.edu.cn

High Mg/Li ratio and high magnesium content make the extraction of lithium from salt lake brine face enormous challenges in the Qaidam Basin, China. Magnesium ion and lithium ion have similar radius and chemical properties, which make it difficult to separate magnesium and lithium ions. The layered double hydroxides (LDHs) is a kind of intercalation material. Because of flexible composition and structure, a large class of functional materials are formed. According to the deformability criterion of lamellar metal-oxygen (MO_6) octahedral in LDHs, we proposed a new process with reaction-coupled separation technology. The Mg^{2+} were almost completely entered into solid phase to form stable MgAl-LDHs by co-precipitation while Li^+ still remain in the solution. The mass ratio of Mg/Li in the solution decreased significantly from 12.66 to 0.08, and the lithium extraction is above 90%^{1,2}. Further, Na/Li separation was carried out from high Na/Li ratio brine (Na/Li=48.7, w/w) after separation of magnesium and lithium. The Li^+ can selectively enter the ordered vacancies within the framework of $\text{Al}(\text{OH})_3$, in which LiAl-LDHs form. The lithium extraction reaches 96%^{3,4}. The reaction-coupled separation technology provides a new idea for the extraction of lithium resources from salt lake brine and high valued utilization of magnesium.



References:

1. X. Guo, S. Hu, C. Wang, H. Duan, X. Xiang, *Ind Eng Chem Res*, 2018, **57**, 6618-6626.
2. S. Hu, Y. Sun, M. Pu, R. Yun, X. Xiang, *Sep Purif Technol*, 2019, **229**, 115813.
3. Y. Sun, X. Guo, S. Hu, X. Xiang, *J Energ Chem*, 2019, **34**, 80-87.
4. Y. Sun, R. Yun, Y. Zang, M. Pu, X. Xiang, *Materials*, 2019, **12**, 1968.

IL16

Characteristics and Mechanism of Cationic Polymerization in Aqueous Media Initiated by Cumyl Alcohol/ $B(C_6F_5)_3$

Shichao You^{1,2}, Jinhao Zhang^{1,2}, Wenli Guo^{1,2}, Yibo Wu^{1,2*}

1. Department of Materials Science and Engineering, Beijing Institute of Petrochemical Technology, Beijing 102617, China;
2. Beijing Key Lab of Special Elastomeric Composite Materials, Beijing 102617, China

Abstract. Aqueous cationic polymerizations of styrene and vinyl ethers were performed for the first time by a CumOH/ $B(C_6F_5)_3$ /Et₂O initiating system in an air atmosphere and alcohols as an initiator in a reproducible manner. Through the careful design of experimental conditions (adding initiator, co-solvents, and surfactant or decreasing the reaction temperature), and the polymerization characteristics were systematically tested and compared in the suspension and emulsion. The significant difference with traditional cationic polymerization is that the polymerization rate in aqueous media using $B(C_6F_5)_3$ /Et₂O as a co-initiator decreases when the temperature is lowered, this result was opposite to that in traditional cationic polymerizations. The polymerization sites are located on the monomer/water surface.

Keywords: cationic polymerization; aqueous media; styrene; $B(C_6F_5)_3$; suspension polymerization; emulsion polymerization;

1. Introduction

Traditional cationic polymerizations techniques are necessary to conduct polymerization under strictly anhydrous conditions and low-temperature circumstance with high energy consumption. Most conventional Lewis acids (LAs) are decomposed in the presence of excess of water toward LA. Chlorinated solvents typically used in cationic polymerization are toxic, and their use should be avoided. In recent years, considerable efforts have been made on the development of alternative, mild, and environmentally friendly polymerization conditions for the cationic polymerization of vinyl monomers using various reaction media, such as ionic liquids, supercritical carbon dioxide, or less-toxic organic solvents (e.g., n-hexane). Alternatively, cationic polymerization in aqueous media has recently emerged as a new and attractive process, because reactions are done at room temperature and in water, which is the cheapest non-toxic reaction medium available. This type of polymerization is also the important direction of development for the present cationic polymerization industry.

The main objective of the present work is to study the characteristics of styrene and vinyl ethers cationic polymerization in aqueous emulsion and suspension. Elementary reactions and polymerization mechanism of styrene cationic polymerization were systematically investigated via molecular calculations, polymerization kinetics, and

terminal structure analysis.

2. Experimental

2.1. Materials

Methanol (J&K Scientific Ltd., 99.9%), ethanol (EtOH, Beijing Chemical Works, 99.7%), cumyl alcohol (CumOH) (J&K Scientific Ltd., 97%), $B(C_6F_5)_3$ (J&K Scientific Ltd., 97%), diethyl ether (Aldrich, 99.5%), isopropanol (IPA, Beijing Chemical Works, 99.5%), hexadecyltrimethylammonium bromide (CTAB, J&K Scientific Ltd., 99%), toluene (Beijing Chemical Works, 99.5%), 4-nonylphenyl-polyethyleneglycol (NP-40, J&K Scientific Ltd.), Sodium dodecyl benzene sulfonate (SDBS, J&K Scientific Ltd., 95%), tetrahydrofuran (THF) (J&K Scientific Ltd., 99.9%), and deuterated chloroform ($CDCl_3$, J&K Scientific Ltd., 99.8%) were used as received. Styrene (SINOPEC Beijing Yanshan Company) was distilled under reduced pressure before use. High purity water was obtained from a Pine-Tree XYF-2-10-H Water Purification System. The LiCl/NaCl/ H_2O eutectic was made by dissolving (23.00 g 0.5426 mol) LiCl (J&K Scientific Ltd., 99%), (1.20 g, 0.0205 mol) NaCl (J&K Scientific Ltd., 99%) into (75.80 g, 4.211 mol) high purity water. n-hexane (Beijing Chemical Works, 99.5%), IBVE (J&K Scientific Ltd., 99.0%), 2-chloroethyl vinyl ether (J&K Scientific Ltd., 97.0%), and n-butyl vinyl ether (J&K Scientific Ltd., 98.0%) were distilled in a nitrogen atmosphere before use.

2.2. Polymerizations

2.2.1. Polymerization in Aqueous Suspension

We carry out the polymerization reactions under air atmosphere in glass tubes. This polymerization is a typical procedure in suspension, it was initiated by adding a solution of $B(C_6F_5)_3$ (0.128 g, 2.5×10^{-4} mol) and diethyl ether (0.2 g) in H_2O (2 mL, 0.13 M) to a mixture consisting of monomer, CumOH (0.034 g, 2.5×10^{-4} mol), and H_2O (3 mL). After the expected reaction time is reached, the suspension media was poured out into excess methanol. The polymer was separated from the solution by centrifugation and dried in a vacuum at the set temperature. By gravimetrically, the monomer conversion was determined.

2.2.2. Cationic Polymerization in Aqueous Emulsion

The polymerizations were achieved under the situation of adding an emulsifier. H_2O (3 mL), monomer, a surfactant (NP-40, CTAB, or SDBS), and CumOH (0.034 g, 2.5×10^{-4} mol) were added to a reactor with mechanical stirring at 150 rpm. Then the reactor was warmed to a set polymerization temperature by immersion for 20 min in an ethanol/water (50/50) bath. $B(C_6F_5)_3$ (0.128 g, 2.5×10^{-4} mol), H_2O (2 mL, 0.13 M), and diethyl ether (5×10^{-4} mol) were mixed in a beaker. The mixture in the beaker was poured afterward into the reactor. Subsequent processing was similar as the polymerization in an aqueous suspension.

2.3. Measurements

By gel permeation chromatography (GPC) can detect the number-average

molecular weight (M_n) and molecular weight distribution (MWD, i.e., M_w/M_n) of the polymers, equipped with four Waters columns connected in the following series: 500, 103, 104, and 105 at 30 °C. The GPC system consists of a Waters e2695 Separations Module, a Waters 2414RI Detector, and a Waters 2489 UV Detector. Using tetrahydrofuran (THF) as the eluent at a flow rate of 1.0 mL/min⁻¹ at room temperature. The columns were calibrated against standard polystyrene samples. The measurements were carried out at room temperature.

NMR spectroscopy of the polymers was performed on a Bruker-500 MHz spectrometer using CDCl₃ as a solvent at 25 °C. ¹H NMR spectra of solutions in CDCl₃ were calibrated to tetramethylsilane as the internal standard ($\delta H = 0.00$).

By a dynamic light scattering (DLS) can test the particle size in the emulsion. This analysis system using the Nanosight LM20.

The reaction system temperature was detected with Testo 176T4, a data logger that records temperature per second.

3. Results and Discussion

3.1. Polymerization in Aqueous Suspension

The aqueous cationic polymerization of IBVE was conducted in H₂O using B(C₆F₅)₃ combined with different concentrations of CumOH at 20 °C (Figure 1). The polymerization sites in H₂O were on the monomer/water surface, because B(C₆F₅)₃ was dissolved in water. By contrast, the number average molecular weight (M_n) decreased as the concentration of CumOH increased (Figure 1b). The increase of M_n with monomer conversion at the later stage of polymerization was due to a coupling reaction during the later stages of the polymerization.

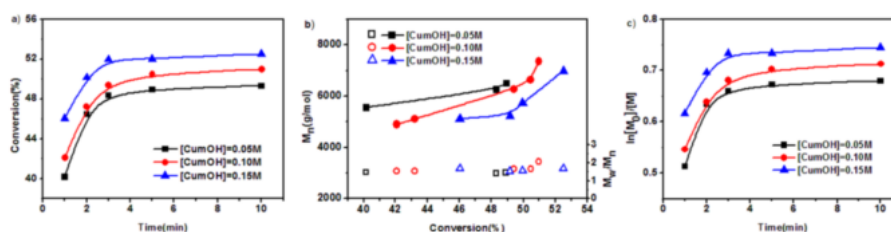


Figure 1. IBVE cationic polymerization initiated by CumOH/B(C₆F₅)₃/Et₂O in H₂O at 20 °C: (a) conversion vs time; (b) M_n and M_w/M_n vs conversion; (c) $\ln[M_0]/[M]$ vs time. [IBVE] = 1.6 M; [B(C₆F₅)₃] = 0.05 M; [Et₂O] = 0.1 M.

3.2. Polymerization in Aqueous Emulsions

To better understand the influence of the aqueous environment on vinyl ether cationic polymerization, poly(IBVE), poly(CEVE), and poly(n-BVE) were synthesized in emulsions (using CTAB, SDBS, and NP-40 as cationic, anionic, and non-ionic surfactants, respectively). Compared with the polymerizations implemented in H₂O, the lower monomer conversion and M_n were obtained in the emulsion at the same reaction time (Figures 2 and 3).

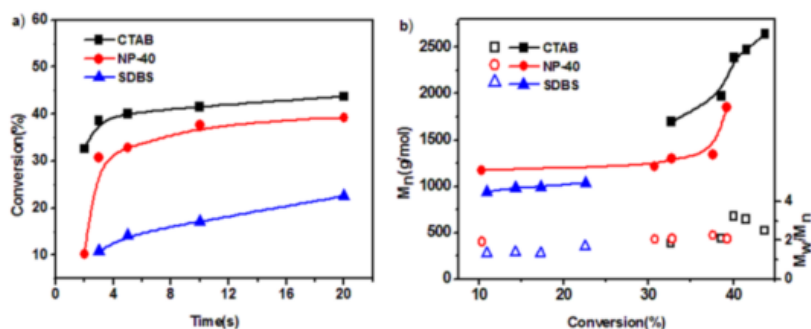


Figure 2. IBVE cationic polymerization initiated by CumOH/B(C₆F₅)₃/Et₂O in emulsion at 20 °C: (a) conversion vs time; (b) *M_n* and *M_w/M_n* vs conversion; [IBVE] = 1.6 M; [CumOH] = [B(C₆F₅)₃] = 0.05 M; [Et₂O] = 0.1 M; CTAB = 0.02 g; NP-40 = 0.02 g; SDBS = 0.02 g.

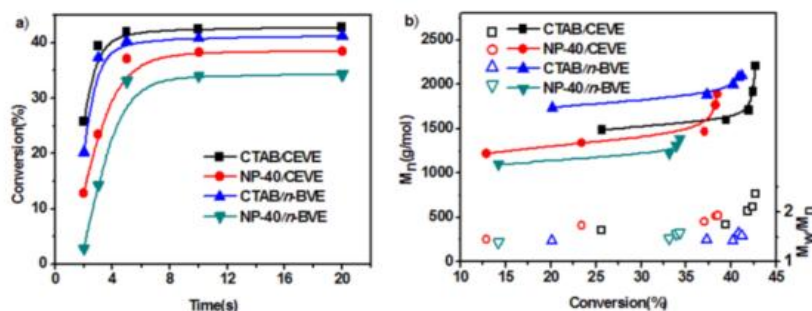
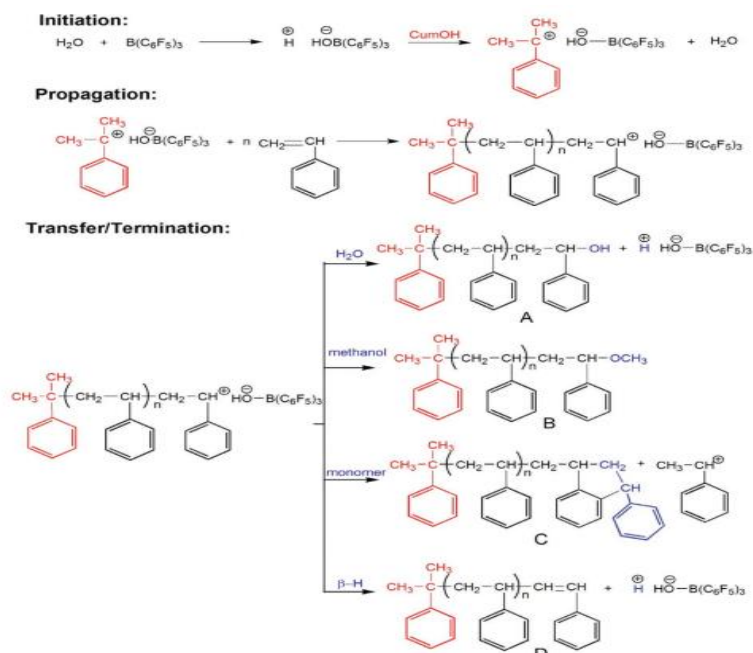


Figure 3. CEVE and *n*-BVE cationic polymerization initiated by CumOH/B(C₆F₅)₃/Et₂O in an emulsion at 20 °C: (a) conversion vs time; (b) *M_n* and *M_w/M_n* vs conversion; [CEVE] = 2.0 M; [*n*-BVE] = 1.6 M; [CumOH] = [B(C₆F₅)₃] = 0.05 M; [Et₂O] = 0.1 M; CTAB = 0.02 g; NP-40 = 0.02 g



Scheme 1. Proposed mechanism for styrene cationic polymerization initiated by CumOH/B(C₆F₅)₃ in aqueous media.

3.3. Proposed Mechanism for Polymerization(styrene)

In the initiation reactions, the water-tolerant LA $B(C_6F_5)_3$ abstracted a -OH group from CumOH, thereby inducing carbocation and $-HO-B(C_6F_5)_3$ counterion. Therefore, the propagations were not very fast, and chain-transfers occurred frequently and diversely. The chain-transfers occurred by chain-breaking via β -H elimination from $-CH_2-$ in the growing carbocation and then by protic reinitiation to create a new polymer chain. Adding methanol to end polymerization, which resulted in the formation of polymer chains with an $-OCH_3$ end group. The chain-transfer to water and monomer resulted in the formation of polymer chains with -OH and indanyl end group.

4. Conclusions

By using $B(C_6F_5)_3/Et_2O$ as a co-initiator and alcohols as an initiator Poly(styrene)s, Poly(IBVE)s, poly(CEVE)s, and poly(*n*-BVE)s were successfully achieved in aqueous suspensions and emulsions in a reproducible manner. Polymerization characteristics were systematically tested and compared in the suspension and emulsion. The polymerization rate surprisingly decreased when the temperature was lowered; this result was opposite to that in traditional cationic polymerizations. The aqueous cationic polymerization sites were located on the monomer/water surface. Accordingly, the mechanism for the aqueous cationic polymerization of styrene and vinyl ethers using CumOH/ $B(C_6F_5)_3/Et_2O$ was proposed.

References:

1. Jinghan Zhang, Yibo Wu, Xiaoning Li, Dan Yang, Min Zhang, Hao Wang, Yuwei Shang, Ping Ren, Xin Mu, Shuxin Li, Wenli Guo. Characteristics and Mechanism of Styrene Cationic Polymerization in Aqueous Media Initiated by Cumyl Alcohol/ $B(C_6F_5)_3$ [J]. *Macromolecular Chemistry and Physics*, 2019, 220(4).
2. Jinghan Zhang, Yibo Wu, Kaixuan Chen, Min Zhang, Liangfa Gong, Dan Yang, Shuxin Li, Wenli Guo. Characteristics and Mechanism of Vinyl Ether Cationic Polymerization in Aqueous Media Initiated by Alcohol/ $B(C_6F_5)_3/Et_2O$ [J]. *Polymers*, 2019, 11, 500

IL17

Collagen from Fish Scales: Extraction and Application in Drug Delivery

Nguyen Thuy Chinh^{1,*}, *Vu Quoc Manh*^{2,3}, *Vu Quoc Trung*⁴, and *Thai Hoang*^{1,2}

¹Institute for Tropical Technology, Vietnam Academy of Science and Technology, 18, Hoang Quoc Viet, Cau Giay District, Ha Noi, 100000, Vietnam

²Graduate University of Science and Technology, Vietnam Academy of Science and Technology, 18 Hoang Quoc Viet, Cau Giay District, Ha Noi, 100000, Vietnam

³Faculty of Foundation Science, College of Printing Industry, Phuc Dien Road, Bac Tu Liem District, Ha Noi, 100000, Vietnam

⁴Faculty of Chemistry, Hanoi National University of Education, No. 136 Xuan Thuy Road, Cau Giay District, Ha Noi, 100000, Vietnam

*E-mail: ntchinh@itt.vast.vn

Collagen from fish scales is focused on study in recent year thanks to its high absorbance ability, biocompatibility as well as non-religious obstruction and cheap sources. Extraction of collagen from fish scales also helps to reduce the environment pollution in fish processing. Bio-polymers increasingly have been studied since they are abundant in nature, renewable, biocompatible and cost – effective. Among them, carrageenan, a water-soluble fiber, found in many seaweeds such as red and brown algae is widely used in the food, cosmetic and pharmaceutical industries with functions such as gelling, thickening and stabilizing, etc. Combination of carrageenan with other biopolymer, collagen for example, could form a new material which has ability to control drug release.

In this study, collagen extracted from Vietnamese fresh-water carp fish scales will be used in combination with carrageenan for the improvement of allopurinol's availability. Allopurinol is known as a xanthine oxidase inhibitor and a medication used to treat gout or kidney stones, and to decrease high blood uric acid levels. The influence of gelation additive and collagen content on morphology, structure, swelling degree and drug release from carrageenan/collagen/allopurinol film was evaluated by methods such as infrared spectroscopy (IR), field emission scanning electron microscopy (FESEM), differential scanning calorimetric (DSC) and ultraviolet-visible spectroscopy (UV-Vis). From the DSC data, FESEM analysis and drug release

of carrageenan/collagen/allopurinol films, the most suitable content of gelation additive and collagen in film is 1 wt.% and 5 wt.%.

Key words: Fish scale collagen, allopurinol, drug release and biomaterials.

Acknowledgements: The authors would like to thank the National Foundation for Science and Technology Development in Vietnam for financial support (subject code 104.02-2017.326, period of 2018–2021).

References:

- 1.K. Naresh, S.A. Shahin, K.D. Vikash, B. Utpal, *Journal of Proteins and Proteomics*, 2010, **1(1)**, 9-14.
- 2.L. Liang, N. Rui, S. Yang, M. Shirui, *Carbohydrate Polymes*, 2014, **103**, 1–11.

Oral Presentation

OL 1 ~ OL 12

OL1

Functionalized Mesoporous Silica Nanoparticles for Anticancer Chemotherapy

Sung Soo Park¹, Moon Hyun Jung², Young-Shin Lee², Jae-Ho Bae², Sun-Hee Kim², Chang-Sik Ha^{1}*

¹ Department of Polymer Science and Engineering, Pusan National University,
Busan 46241, Republic of Korea

² Department of Biochemistry, School of Medicine, Pusan National University,
Yangsan Hospital, Yangsan 50612, Republic of Korea
E-mail: nanopss@pusan.ac.kr

In this work, we studied on the controlled releasing of anticancer drugs controlled by mesoporous silica nanoparticles as supports. First, we synthesized mesoporous silica nanoparticles (MSNs) *via* hydrothermal process using tetraethyl orthosilicate (TEOS) as silica source and cetyltrimethylammonium tosylate (CTATos) as structure directing agent.¹ The mesoporous silica materials modified with carboxyl groups were synthesized by post-synthesis method and drug molecule release behaviour was studied by loading of cisplatin as model drug of anticancer drug. Drug release was about 2 times higher in acidic condition (pH 4.0) than in neutral condition (pH 7.3). With the drug-free samples (Surfactant-extracted MSNs and COOH-MSNs), the cancer cell death did not show any difference. (Cell survival rate of about 82.7~85.7 %) On the other hand, with the sample containing the drug (Pt/COOH-MSNs), the cancer cell death was more pronounced with excellent performance (Cell survival rate 3.6 % for A549, 15.8 % for A2780, and 12.8 % for MCF-7, respectively). Second, we synthesized alkylammonium-functionalized hollow mesoporous silica (HMS) nanoparticles with sphere morphology by using a surfactant mixture composed of zwitterionic (N-dodecyl-N,N-dimethyl-3-ammonio-1-propane sulfonate, DDAPS) and anionic sodium dodecyl sulfate (SDS) surfactants as structure-directing agents, TEOS and alkylammonium alkoxysilane (TMAPS) as silica sources. The HMS have the particle size of ca. 450 nm with the shell thickness of ca. 60 nm. We studied on the controlled releasing of anticancer drug (fludarabine) using the alkylammonium-functionalized HMS nanoparticles as a support of drug molecules. The drug molecules-incorporated HMS nanoparticles showed the

cancer cell (MCF-7) viability of 2.5 % while the cell viability was 1.3 % after treatment for 96 h with the drug molecules (fludarabine).

Acknowledgments:

The work was supported by the National Research Foundation of Korea (NRF) Grant funded by the Ministry of Science and ICT, Korea {Mid-Career Researchers Program (NRF-2017R1A2B3012961); Individual Basic Research Program (NRF-2017R1D1A1B03034414); Brain Korea 21 Plus Program (21A2013800002)}.

References:

1. K. Zhang, L.-L. Xu, J.-G. Jiang, N. Calin, K.-F. Lam, S.-J. Zhang, H.-H. Wu, G.-D. Wu, B. Albela, L. Bonneviot, Peng Wu, *J. Ame. Chem. Soc.*, 2013, **135**, 2427.
2. S. S. Park, B. Ameduri, C.-S. Ha, *Emergent Materials*, 2019, **2**, 45.

OL2

Phosphorylcholine Functionalised MCM-41 Nanoparticles for Controlled Drug Release

Riyasudheen Nechikkattu, Sung Soo Park and Chang-Sik Ha

Department of Polymer Science and Engineering, Pusan National University,
Busan- 46241, Republic of Korea
E-mail: riyas_chem@pusan.ac.kr

Phosphorylcholine functionalized mesoporous silica nanoparticles (MSNs) were prepared for controlled drug release. Phosphorylcholine (PC) groups were generated by post condensation/ surface modification of MCM-41 nanoparticles. The ring-opening reaction of 2-chloro-2-oxo-1,3,2-dioxaphospholane was done subsequent to (3-bromopropyl) trimethoxysilane immobilization on the surface of nanoparticles. Studies revealed the successful introduction of phosphorylcholine groups at the surface, the modified MSN-PC maintains the original structure of MCM-41 and the pore diameter and surface area were reduced by modification. The drug-loaded MSN-PC showed the sustained release of alendronate molecules under physiological pH condition. A partial negative surface charge was generated on MSN-PC at this pH by the deprotonation of silanol groups, and the electrostatic interaction between the phosphorylcholine group and alendronate molecule was disturbed, which triggered the sustained release of the loaded molecules. The nanoparticle showed a significant reduction in the bovine serum albumin adsorption due to the introduction of PC groups onto MSNs.

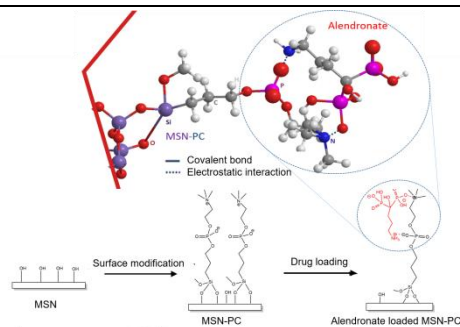


Figure: Schematic representation of preparation of MSN-PC and the interaction between phosphorylcholine group and alendronate drug molecule.

Acknowledgements:

The work was supported by the National Research Foundation of Korea (NRF) Grant funded by the Ministry of Science and ICT, Korea {Mid-Career Researchers Program (NRF-2017R1A2B3012961); Brain Korea 21 Plus Program (21A2013800002)}.

Reference:

1. F. Balas, M. Manzano, P. Horcajada, M. Vallet-Reg, *J. Am. Chem. Soc.*, 2006, **128**, 8116.

OL3

New Approaches to the Functionalization of CNF

Chen Wang, Aleksey Vedyagin, Ilya Mishakov, Yury Bauman and Vladimir Stoyanovskii

Boreskov Institute of Catalysis SB RAS, pr. Lavrentieva 5,
630090 Novosibirsk, Russian Federation
E-mail: chen.wang0726@gmail.com

Among the variety of carbon nanomaterials, functionalized carbon nanofibers (CNF) are considered as materials of high application potential due to the relatively low cost value of their production. The simplicity of their synthesis in comparison with, for example, carbon nanotubes should be mentioned as well. No high purity hydrocarbon sources are required in this case, so any hydrocarbon-containing mixtures (natural gas, associated petroleum gas, domestic gas, etc.) can be used for the catalytic growth of CNF in accordance with so-called carbide-cycle mechanism. As it was reported recently¹, even halogenated organic compounds and their complex mixtures can be transformed into nanostructured carbon using the mentioned approach. Moreover, the bulk items made of nickel or nickel-containing alloys can serve as a catalyst's precursor. For instance, a piece of commercial Ni-Cr wire or a specimen of especially prepared Ni-Cr bulk sample loaded inside the quartz reactor and fed with halogen-containing organics undergo self-disintegration process, which is known as a metal dusting phenomenon, resulting in an appearance of nanosized metal particles catalyzing the growth of carbon fibers.

The second metal in the composition of Ni-based alloys often plays quite important role providing the stable work of the catalyst's particles. Screening of a wide range of additives has revealed that the effect can be negative (additive facilitates a rapid deactivation), neutral (alloy behaves as pure nickel) or positive (improved activity and stability are observed). The Ni-Pd system was found to exceed the Ni-Cr alloy in terms of catalytic efficiency². The results of microscopic studies indicated that the carbonaceous product is mainly represented by long carbon filaments of submicrometer diameter. The prevailing structural type of the carbon fibers can be called a segmental one, which is assumed to reflect the discrete character of the carbon deposition process due to the poisoning effect of chlorine. Both the CNF yield and morphological structure were found to be affected by such process parameters

as temperature and the reaction mixture composition (especially, hydrogen content)³. Within the present research, the effects of addition of organic compounds containing other heteroatoms in their composition into the reaction mixture for one-pot functionalization of CNF materials will be presented and discussed.

This study was supported by the Russian Foundation of Basic Research (project No. 18-29-19053-mk).

References:

1. Y.I. Bauman, I.V. Mishakov, D.V. Korneev, Y.V. Shubin, A.A. Vedyagin, R.A. Buyanov, *Catalysis Today*, 2018, **301**, 147.
2. Y.I. Bauman, I.V. Mishakov, Y.V. Rudneva, P.E. Plyusnin, Y.V. Shubin, D.V. Korneev, A.A. Vedyagin, *Industrial and Engineering Chemistry Research*, 2019, **58**, 685.
3. C. Wang, Y. Bauman, I. Mishakov, A. Vedyagin, *Materials Science Forum*, 2019, **950**, 144.

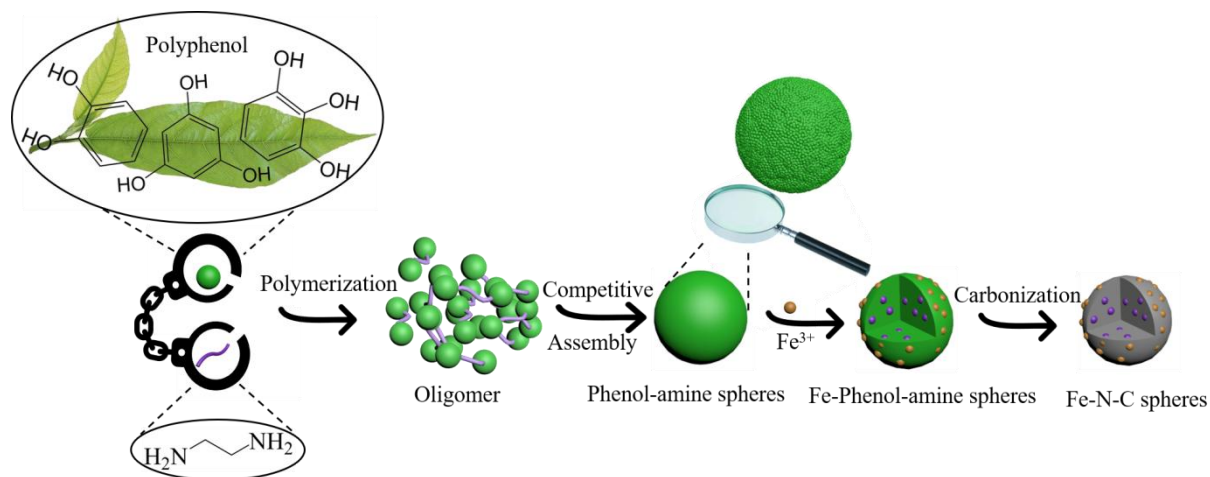
OL4

Tunable Sub-Micrometer N-Doped Carbon Spheres from Phenol-Amine Building Blocks by Competitive Self-Assembly

*Zhiqing Liu, Xin Jia**

School of Chemistry and Chemical Engineering, Shihezi University, Shihezi
832003, P. R. China
E-mail: jjaxin_shzu@foxmail.com

Driven by the design for energy storage systems with high-efficiency and safety, heteroatom doped carbon spheres have drawn extensive attention¹. However, how to prepare such materials through a facile and a controllable manner remains a great challenge². Herein, it is demonstrated that a versatile competitive self-assembly approach to preparing phenol-amine building blocks can be used directly as a precursor, and followed by pyrolysis to develop heteroatom-doped carbon materials. The size of the phenol-amine spheres can be tuned by simply adjusting the ratio of water and co-solvents. Taking advantage of the high density of multi-functional groups on the surfaces of the spheres, Fe³⁺ can be anchored on this spherical template followed with pyrolysis. As a result, a Fe-N-C catalyst was obtained through the coordination between Fe³⁺ and the surface functional groups. The heteroatom-doped carbon materials (FNCS800) exhibit good electrocatalytic activity for the ORR, and with superior durability and well methanol tolerance. The present work sets a landmark in the path of pursuing synthesis of heteroatom-doped carbon spheres that is simple, low-cost, controllable, and easily scaled up from natural products.



References:

1. Zhao, Y.; Nakamura, R.; Kamiya, K.; Nakanishi, S.; Hashimoto, K., Nitrogen-doped carbon nanomaterials as non-metal electrocatalysts for water oxidation. *Nature Communications* **2013**,*4*, 2390.
2. Liu, J.; Qiao, S. Z.; Liu, H.; Chen, J.; Orpe, A.; Zhao, D.; Lu, G. Q., Extension of The Stöber Method to the Preparation of Monodisperse Resorcinol–Formaldehyde Resin Polymer and Carbon Spheres. *Angewandte Chemie International Edition* **2011**,*50* (26), 5947-5951.

OL5

Enhanced Ion Transport in Densified CNT Arrays

Xiaohua Zhang

Center for Soft Condensed Matter Physics and Interdisciplinary Research &
School of Physical Science and Technology and Jiangsu Key Laboratory of
Thin Films, Soochow University, Suzhou 215006, P. R. China
E-mail: zhangxiaohua@suda.edu.cn

We investigate ion transport behavior through a densified vertically aligned carbon nanotube (CNT) array. An electrowetting effect induced by applying a voltage across densified CNT arrays (DCNTAs) leads to an increase in the wettability of a high surface tension liquid both in the intertube channels and inner channels of hydrophobic CNTs. We present evidence from thermal gravimetric analysis (TGA) and transmission electron microscopy (TEM), which shows that this electric activation treatment greatly promotes the formation of water channels in DCNTAs. Moreover, the formation of water channels is of importance in improving the overall ion transport rate through DCNTAs. We find that an enhancement in the overall ion transport rate through electrically activated DCNTAs gives rise to a reduction of electrolyte transfer resistance, and the capacitive performance of CNT-based devices is greatly improved as compared to untreated DCNTAs.

OL6

Novel Metal Chalcogenides as High-Performance Anodes for Sodium-Ion Battery

Xusheng Wang

Technical Institute of Physics and Chemistry, Chinese Academy of Science,
China

High cost and poor reserves of lithium-ion battery (LIB) force us to develop new battery technologies. Sodium-ion battery (SIB) has the advantages of abundant resources, low production cost, environmental friendliness, and high sustainability, thus with a promising application prospect in many fields. It is one of the key factors to realize the practicality of SIB by developing anode materials with high cycling stability, high specific capacity, and high rate capability. This report majorly focuses on the exploration and modification of novel metal chalcogenides (SnSe_2 , SnSSe , FeSe/FeS , and $\text{MoS}_{5.7}$) as high-performance SIB anodes. Based on the design and regulation of unique structure, composition, and sodium-ion-storage mechanism, the cost and capacity delivery of metal chalcogenides are gradually optimized. Stable structures with high resistance against volume expansion are constructed to improve the structural stability, pseudocapacitive behavior is favorable to maintain the morphology and structure of both the material surface and bulk, and thus achieving the goal of long-term cycling stability and high capacity delivery at high current density. These works can provide the foundation and knowledge reserve for the next-step researches and further commercialization of SIBs.



Reporter Introduction: Xusheng Wang is a research assistant at the Technical Institute of Physics and Chemistry, Chinese Academy of Science, China. He obtained the doctor's degree in 2018 from Peking University. He has published more than 20 papers, including *Advanced Materials*, *Angewandte Chemie International Edition*, *Nano Letters*, *ACS Nano*, *Energy Storage Materials*. His research interests focus on the secondary battery systems, especially the development of electrode materials.

OL7

Cobalt-Based Oxide Materials for Cathode of IT-SOFC

YanLi

College of Materials Science and Engineering, Beijing Institute of
Petrochemical Technology, Beijing, 102617

E-mail: yanli@bipt.edu.cn

OL9

Rapid and Facile Ratiometric Luminescent Detection of an Anthrax Biomarker in a Bimetallic Tb/Eu-MOFs

Chuan-Yi Wang, Hao Wang*

Beijing Key Lab of Special Elastomer Composite Materials, College of Materials Science and Engineering, Beijing Institute of Petrochemical Technology, Beijing, 102617
E-mail: wangh@bipt.edu.cn

Metal-organic framework materials (MOFs) are a new type of porous materials that have developed rapidly in the past decade. They have the advantages of high porosity, large specific surface area, convenient synthesis, variable framework size, etc., and have been extensively studied in the detection of small molecules. In this report, we studied bimetallic Tb/Eu-MOFs in zeolite-like topologies with carboxylic acid ligands for rapid and facile ratiometric luminescent detection of an *anthrax* biomarker 2,6-pyridinedicarboxylic acid (DPA) (Fig.1)^[1]. The results indicate that Tb/Eu-MOFs can recognize DPA in methanol solvent (Fig.2). After introducing appropriate concentration of DPA, the emission color of Tb/Eu-MOF-6 changes from yellow to red, which can be observed by naked eyes. LOD value was as low as 4.5 μ M. The combined merits of high selectivity, good reproducibility, rapid and naked-eye recognition of DPA make Tb/Eu-MOF-6 is a promising material for applications in detection.

Keywords: Tb/Eu-MOF, DPA, ratiometric

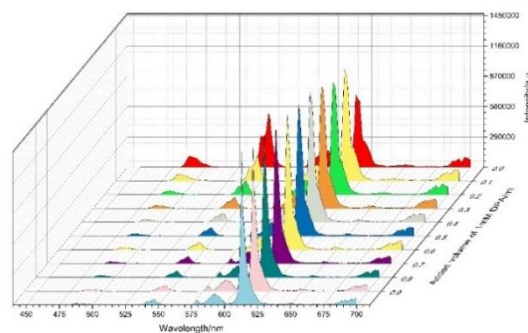
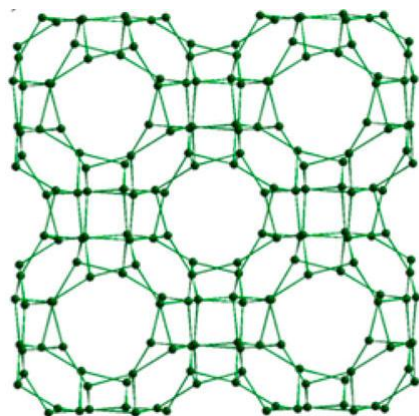


Fig.1 ρ topology of Tb/Eu-MOF Fig.2 Fluorescence spectra titration identification of DPA

References:

1. S.Y. Zhang, W. Shi, P. Cheng, M.J. Zaworotko, *J Am Chem Soc* 2015, **137**, 12203.

OL10

Organic and Polymeric Functional Field Effect Transistors

Lanchao Ma

Beijing Institute of Petrochemical Technology, College of Materials Science and Engineering, No.19 Qingyuan North Road, Daxing District, Beijing, China
E-mail: 0020150027@bipt.edu.cn

Organic/polymeric field effect transistors not only hold great potential in the application of flexible circuits, but are also prone to be endowed with various functionalities, such as photo detection, light emission and so on. Functional field effect transistors make full use of amplification effect of transistors and improve integration level of devices. This talk is about light emitting transistors and photo response transistors, which are realized by selecting and synthesizing organic/polymeric semiconductors, adopting appropriate device configuration and post treatment. Organic light emitting field effect transistors could be used as luminous unit in flexible displays. They are featured with high on-off ratio and large on state current density. Photo response field effect transistors could achieve high light/dark current ratio and responsivity to weak light intensity. Photo response field effect transistors could respond to different wavelength of the spectrum if distinct semiconductor is adopted.

References:

1. C. Di, H. Shen, F. Zhang, D. Zhu, *Accounts of Chemical Research*, 2019, **52**, 1113.
2. W. Li, A. Elzatahry, D. Aldhayan, D. Zhao, *Chem Soc Rev*, 2018, **47**, 8203. L. Ma, D. Qin, Y. Liu, X. Zhan, *J. Mater. Chem. C*, 2018, **6**, 535.

OL11

Thermal Conductive Epoxy Adhesive with Synergy of Hexagonal Boron Nitride and α -Aluminum Oxide Fillers

Dahai Gao, Liyuan Yu

Beijing Institute of Petrochemical Technology, No.19 Qingyuan North Road,
Daxing District, Beijing, 102617, China
E-mail: gao dh@bipt.edu.cn

With the rapid development of electrical manufacturing industry, the structure and performance of thermal conductive adhesives were continuously improved. Recently, high-thermal conductive, insulative, ambient curable and convenient processible adhesives are urgently required in electronic circuits. Several thermal conductive fillers, such as hexagonal boron nitride (h-BN), play a vital role in adhesive products.

Efficient thermal networks should be constructed in the adhesive structure, for enhancement of phonons transmission and showing a high thermal conductivity (TC). Therefore, a large fillers content in thermal conductive composites is necessary. However, it is difficult to realize high h-BN content in polymer adhesives, because it brings about an obvious increase in processing viscosity owing to its 2D layered structure^{1,2}. An appropriate amount of α -aluminum oxide (Al_2O_3) nano particles was added into the adhesive products, in order to restrain the aggregation of BN layers. Although the TC of α - Al_2O_3 shows a medium value of TC ($\sim 30 \text{ W}\cdot\text{m}^{-1}\cdot\text{K}^{-1}$, lower than the value of h-BN, $\sim 300 \text{ W}\cdot\text{m}^{-1}\cdot\text{K}^{-1}$), the space effect of nano particles could promote the thermal networks formed by random distribution of h-BN layers.

The interface thermal resistance was decreased by surface modification of thermal conductive fillers^{3,4}. Amino substituted silane was used to modify h-BN, while epoxide group substituted silane to modify α - Al_2O_3 , which induced linking groups onto the surface of fillers for enhancing the organic/inorganic interface. Epoxy resin 108 was selected for the polymer matrix of adhesives, because of its ambient curable and low processing viscosity. The modified fillers can provide an obvious increase ($\sim 18\%$) in TC compared with the sample filled with unmodified h-BN and α - Al_2O_3 . These surface modifications have not exhibited negative effect in mechanical, electrical insulating, dielectric properties of thermal conductive adhesives.

References:

1. M. Derradji, X. Song, A. Q. Dayo, J. Wang, W. Liu. *Applied Thermal Engineering*, 2017, **115**, 630.
2. C. Yu, J. Zhang, W. Tian, X. Fan, Y. Yao. *RSC Advances*, 2018, **39**, 21948.
3. K. Kim, M. Kim, Y. Hwang, J. Kim. *Ceramics International*, 2014, **40**, 2047.
4. D. S. Muratov, A. A. Stepashkin, S. M. Anshin, D. V. Kuznetsov. *J Alloys and Compounds*, 2018, **735**, 1200.

OL12

Controllable Fabrication of Raspberry-like Porous Polysilsesquioxane Particles

Hongwei Li, Liangyu Lu, Mengyu Ma, and Fuping Dong*

Department of Polymer Materials and Engineering, Guiyang, China

E-mail: asam7thfpdong@gzu.edu.cn

The raspberry-like micro/nano porous structured polysilsesquioxane materials have great potential in the fields of catalysis, medicine and separation due to its own mechanical stability, novel porous structure and easy chemical modification of the surface.

In this paper, a porous polysilsesquioxane material was fabricated with the surface shell composing of hollow nanospheres and the core is solid microspheres. The synthesis of traditional core-shell materials mostly contain a multi-step process that firstly synthesizing core and then growing or assembling shells on the core. In this study, the pre-synthesized polystyrene beads are used as "satellite" shells to be assembly onto a microcore. An organofunctionalized micron-sized raspberry-like polysilsesquioxane material was prepared. After removing the polystyrene template, raspberry-like particles with hollow nanospheres on microspheres were obtained. Through the morphology analysis of the intermediate products at different times in the synthesis process, the gradual formation mechanism of the microspheres was studied, and the material morphology was controlled by adjusting the precursor concentration, the amount of the catalyst and the amount of the stabilizer.

The hollow nano-materials can be loaded with the guest molecules. The catalytic properties of the gold nanoparticles on this raspberry-like particles are investigated with high performance in the catalytic reduction reaction of *p*-nitrophenol to *p*-aminophenol.

References:

1. Lu, L.; Li, J.; Li, H.; Gao, C.; Xie, H.; Xiong, Y.; Luo, Z.; Sun, Q.; Dong, F. Controllable synthesis of hierarchical polysilsesquioxane surfaces: From spheres-on-sphere to bowls-on-sphere structure. *Appl. Surf. Sci.* 2019, **481**, 75-82.
2. Dong, F.; Xie, H.; Zheng, Q.; Ha, C.-S. Superhydrophobic polysilsesquioxane/polystyrene microspheres with controllable morphology: From raspberry-like to flower-like structure. *Rsc Advances* 2017, **7**, 6685-6690.

Poster Presentation

PS 1 ~ PS70

Poster 1

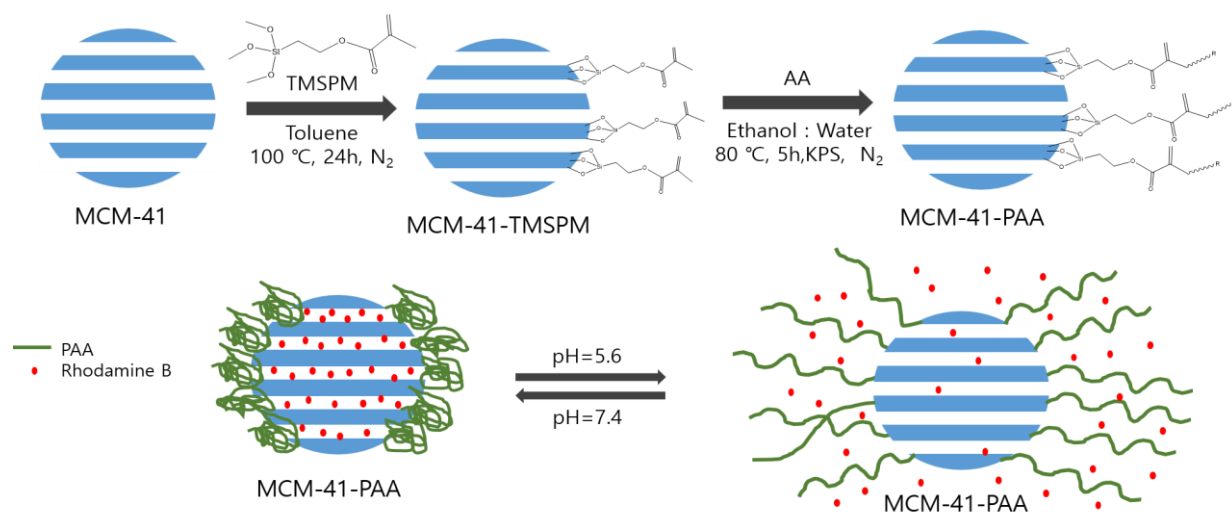
Fabrication of pH-Responsive Poly(acrylic acid)/MCM-41 and Incorporation of Guest Molecules for Sustained Drug Release

Jungwon Kong, Sung-soo Park, Chang-sik Ha

Department of Polymer Science and Engineering, Pusan National University,
Busan, Korea

E-mail: ggong933@gmail.com

We synthesized poly(acrylic acid) modified MCM-41 to get effective pH-responsive nanocarrier. (3-Trimethoxysilyl)propyl methacrylate (TMSPM) functionalized surface was prepared by using post-grafting method, then free-radical polymerization of acrylic acid (AA) was proceeded using potassium persulfate (KPS) as an initiator. The structure and morphology of the modified nanoparticles were characterized by X-ray diffraction, Fourier transform infrared spectroscopy, DLS, SEM, TEM, and N₂ adsorption-desorption analysis. The prepared particles have well-ordered mesoporous structure and large pore size and pore volume that is proper as a carrier for guest particles. We studied on the controlled releasing of guest molecules by using Rhodamine B. The dye molecules were highly loaded into the Poly(acrylic acid) modified MCM-41. The guest molecules-incorporated mesoporous silica particles showed different releasing rate of Rhodamine B under various pH conditions (pH 7.4, 5.6, 4.0). It demonstrated that our current materials have possibilities to be utilized in catalytic applications, drug delivery and so on.



Scheme. Modification process of MCM-41-PAA and pH-responsive behavior of the prepared material.

References:

1. Seema Saroj, Sadhana J. Rajput, *Drug Development and Industrial Pharmacy*, 2018, **44**, 1198
2. Chia-Hung Lee, Leu-Wei Lo, Chung-Yuan Mou, Chung-Shi Yang, *Advanced Functional Materials*, 2008, **18**, 3283

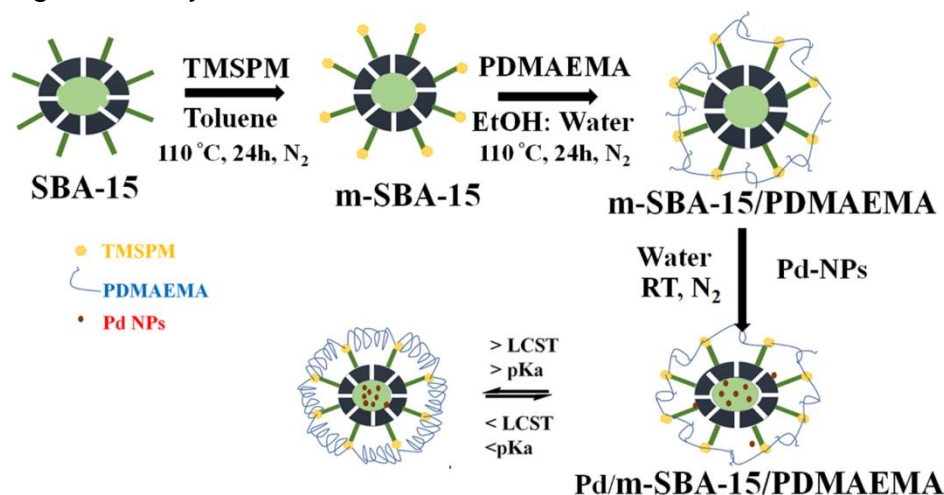
Poster2

Dual Stimuli-Responsive PDMAEMA Functionalized SBA-15 with Pd Nanoparticles Incorporated Hybrid System for Catalytic Application

Anju Maria Thomas, Chang-Sik Ha

Department of Polymer Science and Chemical Engineering, Pusan National University, Busan, Korea
E-mail: anju.05u0@gmail.com

In this work the mesoporous silica SBA-15, was modified with pH and temperature responsive Poly [2-(N,N-dimethylamino)ethyl methacrylate] which was successfully synthesized by free radical polymerization¹. Further monometallic Palladium (Pd) nanoparticles were incorporated in the pre-synthesized SBA-15/PDMAEMA. The morphology and structure of resultant materials were characterized by various techniques. The hybrid material showed on/off catalytic activity during the reduction of 4-nitrophenol (4-NP) to 4-aminophenol (4-AP). It showed good catalytic activity at lower pH and temperature. The results suggest that the Pd/m-SBA-15/PDMAEMA catalyst shows a double stimuli-response on the catalytic reduction². This smart catalyst can be used in various other application such as in controlled catalysis and drug release system.



Scheme 1. Schematic illustration of the synthesis of Pd/m-SBA-15/PDMAEMA hybrid catalyst.

References:

1. J.T. Sun, C.Y. Pan, *J. Phys. Chem. C*, 2010, **114**.
2. P. Shinde, S. Sen Gupta, B. Singh, V. Polshettiwar, B.L.V. Prasad, *J. Mater. Chem. A*, 2017, **5**, 14914-14921.

Controllable Plasmon-Induced Catalytic Reaction by Tip Enhanced Raman Spectroscopy

Yanqi Liu, Yan Zhao*

Institute of Laser Engineering, Beijing University of Technology, Beijing
100124, China

* Corresponding author: zhaoyan@bjut.edu.cn

Controllable catalytic reaction plays a pivotal role in heterogeneous catalysis. Tip enhanced Raman spectroscopy (TERS) is considered as a promising technique to study catalytic reactions due to highly localized sensitivity and nanoscale spatial resolution.^{1,2} Here, we report a facile method for controlling catalytic reaction of 4-nitrobenzenethiol (4NBT) to p, p'-dimercaptoazobenzene (DMAB) on Ag/Au composite films by varying the thickness of Au film. Additionally, catalytic reaction of 4NBT absorbed on Au film can be manipulated on nanoscales by controlling the height between the tip-apex and the sample surface in Ag tip-Au substrate geometry (Figure 1). It is concluded that 'hot electron' induced by localized surface plasmon can significantly promote catalytic reactions based on the finite difference time domain (FDTD) simulations. Our findings offer a novel way for controllable graph drawing of molecular at nanoscale level.

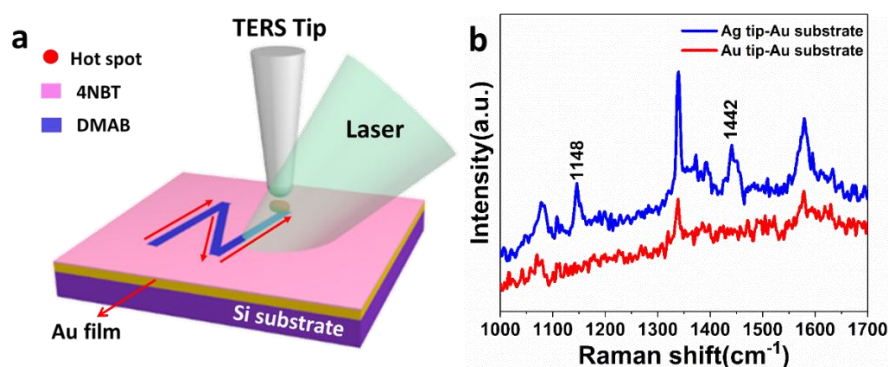


Fig1: (a) Schematic illustration of plasmon-induced catalytic reaction in TERS.(b) TERS spectra of 4NBT in the Ag tip-Au substrate geometry and Au tip-Au substrate geometry under 532 nm laser. The acquisition time was 20 s.

Keywords: tip-enhanced Raman spectroscopy; surface plasmon resonance; catalytic reaction; finite difference time domain

References:

1. E.M. van Schrojenstein Lantman, T. Deckert-Gaudig, A.J. Mank, V. Deckert, B.M. Weckhuysen: *Nat Nanotechnol* 2012, **7**, 583-586.
2. J.H. Zhong, X. Jin, L. Meng, X. Wang, H.S. Su, Z.L. Yang, C.T. Williams, B. Ren, *Nat. Nanotechnol.* 2017, **12**, 132-136.

Poster4

Application of Ag-loaded TiO₂ Nanocolumn Array in Photocatalysis

Xu Jinghan, Zhao Yan

Research Institute of Laser Engineering, Beijing University of Technology, No. 100 Pingle Park, Chaoyang District, Beijing 100124, China
E-mail: S201613001@emails.bjut.edu.cn

Titanium dioxide (TiO₂), as a wide-bandgap semiconductor, is widely used in photocatalytic degradation experiments of organic compounds because of its low cost, non-toxicity, high chemical stability and strong redox ability.¹ By making the material into nanostructure, the specific surface area of TiO₂ can be increased, and the catalytic efficiency of the material can be improved.² At the same time, the combination of Ag and TiO₂ can promote the separation of photogenerated electrons and holes, and further improve the photocatalytic efficiency of the material.³

In this study, TiO₂ was deposited in Anodic Aluminum Oxide (AAO) template by atomic layer deposition (ALD). Ag was deposited on the surface of TiO₂ array by vacuum evaporation, and the thickness of Ag was controlled by deposition time.

The shapes of the arrays are shown in Figure 1. It can be found that TiO₂ nanocolumns are very regular, and as the thickness of Ag increases, the array structure is gradually covered. Figure 1 (f) shows the photocatalytic degradation rate of the array. The degraded dye is methylene blue (MB) and the light source is a 300W Xe lamp. It can be found from the figure 1 (f) that Ag greatly increases the catalytic rate of the TiO₂ array. However, too much Ag hinders the absorption of light by TiO₂ and the contact between TiO₂ and MB, so the catalytic efficiency of the sample decreases with the increase of Ag deposition thickness.

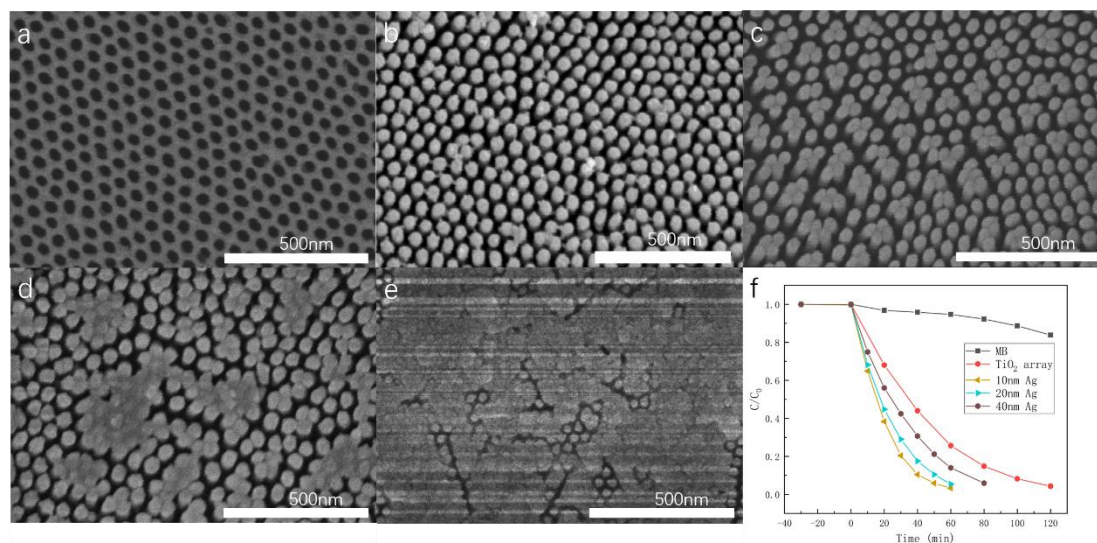


Figure 1. a) AAO template, b) TiO₂ nanocolumn array, c) TiO₂ array of 10 nm thick Ag, d) TiO₂ array of 20 nm thick Ag, e) TiO₂ array of 40 nm thick Ag, f) photocatalytic degradation rate curve of MB solution.

References:

1. Chen X, Mao S S. Chemical reviews, 2007, **107**, 7.
2. Lai L L, Wen W, Fu B, et al. Materials & Design, 2016, **108**: 581-589.
3. Sun Z, Liao T, Kou L. Science China Materials, 2017, **60**, 1.

Poster5

Complexation Behavior of Fulvic Acid with Heavy Metal Ions

Jintong Du^{1,2}, Piyue Gong¹, Aifang Geng², Haiying Huang^{1}*

¹State Key Laboratory of Polymer Physics and Chemistry, Changchun Institute of Applied Chemistry, Chinese Academy of Sciences, Changchun, 130022, P. R. China ²School of Chemistry and Environmental Engineering, Changchun University of Science and Technology, Changchun 130022, China

E-mail: jtdu@ciac.ac.cn

Fulvic acid (FA) is considered to be the most active macromolecules of humic substances in natural organic matter, which plays an important role on regulating the ecological effects of heavy metal ions on earth, such as chemical cycle, migration and transformation.¹ Owing to the higher activity of its functional groups, it can reduce the toxicity of heavy metal ions with much higher sorption capacity compared with humic acid.²⁻³ Nevertheless, it remains challenging for precise description of their structure information and characterization of chemical and physicochemical properties because of its heterogeneous and polydisperse nature, an intensive study of complexation process of FA-metal ions is therefore of fundamental importance.

In this work, we studied the stability, size and morphology of FA complex with CdCl₂ by dynamic light scattering (DLS), scanning electron microscopy (SEM) and transmission electron microscopy (TEM). We found that HA in aqueous solution form rod-like complexes, and their size strongly depends on the pH of solution, i.e. the complexes formed at pH=2.3 and pH=12 are significantly larger than that of other pH values. Addition of CdCl₂ into FA solution leads to the formation of larger aggregates, above a critical metal ion concentration, the solution loses its stability and the aggregates precipitate. In this way, we were able to establish the relationship between ion adsorption and FA complex structure under different conditions, which can gain further insight into the underlying adsorption and aggregation kinetics of FA-metal ions in soil and aquatic environments.

References:

1. O. Oriekhova, S. Stoll, *Chemosphere*, 2016, 144, 131.
2. F. J. Stevenson, *Humus Chemistry: Genesis, Composition, Reactions*, 1994, Wiley-Interscience, New York.
3. S. Lalas, V. Athanasiadis, and V. G. Dourtoglou, *Clean-Soil, Air, Water*, 2018, 46, 1700608

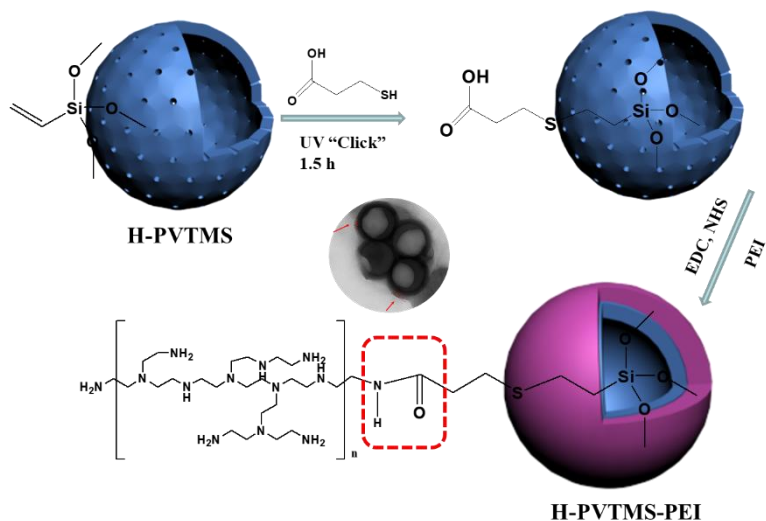
Poster 6

Designed Synthesis of Monodisperse Hollow Polysilsesquioxane@PEI Spheres for Dye Removal

*Yong-Zhu Yan, Saravanan Nagappan, Sung Soo Park and Chang-Sik Ha**

Department of Polymer Science and Engineering, Pusan National University,
Busan- 46241, Republic of Korea
E-mail: zyancam@163.com

Efficient adsorption of pollutants from wastewater is of considerable importance for environmental protection; Thus, the construction of a new type of adsorbent materials with excellent adsorption capacity would be of significant interest. Herein, polysilsesquioxane@PEI hybrid hollow spheres were successfully synthesized in an aqueous medium by using vinyltrimethoxysilane (VTMS) as the precursor, followed by polyethylenimine (PEI) was assembled on the surface of hollow polysilsesquioxane to achieve high density active sites. Accordingly, the low density cavity and the reactive aminogroups on the surface of the hybrid polysilsesquioxane microspheres promise many potential applications. The novel spheres show a high adsorption capacity of 600.3 mg/g for Congo Red, which is higher than the adsorption capacity of single polysilsesquioxane hollow spheres. Adsorption mechanisms consisted of electrostatic interaction between the positively charged amino-groups and the negatively charged pollutant species in the aqueous solution. In the predicted application of polysilsesquioxane@PEI, other anionic dyes and metal ion, might be also effectively adsorbed from solution.



Scheme 1. Schematic Illustration of the Synthetic Procedure for Hollow polysilsesquioxane@PEI Composite

References:

1. F. Dong, W. Guo, S.S. Park, C.S. Ha, *J. Mater. Chem.*, 2011, 21, 10744-10749.
2. Z. Wang, F. Guo, C. Chen, L. Shi, S. Yuan, L. Sun, J. Zhu, *ACS Appl. Mater. Interfaces*, 2015, 7, 3314-3322.

Poster 7

Enhanced Thermal Conductivity of Epoxidized Natural Rubber with Poly(dopamine) Modified Boron Nitride

Jian Hao

College of Materials Science and Engineering, Beijing Institute of
Petrochemical Technology, Beijing, China
Email: 18047862603@163.com

With miniaturization and integration of electronic packaging materials, the removal of excess heat is becoming an increasingly critical issue. However, the low thermal conductivity of elastomers might accumulate the self-generated heat and rise temperature, leading to short life service and performance degradation. Boron nitride (BN) is believed to be an ideal material for heat dissipation due to its relatively high thermal conductivity. However, the weak interfacial bonding force between BN and polymeric matrix leads to an unacceptable increased thermal resistance. Inspired by adhesive proteins in mussels, poly(dopamine) (PDA) was used as the surface modification of BN to improve thermal conductivity of epoxidized natural rubber (ENR) composites. The effect of PDA thickness on microstructure, mechanical properties, dielectric properties and thermal conductivity of ENR composites was systematically investigated.

Keywords: dopamine; borazon; ENR; high thermal conductivity composites

Poster8

Improved Thermal Conductivity of Nitrile Butadiene Rubber by Incorporating Modified Alumina/Boron Nitride Using Dopamine Chemistry

Qiaoyu Han

College of Materials Science and Engineering, Beijing Institute of
Petrochemical Technology, Beijing 102617, China

Nitrile-butadiene rubber (NBR) is a promising candidate for dielectric flexible materials thanks to its strong polarization, mechanical flexibility, easy processing, and low cost. However, in miniaturized and functionalized microelectronic devices, the low thermal conductivity of NBR limits its practical applications. The commonly used method for improving thermal conductivities of polymers is blending with high thermal conductive fillers. However, effective improvement of thermal conductivity is well below expectation due to elevated interfacial thermal resistance existing in polymer composites. Inspired by adhesive proteins in mussels, poly(dopamine) (PDA) was used to modify alumina and boron nitride and these two kind of modified thermal conductive filler were added into NBR matrix simultaneously to improve thermal conductivity of polymer matrix. The results showd that the thermal conductive of NBR composites was improved by decreasing interfacial thermal resistances.

Keywords: Al₂O₃ particles, BN particles, Dopamine, Nitrilerubber, Thermalconductivity, Mechanical properties.

Poster9

**Improved Thermal Conductivity of XNBR Dielectric
Composites by Using Multilayered Core-Shell Structure
Dielectric Particles as High Dielectric Constant Filler**

*Qunqiu Wei, Dan Yang**

College of Materials Science and Engineering, Beijing Institute of
Petrochemical Technology, Beijing, 102617, China.

E-mail: 18810132861@163.com

With the rapid development of modern microelectronic techniques, electronic devices became increasingly integrated, miniaturized, and efficient. The low thermal conductivity of elastomers might accumulate the self-generated heat and rise temperature during the electronic device service, leading to short life service and performance degradation. In this study, the Al₂O₃ microparticles were first modified by poly(catechol/polyamine) (PCPA), followed assembled with graphene oxide, forming Al₂O₃-PCPA-GO core-shell hybrids. The novel hybrids were added into XNBR matrix to obtain high thermal conductive and high dielectric constant elastomer composites. The strong interaction between polar groups in Al₂O₃-PCPA-GO core-shell hybrids and -C≡N groups in XNBR matrix improved dispersion of filler, leading to a high thermal conductivity and high dielectric constant. This method is convenient and effective for its simple reagents, mild reaction conditions, and no-harmful properties, showing potential applications in advanced packaging materials and microelectronic devices.

Keywords: multilayer core-shell hybrids; thermal conductivity; Dielectric elastomer

Poster10

**Improved Electromechanical Properties of
Acrylonitrile-Butadiene Rubber Composites by Modification of
TiO₂ Nanoparticles via Non-Covalent Poly(catechol/polyamine)
Deposition and Covalent Grafting with Silane**

Xinxin Kong

College of Materials Science and Engineering, Beijing Institute of
Petrochemical Technology, Beijing, 102617, China.

E-mail: 5120131575@bipt.edu.cn

The combination of covalent and non-covalent modifications is used to functionalize the TiO₂ nanoparticles to improve the electromechanical properties of the acrylonitrile-butadiene rubber (NBR) composite. The surface of the TiO₂ nanoparticles is first modified by non-covalent deposition of poly(catechol/polyamine) (PCPA), followed by γ -(2,3-epoxypropoxy)-propyltrimethoxy Silane (GPTMS) is grafted to form TiO₂-PCPA-GPTMS. Nanoparticles. PCPA deposition maintains the surface characteristics of the TiO₂ nanoparticles, while the epoxy groups in GPTMS provide a strong interaction with the polar rubber matrix. Mechanical, dielectric and electromechanical properties are improved due to enhanced interfacial interaction between the TiO₂-PCPA-GPTMS nanoparticles and the NBR matrix. The 10 phr TiO₂-PCPA-GPTMS / NBR composite has a relatively high driving strain at a certain voltage, which is higher than the maximum driving strain obtained by pure NBR in this work. Compared to dopamine modification, the methods described herein have shorter reaction times and lower costs, and may have potential applications in the industry.

Keywords: dielectric elastomer; poly(catechol/polyamine); electromechanical properties; silane; interfacial

Poster 11

Preparation of Thermal Conductive Composite with Tannic Acid Modified Boron Nitride

Shan Gao

College of Materials Science and Engineering, Beijing Institute of
Petrochemical Technology, Beijing 102617, China

Problems of heat conduction and dissipation have become one of the key factors restricting rapid development of integrated electronic devices, energy storage and conversion systems. Due to low cost and good processability, polymeric matrix has been commonly used as electronic packaging materials, but the low thermal conductivity limits its application. In order to improve the thermal conductivity of polymeric matrix, many researchers added thermal conductive fillers into polymeric matrix. As the interface compatibility between thermal conductive fillers and polymeric matrix, the high thermal contact resistance lead to a limited improved thermal conductivity of composites. In this paper, tannic acid was used to modify the surface of boron hexagon nitride for decreasing thermal contact resistance. The effect of tannic acid modified boron hexagon nitride on the dispersion, mechanical properties, dielectric properties and thermal conductivity of carboxyl nitrile butadiene rubber composites were studied.

Key words: boron nitride; tannic acid; Thermal conductivity, carboxyl nitrile butadiene rubber; modification

Preparation of High Thermal Conductive Composites with Tannic Acid Modified Carbon Nanotubes

Tingting Hu

College of Materials Science and Engineering, Beijing Institute of
Petrochemical Technology, Beijing 102617, China

Recently, with the advances in technology, the miniaturization of electronic devices is confronted with the issue of heat dissipation. Therefore, there is an urgent need to prepare polymeric materials with high thermal conductivity. Recently, numerous carbon-based materials, including carbon nanotubes, graphite, grapheme, and graphene derivatives have been used as functional fillers to prepare thermally conductive polymer composites. Due to the large length to diameter ratio, carbon nanotubes are widely used in heat conduction material or heat transfer packing material. However, the unmodified carbon nanotubes have a weak interfacial interactivity between polymeric matrixes, leading to an unacceptable increased thermal resistance.

In this study, tannic acid was used as non-covalent bond modifier to modify the surface of carbon nanotubes to decreasing thermal resistance of carboxyl nitrile butadiene rubber composites. The microstructure, mechanical properties, dielectric properties and thermal conductivity of carboxyl nitrile butadiene rubber composites filled with carbon nanotubes before and after tannic acid modification were studied.

Keywords: carbon nanotubes; tannic acid; Thermal conductivity, carboxyl nitrile butadiene rubber; modification

Poster13

High Thermal Conductivity Dielectric Elastomer Composites Were Prepared by Modifying Alumina Particles with Catechol and Tetraethylenepentamine

Jia Ai

College of Materials Science and Engineering, Beijing Institute of
Petrochemical Technology, Beijing 102617, China

Dielectric elastomer (DE) is an electronically active polymer with many excellent properties. However, the thermal conductivity of single dielectric elastomer composite is low, and the poor heat dissipation effect seriously affects the service life and working time of the material. Therefore, it is necessary to add thermal conductive fillers to the original dielectric elastomer composites to improve their thermal conductivity. In order to improve the thermal conductivity of carboxylated nitrile-butadiene rubber (CBNR), alumina particles were used as thermal conductive fillers. In order to make alumina better combine with carboxynitrile rubber, we choose catechol and tetraethylene132entaamine to modify alumina surface, which can effectively improve the binding force between filler particles and matrix. Based on the above point of view, we studied a polyphenol surface modification method to modify alumina and prepare carboxylated nitrile-butadiene rubber with high thermal conductivity as follows:

(1) Alumina was modified by oxidative co-deposition of catechol and polyamine. The catechol group and amino group in PCPA can adsorb alumina, and the modification of PCPA can effectively enhance the binding force between alumina particles and matrix.

(2) high conductivity dielectric elastomers were prepared by emulsion blending.

The results show that the surface modification of polyphenols can effectively improve the thermal conductivity of elastic dielectrics by combining filler particles with matrix.

Keywords: Alumina, Tetraethylene pentaamine, Catechol, Dielectric properties, Thermal conductivity, Carboxyl nitrile butadiene rubber

Poster14

Preparation of High Thermal Conductivity Elastomer Composites with Novel Core/Shell-Structured Thermal Conductive Nanoparticles

Liyan Yu,^{a,b} Dan Yang^{a,b*}

^aCollege of Materials Science and Engineering, Beijing Institute of Petrochemical Technology, Beijing 102617, China

^bBeijing Key Lab of Special Elastomeric Composite Materials, Beijing 102617, China

E-mail: 807845571@qq.com

Owing to the miniaturization of microelectronics and an associated increase in the power densities, the polymeric materials with high thermal conductivity and high dielectric constant (ϵ_r) are becoming increasingly useful for the applications in electronic technology. Nitrile-butadiene rubber (NBR) with relatively high dielectric constant (>10) is a promising candidate for dielectric flexible materials. However, the low thermal conductivity of NBR might accumulate self-generated heat and rise temperature during device service. This could lead to short life service and performance degradation of the device. In order to improve the thermal conductivity of NBR, we incorporated novel core/shell-structured thermal conductive nanoparticles into NBR matrix to prepare high thermal conductive composites. First, TA-Fe chelate was grafted on the surface of alumina nanoparticles to form $\text{Al}_2\text{O}_3@TA\text{-Fe(III)}$. Then the as-prepared nanoparticles were immersed into the silver nanoparticles solution to get $\text{Al}_2\text{O}_3@TA\text{-Fe(III)}@Ag$ core/shell-structured thermal conductive nanoparticles. The novel core/shell-structured thermal conductive nanoparticles were characterized by TG, TEM, XPS and XRD. The microstructures, mechanical properties, dielectric properties and thermal conductivity of NBR composites were systematically studied.

Key words: Alumina, Tannic Acid, NBR, Thermal Conductivity

References:

1. O'Halloran A, O'malley F, McHugh P. A review on dielectric elastomer actuators, technology, applications, and challenges[J]. *Journal of Applied Physics*, 2008, 104(7): 9.
2. Rahim M A, Kempe K, Müllner M, et al. Surface-Confined Amorphous Films from Metal-Coordinated Simple Phenolic Ligands[J]. *Chemistry of Materials*, 2015, 27(16): 5825–5832.
3. Kim H J, Kim D G, Yoon H, et al. Polyphenol/FeIII complex coated membranes having multifunctional properties prepared by a one-step fast assembly[J]. *Advanced Materials Interfaces*, 2015, 2(14): 8529-8536.

Growth and Optoelectronic Properties of Acceptor-Rich ZnO Single-Crystal Microtubes

Qiang Wang^{1,2}, Yin Zhou Yan², Yijian Jiang^{1,2}

¹College of Materials Science and Engineering, Beijing Institute of
Petrochemical Technology, Beijing 102617, China

²Institute of Laser Engineering, Beijing University of Technology, Beijing
100124, China

E-mail: phywang@jhu.edu

As a representative of the 3rd generation semiconductors, the wide band-gap with a large exciton binding energy and biexciton binding energies (on the order of 25 meV thermal energy) at room temperature make ZnO attractive for low-cost and high-efficiency LEDs and lasers near the UV band. However, a major challenge for development of ZnO-based devices is to stabilise the high-quality *p*-type ZnO at room temperature due to the self-compensation or lattice relaxation. Although the native defects in ZnO have been sophisticatedly investigated and understood¹, the stable and reliable acceptors in ZnO bulk are rarely achieved experimentally. On the other hand, the high-Q WGMs lasing in ZnO microrods with tens of microns in diameter was achieved in previous studies². Unfortunately, few studies focused on the tailored ZnO microtube microcavities owing to a lack of fabrication technique. In this work, we report a novel technique to grow high quality free-standing undoped acceptor-rich ZnO microtubes with dimensions of ~100 μm (in diameter) \times 5 mm (in length) by optical vapour supersaturated precipitation, as shown in the Figure 1. The extraordinary optoelectronic properties of the ZnO microtube are revealed, and several novel applications (e.g. mimetic *p-n* homojunction, low-threshold UV microlasers, multicolor light source, etc.) are demonstrated. It opens up new ways to achieve novel ZnO-based electronic and optoelectronic devices for a variety of applications.

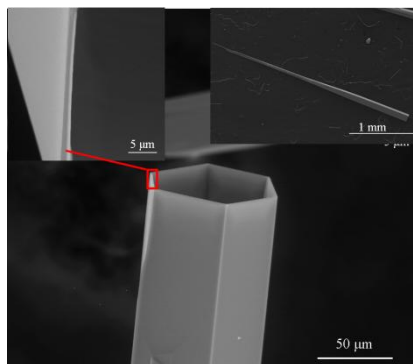


Figure 1. The micromorphology of a single ZnO microtube.

References:

1. A. Janotti, C. G. Van de Walle, *Phys. Rev. B*, 2007, **76**, 165202.
2. J. Dai, , C. X. Xu, K. Zheng, C. G. Lv, Y. P. Cui, *Appl. Phys. Lett.*, 2009, **95**, 241110.

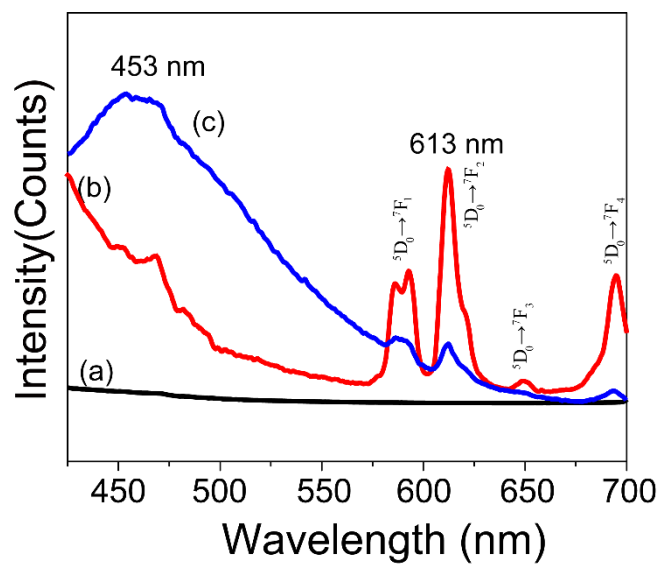
Poster 16

The Preparation and Properties Investigation of 5-Aminolevulinic Acid Intercalated Composites

Qingyang Gu, Jinyan Li

Beijing Institute of Petrochemical Technology, No.19 of Qingyuan Road,
Huangcun Town, Daxing District, Beijing, 102617
E-mail: guqingyang@bipt.edu.cn

Layered rare-earth hydroxides (LRHs), one new intriguing family of layered materials, with general formula of $[\text{RE}(\text{OH})_{2.5} \cdot x\text{H}_2\text{O}] \cdot [\text{A}^n]_{0.5/n}$ (RE = rare-earth ions, A = anions), have attracted increasing attention due to the rich intercalation chemistry^{1,2}. 5-aminolevulinic acid (5-ALA) is intercalated into the gallery of NO_3^- type layered europium hydroxide ($\text{NO}_3\text{-LEuH}$) by ion-exchange method, forming the composite of 5-ALA-LEuH. The prepared products display XRD patterns with series of diffractions attributing to layered materials. The composite corresponds to a monolayered vertical arrangement. The thermal stability of the composite is enhanced after intercalation. The composite shows blue emission at 453 nm under the excitation of 395 nm. This work may be beneficial to the fabrication of multifunctional drug molecule intercalated layered rare-earth hydroxides (LRHs) hybrid, which may have wide applications in drug deliver materials.



References:

1. J.B. Liang, R. Ma, F.X. Geng, Y. Ebina, T. Sasaki, *Chem. Mater.*, 2010, **22**, 6001.
2. F. Geng, Y. Matsushita, R. Ma, H. Xin, M. Tanaka, N. Iyi, T. Sasaki, *Inorg. Chem.*, 2009, **48**, 6724.

Poster 17

Toughness Enhancement of Poly(Lactic Acid) through Hybridisation with Epoxide-Functionalized Silane via Reactive Extrusion

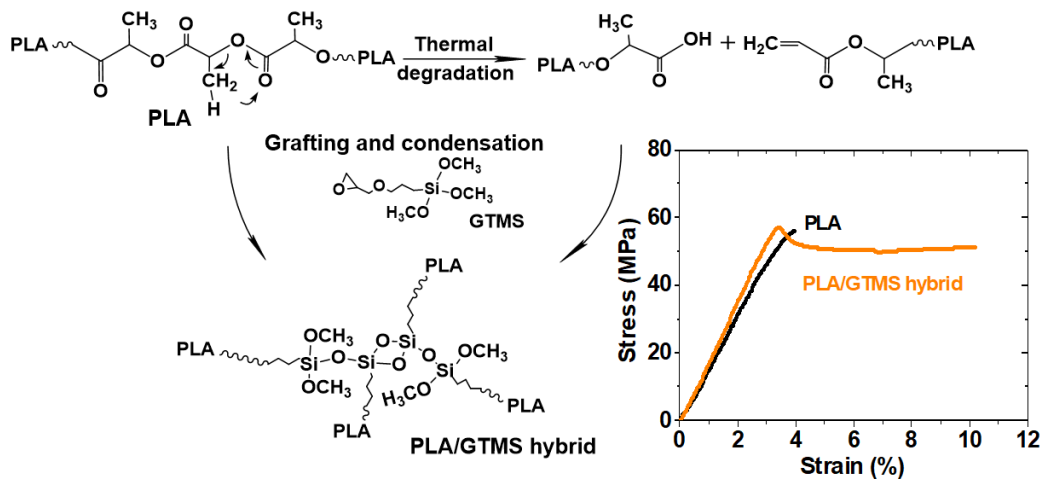
Jae-Choon Lee^{a,b}, Myeon-Cheon Choi^a, Dong-Hee Choi^b, Chang-Sik Ha^a

^a Department of Polymer Science and Engineering, Pusan National University, Busan 46241, South Korea

^b Technical Research Laboratories, WAPS Co. Ltd., 45, Centumdong-ro, Haeundae-gu, Busan, 48059, Korea

E-mail: jchlee@waps.com

Poly(lactic acid) (PLA) was hybridized with epoxide-functionalised silane (GTMS) through reactive extrusion. The GTMS was successfully grafted to PLA via ring-opening reaction by nucleophilic end groups of PLA. For the hybridisation, PLA was extruded with various amounts of GTMS between 0 and 2.0 phr at 200°C. The PLA hybrids were characterised by Fourier transform infrared (FTIR) spectra and scanning electron microscopy. Their properties were investigated through tensile testing, differential scanning calorimetry, thermogravimetric analysis, dynamic mechanical analyzer, and rheological characterization. The glass transition temperature of the hybrids decreased to 52.7°C compared to that of PLA (60.1°C). The toughness was enhanced significantly by approximately 380% with only 0.5 phr loading of GTMS. The hydrolytic degradation was also delayed by the hybridised GTMS in the PLA matrix. In conclusion, hybridisation by GTMS influenced thermal, mechanical and degradable properties of the PLA hybrids substantially.



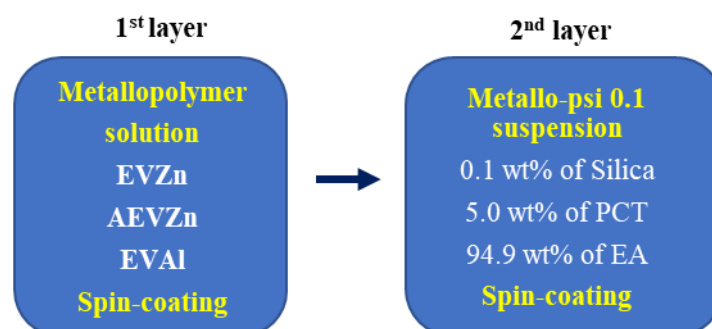
Design and Fabrication of Robust and Transparent Amphiphilic Metallopolymer Coatings

*Yubin Jeon, Saravanan Nagappan, Chang-sik Ha**

Department of Polymer Science and Engineering, Pusan National University,
Busan 46241, Republic of Korea
E-mail: yoojeon@gmail.com

The control of surface wettability through a combination of surface roughness, chemical composition, and structural modification has attracted significant attention for a variety of applications.

In this report, we introduce an amphiphilic metallopolymer, which involves transition metal ions for exhibiting its own property, such as anti-microbial activity, by two steps of spin-coating method. At first step of coating, the glass substrates which were coated with metallopolymer solution showed hydrophobic property, while at subsequent second step, spin-coated with psi 0.1 suspension exhibited hydrophilic property. The combination of these features rendered our novel coating materials as anti-bacterial, anti-fog property with extremely high hardness and transparency.



Scheme 1. Recapulative table of layer by layer (LBL) process for amphiphilic metallopolymer coatings.

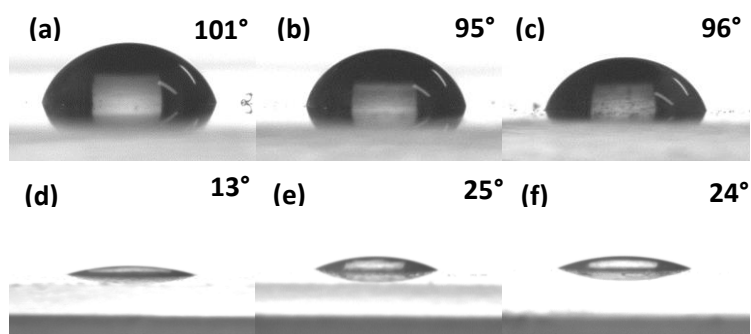


Figure 1. Water Contact Angle of glass substrate coated with metallopolymer solutions (a~c) and psi-0.1 suspension by multilayer method (d~f).

References:

1. S Nagappan, SS Park, EJ Yu, HJ Cho, JJ Park, WK Lee, CS Ha, *Journal of Materials Chemistry A*, 2013, **1 (39)**, 12144-12153
2. S Nagappan, MC Choi, G Sung SS Park, MS Moorthy, SW Chu, WK Lee, CS Ha, *Macromolecular Research*, 2013, **21(6)**, 669-680

Poster19

Anion Exchangeable Separator Mimicking Spiderweb for Lithium Sulfur Battery

Yong-Hyeok Lee, Sang-young Lee*

Ulsan National Institute of Science and Technology, Ulsan 44919, Korea

Email: for723@unist.ac.kr

Lithium-sulfur (Li-S) batteries have garnered considerable interest as a promising alternative to current state-of-the-art Li-ion batteries. However, the shuttle effect poses a formidable challenge to development of Li-S batteries. Considering that all ions in electrolytes move through separators between electrodes, significant attention should be paid to separators to prevent the shuttle effect. Here, we demonstrate a new class of spiderweb-mimic, anion-exchangeable separators based on polyionic liquids (“spiderweb separators”) to address the aforementioned issue. The spiderweb separator consists of sandwich-type functional nanomats (top/bottom layers = MWCNTs-wrapped PEI nanomats, middle layer = PVIm[TFSI]/PVdF-HFP nanomat) on PE separator. The middle nanomat layer enables (discharge voltage-dependent) reversible trap/release of polysulfides via an anion exchange reaction between TFSI- anions (from PVIm[TFSI]) and polysulfides. The top/bottom nanomat layers respectively act as an upper current collector and a blocking layer to prevent crossover of polysulfides to Li anodes. The spiderweb separator prevents the shuttle effect while ensuring facile ion transport, leading to exceptional improvement in the electrochemical performance (capacity = 819 mAh g⁻¹ and cycling retention = 72% (at 2.0 C/2.0 C) after 300 cycles).

Keywords: Lithium sulfur battery, Functional membrane, Anion exchange, Electrospinning, Poly ionic liquid

Complexation Behavior of Fulvic Acid with Heavy Metal Ions

Jintong Du^{1,2}, Piyue Gong¹, Aifang Geng², Haiying Huang^{1*}

¹State Key Laboratory of Polymer Physics and Chemistry, Changchun Institute of Applied Chemistry, Chinese Academy of Sciences, Changchun, 130022, P. R. China

²School of Chemistry and Environmental Engineering, Changchun University of Science and Technology, Changchun 130022, China E-mail: jtdu@ciac.ac.cn

Fulvic acid (FA) is considered to be the most active macromolecules of humic substances in natural organic matter, which plays an important role on regulating the ecological effects of heavy metal ions on earth, such as chemical cycle, migration and transformation.¹ Owing to the higher activity of its functional groups, it can reduce the toxicity of heavy metal ions with much higher sorption capacity compared with humic acid.²⁻³ Nevertheless, it remains challenging for precise description of their structure information and characterization of chemical and physicochemical properties because of its heterogeneous and polydisperse nature, an intensive study of complexation process of FA-metal ions is therefore of fundamental importance.

In this work, we studied the stability, size and morphology of FA complex with CdCl₂ by dynamic light scattering (DLS), scanning electron microscopy (SEM) and transmission electron microscopy (TEM). We found that HA in aqueous solution form rod-like complexes, and their size strongly depends on the pH of solution, i.e. the complexes formed at pH=2.3 and pH=12 are significantly larger than that of other pH values. Addition of CdCl₂ into FA solution leads to the formation of larger aggregates, above a critical metal ion concentration, the solution loses its stability and the aggregates precipitate. In this way, we were able to establish the relationship between ion adsorption and FA complex structure under different conditions, which can gain further insight into the underlying adsorption and aggregation kinetics of FA-metal ions in soil and aquatic environments.

References:

1. O. Oriekhova, S. Stoll, *Chemosphere*, 2016, 144, 131.
2. F. J. Stevenson, *Humus Chemistry: Genesis, Composition, Reactions*, 1994, Wiley-Interscience, New York.
3. S. Lalas, V. Athanasiadis, and V. G. Dourtoglou, *Clean-Soil, Air, Water*, 2018, 46, 1700608.

Poster21

Sealing of PEO Layers on Ti Alloy with Zirconia-Filled Sol-Gel Coatings and its Tribocorrosion Performance

Tianlu Li^a, You Zhang^a, Li Li^a, Kang Wang^a, Fei Chen^{a,b,*}

a College of Materials Science & Engineering, Beijing Institute of Petrochemical Technology, Beijing 102617, China

b Beijing Key Lab of Special Elastomer Composite Materials, Department of Material Science and Engineering, Beijing Institute of Petroleum Technology, Beijing 102617, China

* Corresponding author.

E-mail: chenfei@bipt.edu.cn

In the ocean titanium alloy not only suffered friction, but also corrosion of sea. In a certain extent, it limits its application. Therefore, dealing with the surface of titanium alloy is essential. Thus, the protective composite coating can be deposited on the titanium alloy by plasma electrolytic oxidation (PEO)/sol-gel technology. The coating consists of a PEO layer and different levels of ZrO₂ sol-gel layers. The phase composition and morphology of the composite coating were analyzed to determine the construction and performance of the coating. The static corrosion resistance of the sample was measured using electrochemical impedance spectroscopy (EIS) and polarization. The tribocorrosion performance is measured by the coefficient of friction (COF) in the reciprocating frictional motion, the open circuit potential (OCP) during the corrosion process. The results show that ZrO₂ particles have the best performance when the concentration is 10g.

Poster22

Preparation and Characterization of Black Phosphorus-Carbon Nanotubes Composites

Shangzhou Liu, Ziqian Yu, Xiaorui Wang, Huiqin Lian*

College of Materials Science and Engineering, Beijing Institute of Petrochemical Technology, Beijing 102617, China
E-mail: lianhuiqin@bipt.edu.cn

As a layered 2D material, black phosphorus (BP) has virtues of tunable bandgap by controlling the number of layers and the high surface area, it has the potential application in the field of energy storage with high energy density. However, as a semiconductor material, pure BP has low conductivity which limits its application as an electrode material. It is well known that carbon nanotube has excellent conductivity which is a good candidate electrode material. Therefore, it is reasonable to fabricate an electrode using BP- CNT composite which combine to improve the performance of energy storage device.

A novel BP /CNT composite were prepared through in-situ growth of BP on the surface of CNT using metal based catalyst through two-step method. First, metal based catalyst-CNTs composite was fabricated. Then the BP growth on the surface on the catalyst-CNTs composite surface forming the CNT-BP composite materials. Such CNT-BP materials with uniform constructure provides ideal functional properties to enhance the energy storage capacity.

References:

1. Anasori B, Lukatskaya M R, Gogotsi Y. *Nature Reviews Materials*, 2017, **2(2)**:16098.
2. Liu H, Neal A T, Zhu Z. *ACS nano*, 2014, **8(4)**: 4033-4041.

Preparation of P(NIPAM-co-AMIM[X]) Microgel and Rheological Properties of Aqueous Solution

*Qing Xu Wen, Yong Wang, and Ying Dan Liu**

State Key Lab of Metastable Materials Science and Technology, and College of Materials Science and Engineering, Yanshan University, Qinhuangdao, China

E-mail: ydliu@ysu.edu.cn

Poly(N-isopropylacrylamide) (PNIPAM) is a kind of thermosensitive polymer. As the temperature increases, it presents a phase transition with the lower critical solution temperature (LCST) of about 32°C. As a kind of intelligent polymer material, PNIPAM has unique temperature sensitivity, which makes it widely used in biochemistry, communication sensing, catalysis, ion adsorption¹ and other fields. Ionic liquid (IL) is an organic or inorganic salt composed of ions in a liquid state at room temperature². It has stability, high flame retardancy, low saturated vapor pressure and high ion conductivity therefore can be applied in fields such as catalysts, polymer chemistry, energy engineering, and bioengineering³.

In this study, we used 1-allyl-3-methylimidazolium salt (AMIM[X]) (ion X is Cl⁻ and BF₄⁻) as the comonomer to prepare copolymers of NIPAM and ILs. The effect of counterion on the system was investigated by selecting different counter anions. The rheological behavior, its mechanical properties and the influence of comonomer on the system were studied by rheological properties. Rheology analysis showed that below the phase transition temperature, the system was a low viscosity Newtonian fluid. Above the phase transition temperature, it behaved as a highly viscous pseudoplastic fluid. This was due to the introduction of an ion system. Different counterions had different effects on the aqueous solution of the copolymer. By selecting the cation monomers of the two counterions of Cl⁻ and BF₄⁻ and changing the proportion of comonomers, it was found BF₄⁻ interacted with water more strongly than Cl⁻. Therefore the system had lower viscosity and higher phase transition temperature.

References:

1. M. Muratalin, P.F. Luckham, *J Colloid Interface Sci*, 2013, **396**, 1-8.
2. E.J. Kim, S.H. Cho, S.H. Yuk, *Biomaterials*, 2001, **22(18)**, 2495-2499.
3. T.L. Greaves, C.J. Drummond, *Chem Rev*, 2008, **108(1)**, 206-237.

Poster24

High Performance of Supercapacitor Based on Simultaneous Redox of Polyaniline and Bromide Ions

Lei Zu, Huiqin Lian, Xing Gao, Ce li and Xiuguo Cui**

Beijing Key Lab of Special Elastomer Composite Materials, College of Materials Science and Engineering, Beijing Institute of Petrochemical Technology, Beijing 102617, PR China

* Corresponding author: lianhuiqin@bipt.edu.cn; cuixiuguo@bipt.edu.cn

A novel supercapacitor system with an ultrahigh electrochemical performance was prepared by applying a multi-walled carbon nanotubes (MWCNTs) – polyaniline (PANI) composite electrode and a redox potassium bromide (KBr) electrolyte.^{1,2} The composite electrode possessed a good conductivity and a consecutive 3D conductive network. The amazing electrochemical performance came from the simultaneous redox reaction in both electrode and electrolyte. The maximum discharge specific capacitance was up to 3100 F/g (0.1 A/g) when the concentration of KBr electrolyte was only 0.01 M in a three-electrode system. After 1000 charge-discharge cycles, it still reached to 1340 F/g when the current density was increased to 1 A/g. Furthermore, the specific capacitance, energy density and power density of 652 F/g, 80.7 Wh/kg and 401.7 W/kg, respectively, were also obtained in an asymmetric two-electrode system.

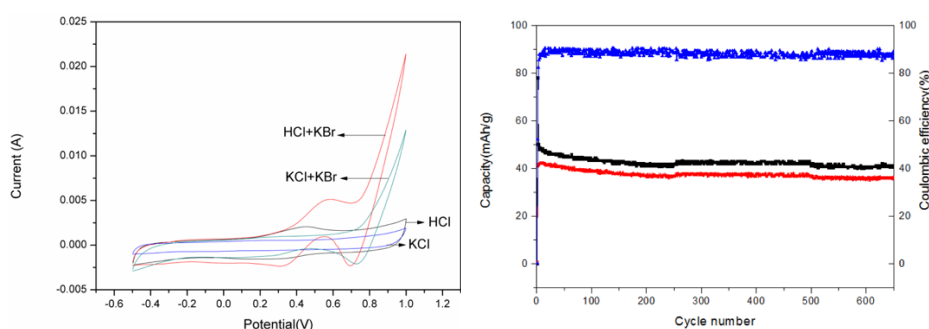


Fig1: (a) CV curves of MWCNT-polyaniline in KBr electrolyte.(b) Charging-discharging stability of MWCNT-polyaniline in KBr electrolyte.

Keywords: Supercapacitors; Simultaneous redox; Polyaniline; Bromide ions

References:

1. X. Wang, R.S. Chandrabose, S.E. Chun, et al. High Energy Density Aqueous Electrochemical Capacitors with a KI-KOH Electrolyte.[J]. *Acs Appl. Mater. Inter.* 2015, **7**, 19978.
2. S. Roldán, C. Blanco, M. Granda, et al. Towards a Further Generation of High-Energy Carbon-Based Capacitors by Using Redox-Active Electrolytes.[J]. *Angew. Chem. Inte. Edit.* 2011, **50**, 1699.

One-Dimensional Nanohybrid Based on Cobalt Porphyrin and Carbon Nanotube for Lithium-Ion Battery Anodes

Kihun Jeong, Ju-Myung Kim, and Sang-Young Lee

Energy and Chemical Engineering, Ulsan National Institute of Science and Technology (UNIST), Ulsan 44919, Republic of Korea
E-mail: jkh1905@unist.ac.kr

Multi-redox organic electrode materials have been emerging alternatives to the widespread inorganic counterparts in advanced power sources due to their design diversity, light weight, flexibility, and environmental benignity.¹ However, their electrically insulating nature, limited capacity, and poor durability have posed formidable challenges for the practical application.

Here, we present a one-dimensional (1D) nanohybrid comprising a multiwalled carbon nanotube (MWCNT) core and a cobalt porphyrin shell (**Figure 1**) as a new class of lithium-ion battery (LIB) anode materials.² π -conjugated *meso*-tetrakis(4-carboxyphenyl) porphyrinato cobalt (CoTCPP) shows good affinity for MWCNT and reversible multi-electron redox capability, leading to the successful formation of the 1D nanohybrid with high specific capacity. The resultant nanohybrid, due to its structural uniqueness, facilitates electron transport and electrolyte accessibility, which contribute to improving redox kinetics.

Furthermore, intrigued by the 1D structure of the nanohybrid, an all-fibrous nanomat anode was fabricated through concurrent electro-spraying/-spinning processes. The nanomat anode provides bicontinuous electron and ion conduction pathways, which eventually realizes the well-distinguishable lithiation behavior of CoTCPP and exceptional electrochemical performances with a long-term stability.

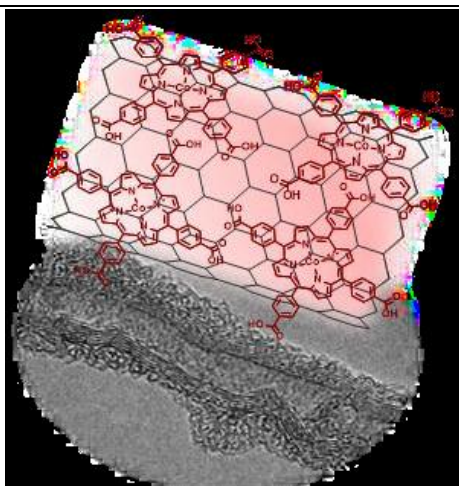


Figure 1. 1D nanohybrid based on MWCNT (core) and CoTCPP (shell).

References

1. T. B. Schon, B. T. McAllister, P. F. Li, D. S. Seferos, *Chem. Soc. Rev.*, **2016**, **45**, 6345.
2. K. Jeong, J.-M. Kim, S. H. Kim, G. Y. Jung, J. Yoo, S.-H. Kim, S. K. Kwak, and S.-Y. Lee, *Adv. Funct. Mater.*, **2019**, **29**, 1806937.

Fabrication of Acceptor-Rich ZnO Microtube/*n*-ZnS Heterojunctions for Highly Efficient Photodegradation of Organic Dyes

Wu Xia^a, Yue Wang^a, Yinzhou Yan^b, Yijian Jiang^b

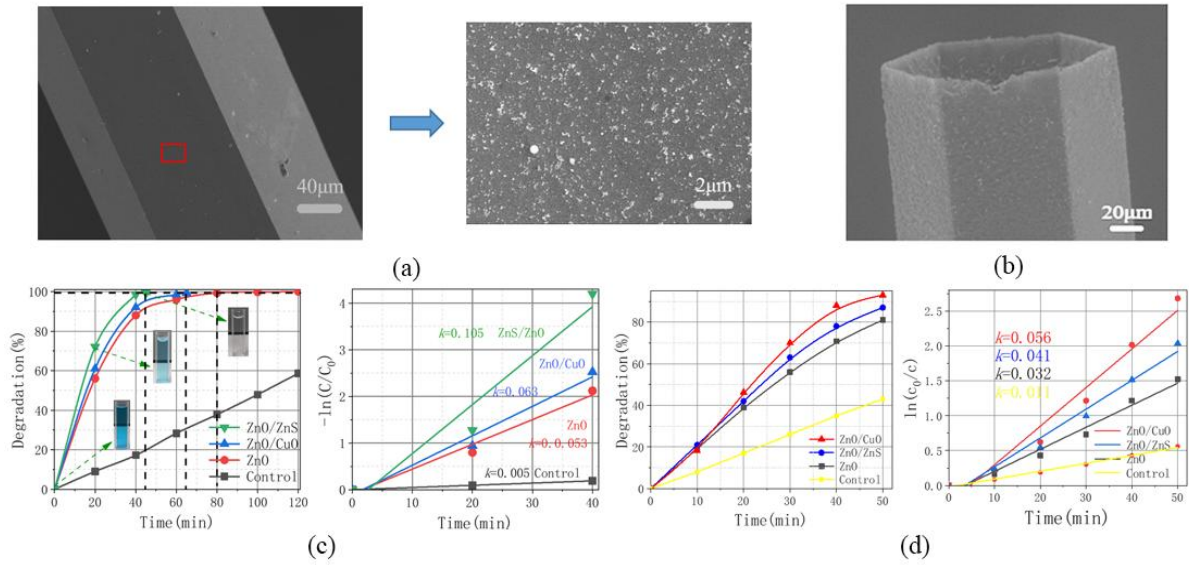
^aCollege of Applied Sciences, Beijing University of Technology, Beijing 100124, P. R. China

^b Institute of Laser Engineering, Beijing University of Technology, Beijing 100124, P. R. China

E-mail: yjjiang@bjut.edu.cn

The acceptor-rich ZnO (A-ZnO) microtubes fabricated by optical vaporization supersaturated precipitation (OVSP) process massive Zn-vacancy-related shallow acceptor carries and extraordinary optical properties, e.g. temperature-dependent luminescence, ultralow-threshold UV lasing, on-chip integrated photocatalysis, etc. Designing heterojunction to separate photogenerated carriers and broaden working band is a feasible way to further improve the catalytic efficiency for degradation of organic dyes. Considering the high concentration of acceptor carries of A-ZnO microtubes, the Fermi level is lower than undoped *n*-ZnO. Therefore, it is essential to select a suitable *n*-type material for a heterojunction structure with A-ZnO microtube. In this work, we employ solid state reaction to deposit *p*-CuO and *n*-ZnS on the surface of A-ZnO microtube, respectively, to explore the effect of heterojunction on the efficiency and stability of photocatalytic performance. Considering the massive acceptor carries, A-ZnO/*n*-ZnS forms a heterojunction of type II, significantly enhancing the separation process of photogenerated carriers. The *p*-CuO/A-ZnO heterojunction has a rate of increased photodegradation ~1.2 times higher than the A-ZnO microtube.

Fig.1. Morphology and photocatalytic degradation rate of A-ZnO based heterojunctions. (a) Morphology of A-ZnO/*n*-ZnS. (b) Morphology of *p*-CuO/A-ZnO. (c) Degradation rate of



A-ZnO based heterojunctions and the first-order kinetics. (d) Degradation efficiency of traditional *n*-ZnO based heterojunctions and the first-order kinetics.

Comparably, the rate of A-ZnO/*n*-ZnS heterojunction increased by ~1.8 times indicates that the V_{Zn} -related acceptor carries in A-ZnO microtube are activated efficiently. The present work provides a novel way for the design of a ZnO-based photocatalytic heterojunction for high-efficient on-chip degradation.

References:

1. W. Xia, *et al.* **APPL. SURF. SCI.** Submitted

The Electroluminescence of Ga: ZnO Microrod Grown by Optical Vapor Supersaturated Precipitation

Cheng Xing, Yinzhou Yan, Qiang Wang, Yijian Jiang

Institute of Laser Engineering, Beijing University of Technology, Beijing 100124,
China.

E-mail: yyan@bjut.edu.cn

ZnO is the most used host material for low threshold ultraviolet laser on chip due to its wide bandgap of 3.37 eV and large binding energy of 60 meV. Unfortunately, the limit in preparation of *p*-type ZnO restricts the development of ZnO-based homojunction for optoelectronic devices in the UV band. Our previous work has demonstrated the feasibility to realize undoped acceptor-rich ZnO by optical vapor supersaturated precipitation (OVSP)^[1]. In addition, the high finish quality of the ZnO single-crystal microtube grown by OVSP can be used as an optical microcavity with superior performance in high-efficiency fluorescence control, low-threshold ultraviolet laser and on-chip integrated photocatalysis^[2].

Here we report a novel technique to manipulate the energy band structure of Ga: ZnO (GZO) microrod by carbon-thermal optical vapor supersaturated precipitation (CT-OVSP). The typical dimensions of the microrod are ~100 μm (in diameter) \times 1.5 mm (in length). The major defects are confirmed from the O and Zn related vacancies by XPS, Raman and temperature-dependent PL spectra. The visible electroluminescence (EL) at 520 nm with a significant redshift up to ~100 nm can be achieved by increasing the injection current density. Meanwhile, the near infrared emission at 950-910 nm was blue shifted by ~40 nm. The EL color is therefore manipulated efficiently in the metal-semiconductor-metal structure. The present work provides a novel platform to exploit multi-wavelength light sources in GZO for light/displaying in nanophotonics.

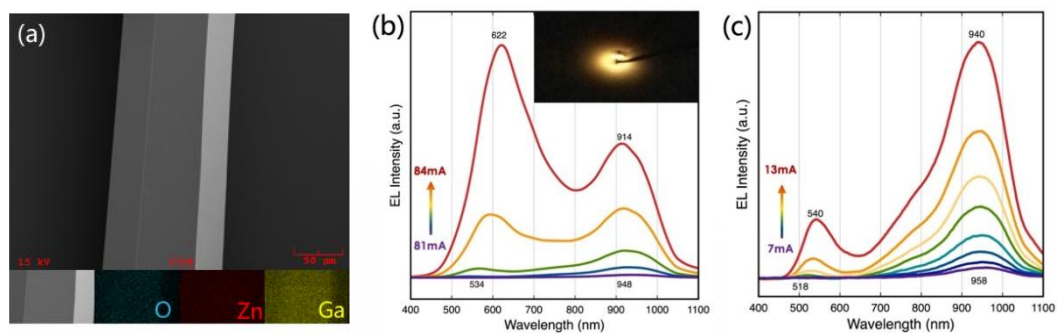


Figure 1. SEM, EDS and EL spectra of ofGZO microrod. (a) SEM and EDS of a typical GZO microrod. (b), (c) EL spectra of GZO microrod grown in (b) 15%-O₂/85%-Ar and (c) 25%-O₂/75%-Ar ambience.

References:

1. Wang Q, Yan Y*, *et al. Sci. Rep.*, 2016, **6**, 27341.
2. Wang Q, Yan Y*, *et al. NPG Asia Mater.*, 2017, **9**, e44.

Giant Enhancement of Unidirectional Photoluminescence by a Microsphere-Cavity-Array capping on QDs/PDMS Composite Film for Flexible Lighting and Displays

Lixue Yang¹, Lin Li², Yinzhou Yan¹, Yijian Jiang¹

¹ Institute of Laser Engineering, Beijing University of Technology, Beijing
100124, China

² Laser Processing Research Centre, School of Mechanical, Aerospace and
Civil Engineering, The University of Manchester, Manchester M13 9PL, UK
E-mail: yyan@bjut.edu.cn

The development of quantum dots (QDs) composite films for lighting and displays is of great importance, owing to their exceptional mechanical flexibility, chemical stability, and optical tunability. Unfortunately, the QDs/polymer film always suffers from the low quantum yield due to nonradiative processes in solid films. Although plasmonic and photonic crystals nanostructures have been proven to be an effective approach to enhance QDs-PL emission, the narrow working spectral bands restrict their applications in white-light illumination/displaying and the flexibility is unresolved so far. Herein, we report a novel method to boost and direct PL emission from the flexible QDs/PDMS composite film by a dielectric microsphere-cavity-array (MCA). The PL enhancement ratio is up to unprecedented three orders of magnitude with a highly-unidirectional emission angle of $\sim 9^\circ$. The light field regulation by optical whispering-gallery resonance and directional antenna effect in the micro-scale is revealed to interpret the mechanism of PL enhancement. Moreover, the enhanced white-light emission is realized, for the first time, by the MCA-capped RGB-QDs hybrid composite film structure. The present work opens up new opportunities for full-color luminescence enhancement in QDs-based flexible nanophotonic devices for energy-saving and highly-directional lighting/displays in future.

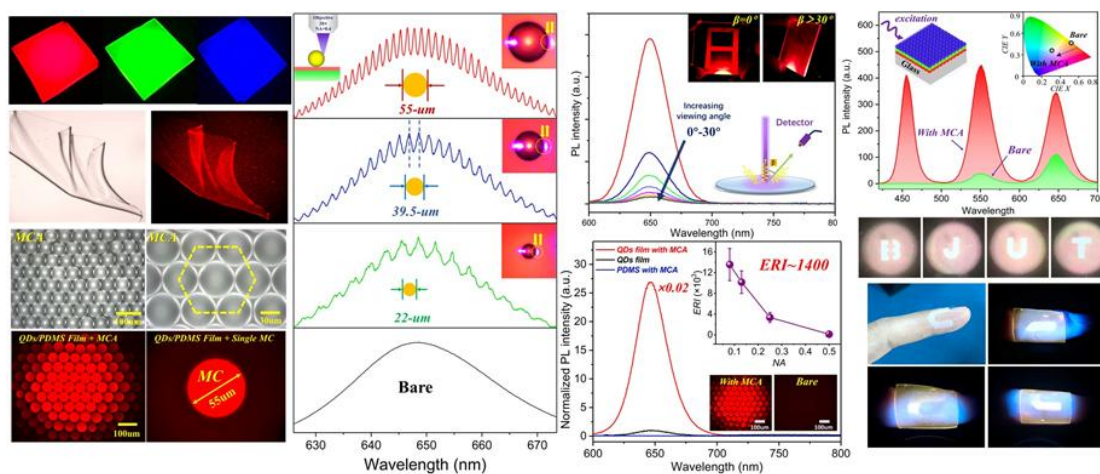


Figure 1 Optical properties of MCA-capped QDs/PDMS composite film

References:

- 1.L. Yang, *et al. Adv. Opt. Mater.* Under Review

Preparation of Aluminum-Based Silver Nanoarrays and the Ultraviolet-Visible-Near Infrared Absorption Properties

Lingling Liang, Yan Zhao and Chao Feng**

Institute of Laser Engineering, Beijing University of Technology, Beijing
100124, China

* Corresponding author: zhaoyan@bjut.edu.cn

Highly ordered periodic Ag nanosphere arrays were fabricated by vacuum evaporation based on AAO template. The size (diameter) and gap of silver nanospheres in the array are adjusted by controlling the thickness of evaporation, so that the absorption peaks and bandwidths of ultraviolet-visible-near infrared (UV-Vis-NIR) are modulated. On the basis of this, combined with FDTD (finite-difference time-domain) simulation, the absorption spectrum shows that ultraviolet strong absorption is Fano resonance induced by asymmetric dielectric environment of silver and aluminium; visible band absorption originates from local surface plasmon resonance of silver nanoparticles and near infrared band strong absorption is surface lattice resonance of silver nanosphere arrays (Figure 1). The study of continuous tunable technology of ultraviolet-visible-near infrared absorption peak position and peak width provides guidance for plasmonic metallic nanostructures, which is significant for solar cells, surface plasmon sensor devices, photocatalysis application^{1, 2}.

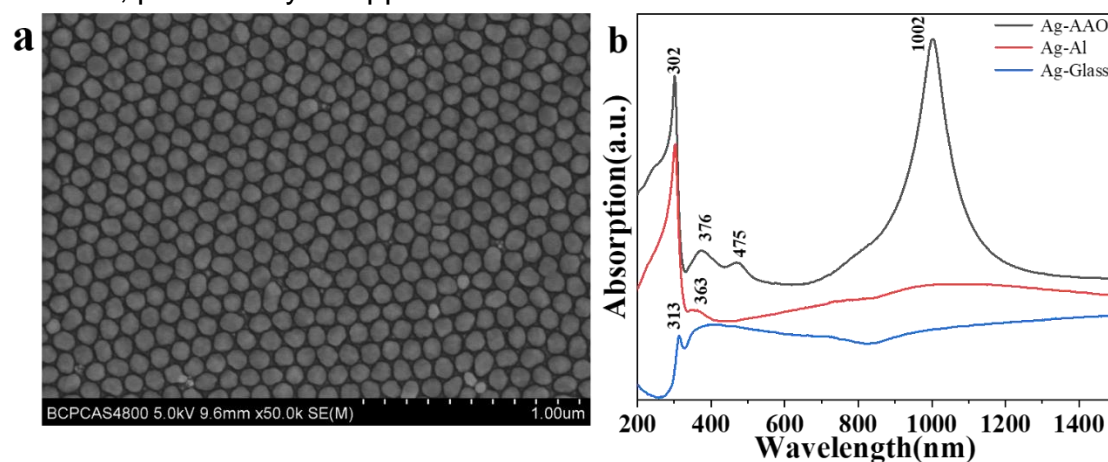


Fig1: (a) SEM image of periodic array of Ag nanospheres.(b) Absorption spectrum of silver composite structures prepared from different substrates

Keywords: Localized Surface Plasmon; band-width; peak-position; finite difference time domain; Farnot resonance

References:

1. Offermans P, Schaafsma M C, Rodriguez S R, et al. Universal scaling of the figure of merit of plasmonic sensors. [J]. *Acs Nano*, 2015, 5(6):5151-5157.
2. K. Ren, P. Yin, Y. Zhou, X. Cao, C. Dong, L. Cui, H. Liu, X. Du. Localized defects on copper sulfide surface for enhanced plasmon resonance and cater splitting [J]. *Small*, 2017, 13, 1700867.

Monolithic Heteronanomat Paper Air Cathodes Toward Origami-Foldable/Rechargeable Zn–Air Batteries

*Dongque Lee, Sang-Young Lee **

Ulsan National Institute of Science and Technology, Ulsan 44919, Korea
E-mail: lighter0919@gmail.com

The ongoing surge in demand for flexible/wearable electronics spurs us to explore high-performance power sources with various form factors. Here we demonstrate monolithic heteronanomat (MH) paper air cathodes as a new electrode platform to enable the fabrication of origami-foldable zinc (Zn)–air batteries with reliable electrochemical rechargeability. The MH paper air cathodes consist of one-dimensional (1D) bifunctional catalyst mixtures (NdBa_{0.5}Sr_{0.5}Co_{1.5}Fe_{0.5}O_{5+δ} double perovskite (NBSCF) nanofibers for the oxygen evolution reaction and nitrogen-doped carbon nanotubes (N-CNTs) for the oxygen reduction reaction), cellulose nanofibers (CNFs), and polytetrafluoroethylene (PTFE) nanoparticles, without the incorporation of conventional current collectors and gas diffusion layers. The CNFs and PTFE nanoparticles act as hydrophilic and hydrophobic binders, respectively, to construct three-dimensional (3D) bicontinuous electrolyte/air channels in the MH paper air cathodes. The well-developed electrolyte/air transport pathways, in combination with the rational design of the 1D bifunctional catalyst mixtures, enables the resultant Zn–air batteries (MH paper air cathode | CNF separator membrane | Zn–foil anode) to exhibit highly efficient charge/discharge performance and cyclability. In addition, the highly entangled network structure (based on a fibrous mixture of NBSCFs, N-CNTs, and CNFs) of the MH paper air cathode substantially improves its mechanical flexibility under various deformation modes, enabling the resultant Zn–air battery to be folded into a paper-airplane shape via origami folding.

Keywords: Zn–air batteries; Monolithic heteronanomat; Paper air cathodes; Origami–folding; Electrochemical rechargeability

Poster31

Ultrahigh Areal-Number-Density Printable On-chip Microsupercapacitor

*Kwon-Hyung Lee, Sang-Young Lee**

Ulsan National Institute of Science and Technology, Ulsan 44919, Korea

Email: kwon@unist.ac.kr

Microsupercapacitors (MSCs) have garnered considerable attention as a promising power source for microelectronics and miniaturized portable/wearable devices. However, their practical application has been hindered by the manufacturing complexity and dimensional limits. Here, we develop a new class of ultrahigh areal-number-density solid-state MSCs (UHD SS–MSCs) on a chip via electrohydrodynamic (EHD) jet-printing. This is, to the best of our knowledge, the first study to exploit EHD jet-printing in the MSCs. The activated carbon-based electrode inks are EHD jet-printed, creating interdigitated electrodes with fine feature sizes. Subsequently, a drying-free, ultraviolet-cured solid-state gel electrolyte is introduced to ensure electrochemical isolation between the SS–MSCs, enabling dense SS–MSC integration with on-demand (in-series/in-parallel) cell connection on a chip. The resulting on-chip UHD SS–MSCs exhibit exceptional areal-number-density (36 unit cells integrated on a chip (area = 8.0 × 8.2 mm²), 55.3 cells cm⁻²) and areal-operating-voltage (65.9 V cm⁻²).

1D Elementals-Internetworked Nanomat Electrode for High-Capacity Li-Ion Battery Cathodes

*Ju-Myung Kim, Sang-Young Lee**

Ulsan National Institute of Science and Technology, Ulsan 44919, Korea
Email: jmkst@unist.ac.kr

To date, numerous studies have been undertaken to incessantly improve electrochemical performances of lithium-ion batteries, with a particular focus on their energy density. Unfortunately, such a stereotyped electrode architecture often gives rise to non-uniform and sluggish electron/ion transport particularly in their through-thickness direction and is also vulnerable to structural disruption upon mechanical deformation. Here, as a facile and versatile electrode strategy to resolve the long-standing challenges of conventional electrodes mentioned above, we demonstrate a new class of nanomat-architected electrodes (referred to as nanomat electrodes), which comprise one-dimensional (1D) elementals of polyacrylonitrile (PAN) nanofibers/multi-walled carbon nanotubes (MWNTs)-mediated nanomat and densely packed electrode active particles. The nanomat electrodes are fabricated through simultaneous electrospinning (for MWNTs/electrode active powders) and electrospinning process (for PAN nanofibers) without the use of typical polymer binders, carbon powder conductive additives and metallic foil current collectors.

Keywords: Li-ion, Battery, Cathode, High-capacity

Single Lithium-Ion Conducting Covalent Organic Framework

Sodam Park, Sang-Young Lee*

Ulsan National Institute of Science and Technology, Ulsan 44919, Korea
Email: souldotcom@unist.ac.kr

Among numerous battery systems explored to date, all-solid-state lithium (Li) batteries and Li metal batteries have been extensively investigated as promising candidates for next-generation batteries, whose key technologies lie in solid-state Li-ion conductor. Previous studies on the solid-state Li-ion conductors have focused on inorganic sulfides/oxides or polymer-based ones. In addition to these traditional approaches, a new concept of solid-state Li-ion conductors based on porous crystalline materials such as covalent organic frameworks (COFs) and metal-organic frameworks (MOFs) has been pioneered as an appealing alternative due to their directional ion conduction pathways through the ordered pores and versatile structural design. We have demonstrated lithium sulfonated COF (TpPa-SO₃Li) designed to provide the well-defined ion channels, high number density of Li-ions, and covalently tethered anion groups. TpPa-SO₃Li to show the exceptional ion conduction characteristics ($\sigma=2.7\times 10^{-5}$ S cm⁻¹, $t_{\text{Li}^+}=0.9$ at room temperature, and $E_a=0.18$ eV), eventually contributing to the stable cycling of Li plating/stripping on Li metal electrodes. This study provides a new electrolyte strategy for next-generation batteries that are in urgent need of high-performance solid-state single-ion conductors.

Keywords: Single lithium-ion conductor, covalent organic framework

Poster34

Direct Ink Writing Based Solid-State Supercapacitors for Smart Contact Lenses

*Ahn David Byungsun, Sang-Young Lee**

Ulsan National Institute of Science and Technology, Ulsan 44919, Korea

Email: dave1231@unist.ac.kr

Recent advances in smart contact lenses are essential to the realization of medical applications and visual imaging for augmented reality through wireless communication systems. However, previous research on smart contact lens has been driven by a wired system or wireless power transfer with temporal and spatial restrictions, which can limit their continuous use and require energy storage devices. However, conventional rigid, large-sized, and fixed-shaped batteries are not suitable for the soft, smart contact lens. In this research, a wirelessly-rechargeable, solid-state supercapacitor integrated into a smart contact lens is realized. The solid-state supercapacitor was fabricated using a microscale direct ink writing (DIW) process. After printing the supercapacitor, all device components (antenna, rectifier, and LED) are fully integrated with stretchable structures for this soft lens without obstructing vision which provides a promising future of smart contact lenses.

Keywords: supercapacitor, solid-state, direct ink writing

Poster35

Antioxidative Lithium Storage Based on Nanoconfinement of Carbon Nanotube Bundles

*Seok-Kyu Cho, Sang-Young Lee**

Department of Energy Engineering, School of Energy and Chemical Engineering, Ulsan National Institute of Science and Technology (UNIST),
Ulsan 44919, Korea
Email: skcho@unist.ac.kr

Lithium (Li) metal has garnered considerable attention in next-generation battery anodes. However, its environmental vulnerability, along with the electrochemical instability and safety failures, poses a formidable challenge to commercial use. Here, we describe a new class of antioxidative Li reservoir based on interstitial channels of single-walled carbon nanotube (SWCNT) bundles. The Li preferentially confined in the interstitial channels exhibits unusual thermodynamic stability and exceptional capacity even after exposure to harsh environmental conditions, thereby enabling us to propose a new lithiation/delithiation mechanism in carbon nanotubes. To explore practical application of this approach, the Li confined in the SWCNT bundles is electrochemically extracted and subsequently plated on a copper foil. The resulting Li-plated copper foil shows reliable charge/discharge behavior comparable to those of pristine Li foils. Benefiting from the confinement effect of the interstitial channels, the SWCNT bundles hold great promise as an environmentally tolerant, high-capacity Li reservoir.

Keywords: Carbon nanotube bundles, Interstitial channels, Confinement, Antioxidation, Lithium storage

High-Performance Organic Electrode Using Heteromat-Framed Scaffold for Lithium-Ion Batteries

Seung Hyeok Kim, Sang Young Lee*

Ulsan National Institute of Science and Technology, Ulsan 44919, Korea
Email: tliver@unist.ac.kr

Electroactive organic-based electrode materials have garnered considerable attention as an emerging candidate to replace inorganic counterparts because of their lightweight, mechanical flexibility, and molecular diversity. Yet, their low energy and power densities associated with poor electronic conductivity and limited ion accessibility often impose a critical impediment for practical applications. Herein, we report that all-fibrous heteromat framework comprising intermingled polyacrylonitrile nanofibers and carbon nanotubes offers three-dimensional bicontinuous electron/ion conductive pathways toward organic-based active materials. At the same time, the framework eliminates heavy metallic current collectors to allow the overall mechanical flexibility of the rechargeable system. Nickel 2,6-naphthalenedicarboxylate (NiNDC) is prepared as a model organic-based anode material for this electrode strategy. Driven by the structural uniqueness, the self-standing heteromatNiNDC anode ultimately affords facile redox kinetics and outstanding electrochemical performance, while surpassing the performance of conventional lithium-ion battery organic-based anodes.

Keywords: Lithium-ion batteries; Organic ligand; High energy density; Heteromat structure; Flexibility

Poster37

Improving Optical and Electrical Properties of GaN Epitaxial Wafers and Enhancing Luminescent Properties of GaN-Based Light-Emitting-Diode with Excimer Laser Irradiation

Yijian Jiang^{1, 2*}, Haoqi Tan², Yan Zhao²

¹Beijing Institute of Petrochemical Technology, Beijing 102617, China

²Institute of Laser Engineering, Beijing University of Technology, Beijing 100124, China

The effect of 248 nm KrF excimer laser irradiation on the properties of epitaxial wafers with a p-GaN surface were investigated. The GaN epitaxial wafers with a p-GaN surface were irradiated with an excimer laser at different energy densities and pulse numbers. The irradiated samples were annealed in oxygen. The laser irradiation-induced changes in optical and electrical properties of GaN epitaxial wafers were examined using PL, I–V, XPS, SIMS and Hall test system measurements. Experimental results show that under an appropriate laser irradiated condition, optical and electrical properties of the samples were improved to different degrees. The samples which were annealed after irradiation have better electrical properties such as the hole concentration and sheet resistance than those without annealing. We hypothesize that the pulsed KrF excimer laser irradiation dissociates the Mg–H complexes and annealing treatment allows the hydrogen to diffuse out more completely under the oxygen atmosphere at a proper temperature. Under appropriate laser conditions and O₂-activated annealing, the light output of the laser-irradiated GaN-Based LED sample is about 1.44 times that of a conventional LED at 20 mA. It is found that the wall plug efficiency is 10% higher at 20 mA and the reverse leakage current is 80% lower at 5V.

* Corresponding author : jiangyijian@bipt.edu.cn

Poster38

Synthesis of Silver nanofiber Transparent Electrodes by Silver Mirror Reaction with Electrospun Nanofiber Template

Chunnuan Du, Xiaohui Lv, Yang Liu, Zikang Jia, Jianxiang Yu¹

College of Materials Science and Engineering, Institute of Petrochemical
Technology, Beijing, 102600, China

Abstract. Electrospinning and silver mirror reaction (SMR) were combined to synthesize silver nanofiber membrane. The sheet resistance (R_s) and transmittance (T) values reach around $51\Omega/\text{sq}$ and 83%, respectively. In this method, Poly(acrylonitrile-co-phenylethylene) (P(AN-S)) nanofiber act as the template and silver on the nanofiber surface act as seed. In SMR process, silver deposited on the surface of nanofiber and developed into silver nanofiber. The membrane was characterized by scanning electron microscopy (SEM), energy dispersive spectrometer (EDS) and X-ray diffraction (XRD). This process is easily controlled and takes place at ambient condition, which gives a new opportunity for transparent conducting flexible electronics.

Key words: nanoparticles; electrospinning; polymer composites; deposition

1. Introduction

Transparent conductors with suitable conductivity and transparency play important roles in many optoelectronic devices such as touchscreens, displays and solar cells. Sheet resistance (R_s) and transmittance (T) are the two important basic parameters for transparent electrodes. Currently, the dominant material for transparent conductors is indium tin oxide (ITO), but it's rare, high cost and brittleness, which limit its applications. So various candidates are being developed such as carbon nanotube, graphene, and silver nanofiber networks (C.F. Guo *et al.* 2015, P.C. Hsue *et al.* 2014). Among these novel transparent conductors, silver nanofiber networks are the most promising because of their high electrical conductivity and transmittance. There are many reported methods to prepare silver nanofibers, such as chemical synthesis, electrochemical process, hydrothermal method and ultraviolet irradiation photo detection technique (M. Huang *et al.* 2014, Y.S.K. Abe *et al.* 2007, H.S. Lee *et al.* 2015, H. Wu. *et al.* 2010.). Now preparation techniques of silver nanofibers have been developed, but there are still many problems in the application, for example, the sheet

¹Corresponding author, Dr. Jianxiang Yu, E-mail; yujianxiang@bipt.edu.cn

resistance is too large because silver fibers can't connect with each other in polymer matrix. Here we propose a facile method including electrospinning and silver mirror reaction to prepare silver nanofiber networks.

The process of preparing silver nanofibers transparent electrodes is shown in Fig. 1, partial AgNO_3 decomposed into silver nanoparticle in *N, N*-Dimethylformamide (DMF) when preparing the solution, so the colorless transparent solution turned into brown. The electrospun P(AN-S) nanofiber networks were applied as the template for silver deposition. In this work, because electrospinning can produce ultralong nanofiber, so silver nanofiber was obtained by SMR on the surface of electrospun P(AN-S) nanofiber.

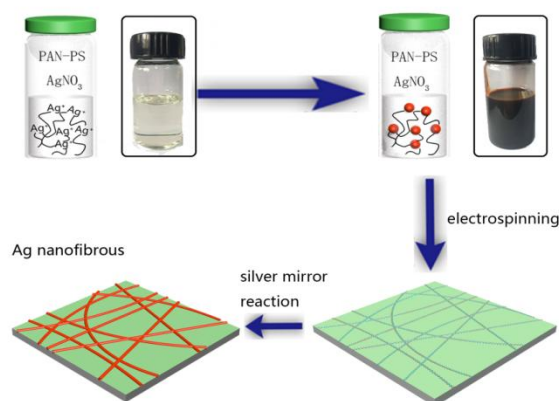


Fig.1. Schematic of silver nanofiber transparent electrodes

2. Materials and methods

2.1 Materials

P(AN-S) ($M_w=80000$, containing 31 wt.% AN units) was supplied by Sinopec Beijing Yanshan Co. (China). *N, N*-dimethylformamide (DMF) was purchased from Tiantai Chemicals Co. (China). Silver nitrate (AgNO_3), ammonium hydroxide (25 wt.%–28 wt.%) were supplied by Beijing Chemical Reagent Co. (China).

2.2 Electrospinning

P(AN-S) was first dissolved in DMF at 25 wt.% and stirred at room temperature for 12 h to obtain a transparent homogenous solution, then AgNO_3 was added into P(AN-S) solution and the concentration of AgNO_3 was adjusted to 10 wt.%. As the solutions were stirred overnight (12 h), the dark brown solution was obtained indicating the formation of silver nanoparticles in the electrospinning solution (A. Celebioglu *et al.* 2014). The electrospinning process was performed at room temperature, the solution was collected into a 5 mL injection syringe with a single nozzle, and the syringe was fixed on an electric pump set to maintain flow rate of the spin dope at 0.4 mL/h. A high-voltage power supply was employed to apply positive charge between the syringe tip and collector. The voltage used for electrospinning was 20 kV. Glass slide or PET sheet on aluminum foil was used as collector, and the tip-to-collector distance was fixed at 20 cm. For comparison, P(AN-S) solutions without AgNO_3 were also electrospun into membrane.

2.3 Silver nanoparticles loaded by SMR process

$[\text{Ag}(\text{NH}_3)_2]^+$ solution, was prepared by adding NH_4OH into 5g/L AgNO_3 aqueous solution dropwisely until the solution became clear again. The P(AN-S) nanofibrous membranes were immersed into 5g/L of glucose aqueous solution. The $[\text{Ag}(\text{NH}_3)_2]^+$ solution was then added dropwisely into the glucose aqueous solution for 20 min. The samples were washed with distilled water for three times.

2.4 Characterization

The morphology of nanofiber membrane before and after SMR was observed by a scanning electron microscope (Hitachi S-4300, Hitachi Co., Japan) with an accelerating voltage of 20 kV. Energy dispersive spectrometer (EDS) was used in conjunction with SEM for elemental analysis of the surface component. The XRD patterns of the samples were recorded on a wide-angle X-ray diffraction analyzer (WAXD, DX-2800, Dandong Haoyuan instrument Co., Ltd., China) under area detector operating at a voltage of 40 kV and a current of 200 mA using Cu K α radiation ($\lambda = 0.154$ nm), the scanning rate was 3°/min in the 2θ range from 10° to 90°. The sheet resistance was measured by a four-point probe tester (RTS-4, Suzhou Jingge Electronic Co., Ltd., China.). The average value was obtained from three position measurements for each sample. Light transmission scans were conducted using a WGW (QT005, Shanghai instrument scientific instrument Co., Ltd., China), white light, and a transmission scanner with a bit depth of 48 bits per pixel and a spatial resolution of 6400 dpi.

3. Results and discussion

The reduction of partial AgNO_3 into silver was achieved in P(AN-S) solution and P(AN-S) also stabilize the Silver nanoparticle by keeping them from aggregating [8]. Glass slide was spin-coated with 10 μm thick P(AN-S) polymer film before electrospinning, which can reduce silver deposition onto the substrate. Fig.1 showed the SEM morphology of sample, the spinning time was 1min, SMR time was 20min, the nanofiber is smooth and uniform before SMR, their average fiber diameters were about 400nm (Fig.2A), and they grew to 500-600nm after SMR reaction (Fig.2B), the surface of silver nanofiber is rougher than P(AN-S) nanofiber for the formation of silver crystal.

To prove the presence of silver crystal loaded on the surface of P(AN-S) nanofibers and investigate their crystal structure, X-ray analysis was used. The crystalline characteristics of the silver nanoparticles on P(AN-S) nanofiber membranes before and after SMR and P(AN-S) membrane are shown in Fig.2C. There are two wide diffraction peaks in XRD spectra of P(AN-S) nanofibers membrane, while the peaks become weaken when AgNO_3 were added into polymers, which destroyed the crystalline of polymer. When silver nanofibers formed from P(AN-S)/ AgNO_3 nanofibers by SMR, it has 4 diffraction peaks at $2\theta = 38.1, 44.3, 64.4$ and 77.5 , which belongs to (111), (200), (220) and (311) crystalline planes of silver, respectively, and there are not additional peaks about Ag_2O , this result is close to reference (Y. Shiet *al.* 2015). We could conclude that the silver existed in the form of single silver instead of Ag_2O .

Elementary analysis of Ag/P(AN-S) nanofibers was carried out by SEM-EDS, as shown in Fig. 2E. The results showed that carbon, oxygen and silver were the

principal elements. EDS analysis thus provided direct evidence that silver particles existed on the P(AN-S) nanofibers surface. As seen in Fig.2E, the silver content of Ag/P(AN-S) nanofibers reached 30.14 wt.%, The loaded silver content seemed to be high after SMR due to the strong anchoring mechanism of the ion–dipole interaction and the subsequent reduction of the silver particles on the large surface area of the P(AN-S) nanofibrous membranes (A. Celebioglu *et al.* 2014, Y. Shiet *et al.* 2015). EDS mapping (Fig.2D) of Ag/P(AN-S) nanofibers reveal the morphology, the yellow color in the EDS represents Ag characteristic radiation, and the Silver seed catalysts successfully facilitate deposition on the polymer nanofibers. the Silver nanofibers in our study are generally 500-600 nm in diameter, With the electrospun P(AN-S) nanofibers being about 400nm, the thickness of Silver is about 100-200 nm.

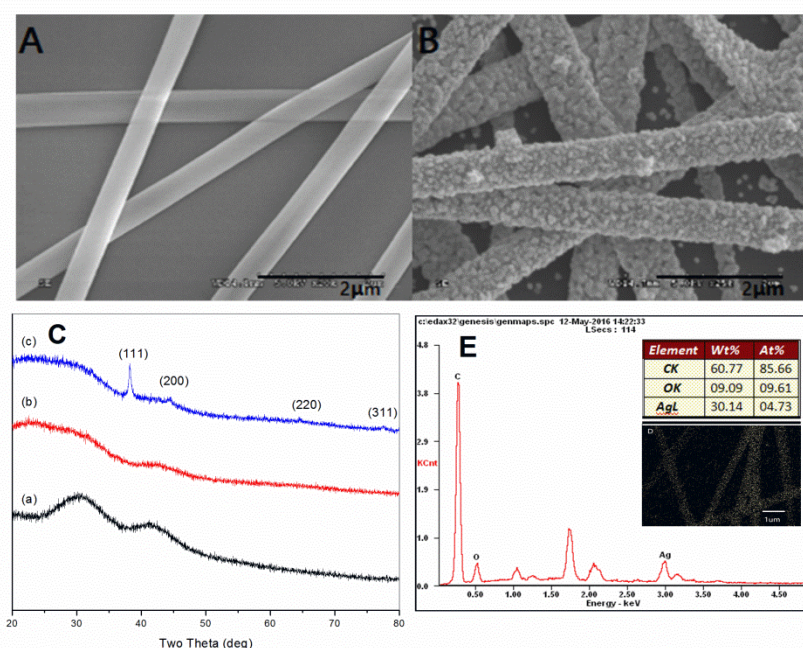


Fig.2.(A) SEM image of P(AN-S)/AgNO₃ nanofibers before SMR process, (B) SEM image of P(AN-S)/AgNO₃ nanofibers after SMR process,(C) XRD spectra of (a) P(AN-S) nanofibers, (b) P(AN-S)/AgNO₃ nanofibers (before SMR) (c) Silver nanofibers (after SMR). D: EDS mapping of silver nanofibers. E: EDS analysis of silver nanofibers.

Fig.3A shows the Rs–T relationship of silver nanofibers membrane in different parameters, which are effected by the process of electrospinning and silver mirror reaction. The best sample we prepared under the condition as list in experiment part has Rs and T values of 51Ω/sq and 83%, respectively, which are comparable to conventional transparent conductors. Actually, the performance requirement is depended on the application, electrode of large area displays requires low Rs of 20Ω/sq, and touch screens require Rs in the scope of 400–600Ω/sq (K. Azuma *et al.* 2014).

The silver nanofibers membrane also exhibit superior bending resistance compared to ITO. Fig.3B shows a bending test result of Silver nanofibers membrane collected on polyethylene terephthalate (PET) substrate. The bending test was carried out 100

times, with a bending radius of 4 mm. Rs of the ITO film increases 55 times after 100 cycles, while that of silver nanofibers almost not changed, this result are similar with reference (P.C. Hsuet *al.* 2014), silver nanofibers is composed of close packed silver crystal, which has good resistance to bending performance.

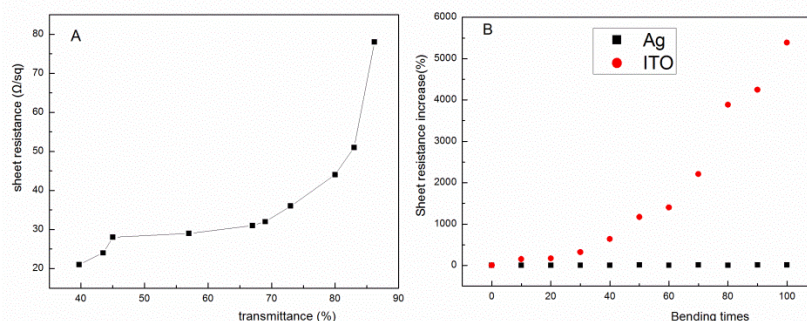


Fig.3.(A) Rs-T performance of Silver nanofiber membrane. (B) Percentage sheet resistance change after 100 bending cycles. The bending radius is 4 mm.

4. Conclusions

In summarize, silver nanofiber membrane was prepared by electrospinning and silver mirror reaction. This facile approach can produce transparent conductive film with comparable performance to conventional transparent conductors. The process was carried out at ambient condition and easily controlled, it has a much wider applicability and lower energy cost for flexible electronics. Further studies about the Silver nanofiber membrane are in progress, the better results will be reported in the future.

Acknowledgements

This work was supported by URT program of Beijing Institute of Petrochemical Technology (2017J00116 and 2018X00060).

References

1. C.F. Guo, Z.F. Ren. (2015), "Flexible transparent conductors based on metal nanofiber networks", *Mater. Today.* 3, 143-154.
2. P.C. Hsu, D. Kong, S. Wang. (2014), "Electrolessly deposited electrospun metal nanofiber transparent electrodes", *J. Am. Chem. Soc.* 136, 10593-10596.
3. M. Huang. (2014), "Novel hybrid electrode using transparent conductive oxide and silver nanoparticle mesh for silicon solar cell applications", *Energy Procedia*, 55, 670-678.
4. Y.S.K. Abe. (2007), "Transparent conductive film having sandwich structure of gallium-indium-oxide -silver-gallium-indium-oxide", *Mater. Lett.* 61, 3897-3900.
5. H.S. Lee. (2015), "Synthesis of dimension-controlled silver nanofibers for highly conductive and transparent nanofiber films", *Acta Mater.*, 83, 84-90.

6. H. Wu, L. Hu, M.W. Rowell. (2010), "Electrospun metal nanofiber webs as high-performance transparent electrode", *Nano Lett. Energy Procedia*, 10, 4242-4248.
7. A. Celebioglu, Z. Aytac, O.C.O. Umu. (2014), "One-step synthesis of size-tunable Silver nanoparticles incorporated in electrospun PVA/cyclodextrin nanofibers", *Carbohydr. Polym.*, 99, 808-816.
8. Y. Shi, Y. Li, J. Zhang. (2015), "Electrospun polyacrylonitrile nanofibers loaded with silver nanoparticles by silver mirror reaction", *Mater. Sci. Eng., C*. 51, 346-355.
9. K. Azuma, K. Sakajiri, H. Matsumoto, S. Kang, J. Watanabe, M. Tokita. (2014), "Facile fabrication of transparent and conductive nanofiber networks by wet chemical etching with an electrospun nanofiber mask template", *Mater. Lett.* 115, 187-189.

Poster39

Vertically Aligned MoS₂ Thin Films Prepared by RF-Magnetron Sputtering Method as Electrocatalysts for Hydrogen Evolution Reactions

XuePing Chen ^{a,b}, GuangJian Xing ^a, Linfeng Xu ^a, HuiQin Lian^a, Yanyan Wang^{a,*}

^a Beijing Key Lab of Special Elastomer Composite Materials, College of Materials Science and Engineering, Beijing Institute of Petrochemical Technology, 102617 Beijing, China

^b College of Materials Science and Engineering, Beijing University of Chemical Technology, 100029 Beijing, China
E-mail: wangyanyan528@bipt.edu.cn

A series of 50 nm-thick molybdenum disulfide (MoS₂) thin films were prepared by radio frequency (RF) magnetron sputtering method under Argon (Ar) pressure of 4 Pa, 2 Pa, 0.8 Pa and 0.5 Pa respectively. According to the morphology observed by Atomic Force Microscope (AFM) and the structure characterized by X-ray diffraction (XRD) and Raman spectra, the MoS₂ thin films exhibited a nearly vertically aligned morphology. The vertical aligning is an ideal edge-terminated structure to expose a most active sites, which results in a superior electrocatalytic hydrogen evolution reaction (HER) performance. Especially for the MoS₂ thin film under 0.8Pa exhibits a best HER performance, whose onset overpotential of the linear sweep voltammetry curve at the current density of 10mA/cm² is 149 mV, expected to be an ideal alternative electrocatalysts for platinum (Pt).

Preparation of Polyurethane Solid Electrolytes Adding Nanocarbon Material For Dye-sensitized Solar Cells

*Hongyu Feng, Tong Zhao, Yuhua Dai**

College of Materials Science and Engineering, Beijing Institute of Petrochemical Technology, Beijing 102617, P. R. China
E-mail: daiyuhua@bipt.edu.cn

Dye-sensitized solar cells (DSSCs) have become an important development direction of solar cells due to their commercial potential^{1, 2}. DSSC consists of a nano TiO₂ film of the photo electrode, dye molecules absorbed on the surface of TiO₂ film, an electrolyte layer and a Pt counter electrode. Among these, the electrolyte plays a key role in electron transport and dye molecular regeneration. The electrolyte usually used in the DSSCs is an I⁻/I³⁻ redox couple in an organic solvent. In this work, polyurethane solid electrolyte was synthesized by polyethylene glycol (PEG) and toluene diisocyanate (TDI). 1-methyl-2-pyrrolidone (NMP) was used as organic solvent, NaI/I₂ as redox couple, and a certain amount of graphene, multi-walled carbon nanotubes, multi-walled carbon nanotubes were added respectively. It was found that the DSSC based on polyurethane solid electrolyte, which doped 4×10⁻³ g of graphene obtained the highest power conversion efficiency (PCE) of 3.36% at 100 mW/cm².

Keywords: Polyurethane, graphene, Iodine, Sodiumiodide, Dye-sensitized solar cells

Reference:

1. S. Mozaffari, M. R. Nateghi and M. B. Zarandi, *Renewable and Sustainable Energy Reviews*, 2017, **71**, 675-686.
2. J. Liu, Y. Li, M. Li, S. Arumugam and S. P. Beeby, *IEEE Journal of Photovoltaics*, 2019, **9**, 1020-1024.

Preparation and Characterization of Polybenzimidazole Based 3D Printable Photocurable Dental Resin

Minyoung Lee, Wanhee Jeong, Ildoo Chung

Department of Polymer Science and Engineering, Pusan National University,
Busan 46241, Republic of Korea
E-mail: minyoung@pusan.ac.kr

Polybenzimidazole is well known for its thermal stability, chemical resistance, and excellent mechanical properties. Most resin monomers, which have been used in dental applications, need strong durability, small shrinkage, biocompatibility, and easy polymerization. Therefore, based on the properties of PBI, it is expected to overcome the problems of conventional dental restorative materials.

In this study, poly[2,2'-(m-phenylene)-5,5'-bibenzimidazole](PBI) was synthesized through condensation polymerization from isophthalic acid (IPA) and 3,3'-diaminobenzidine (DAB) in polyphosphoric acid (PPA) at 200°C for 24 hours. In addition, carboxylic acid-terminated PBI oligomer was synthesized by adjusting the mol ratio between IPA and DAB. Photopolymerizable PBI was also synthesized from carboxy-PBI oligomer and 2-hydroxyethyl methacrylate (HEMA) by Steglich esterification, and characterized by FT-IR, ¹H-NMR, ¹³C-NMR, TGA and GPC.

The synthesized polymer was formulated with ethoxylated bis-GMA (EBPDMA) in various ratios, and Irgacure 819 as a photoinitiator, photopolymerized by DLP 3D printer, then finally used to evaluate their compressive strength by universal testing machine (UTM).

References:

1. A. Ainla, D. Brandell, *Solid State Ionics*, 2007, **178**, 582
2. S. C. Kumbharkar, U. K. Kharul, *European Polymer Journal*, 2009, **45**, 3364.

Poster42

Preparation and Characterization of Poly(Ether Ether Ketone) Based 3D Printable Photocurable Dental Resin

Minyoung Lee, Wanhee Jeong, Ildoo Chung

Department of Polymer Science and Engineering, Pusan National University,
Busan 46241, Republic of Korea
E-mail: minyoung@pusan.ac.kr

Dental resins need strong durability, low shrinkage, biocompatibility and easy polymerization. In order to get better chemical and mechanical properties, we focused on poly(ether ether ketone) (PEEK) structure, which has excellent chemical, sterilization resistance, and mechanical properties, and synthesized etheretherketone based oligomer to investigate the possibility as dental restorative materials.

This study aims to synthesize methacryloyl-etheretherketone (MA-EEK) using hydroxyl-terminated etheretherketone (HEEK) and methacryloyl chloride (MAC) and characterize them by FT-IR, ¹H-NMR spectroscopies. The resin mixture was prepared by mixing MA-EEK and ethoxylated bis-GMA (EBPDMA) with the various ratio, and a silica derivative was added to improve the mechanical properties of the dental composite resin. To evaluate the mechanical properties, It was photopolymerized by DLP 3D printer and measured their mechanical properties, such as compressive and flexural strength.

This study investigated the possibility of dental resin by synthesizing resin monomer based on PEEK structure. It was characterized by FT-IR, ¹H-NMR and GPC, cured using a DLP 3D printer and glass tube, and mechanical properties were confirmed using UTM. The compressive strength of MA-EEK resin was higher than that of pure EBPDMA resin. The higher the MA-EEK ratio, the higher the compressive strength.

References:

1. K. B. Sagomonyants, M. L. Jarman-Smith, J. N. Devine, M. S. Aronow, G. A. Gronowicz, *Biomaterials*, 2008, 29, 1563

Poster43

Synthesis and Characterization of Carboxylic β -Cyclodextrin with Vitamin E/C

Mijin Jeong, Injun Song and Ildoo Chung

Department of Polymer Science and Engineering, Pusan National University
Busan 46241, Republic of Korea
E-mail: jmj2429@pusan.ac.kr

Vitamin E is a group of eight compounds that includes four tocopherols and four tocotrienols. Among all tocopherol isoform, α -tocopherol (α -TO) has the highest antioxidant and biological activity and can be used in cosmetic, pharmaceutical, and food industry. Also, Vitamin C, known as L-ascorbic acid (AA) is one of the interesting and well-known acids in nature which has bioactivity and anti-oxidation property.

However, α -TO and AA are readily oxidized by light, air, oxidizing agents or heat, resulting in the reduction of their antioxidant value. Cyclodextrin (CD) can enhance the solubility and chemical stability of compounds in aqueous solution leading to increase the bioavailability. To increase bioavailability and solubility of α -tocopherol (α -TO) and L-ascorbic acid (AA), we prepared carboxylic β -cyclodextrin with AA and α -TO.

The oxidized β -CD, carboxy- β -CD was synthesized from TEMPO, NaBr, NaClO₄ and characterized by FT-IR, MALDI-TOF, ¹H-NMR, ¹³C-NMR spectroscopies. C- β -CD-AA and C- β -CD-TO were synthesized from C- β -CD with ascorbic acid or α -tocopherol by using DCC(1-ethyl-3-(3-dimethylaminopropyl)carbodiimide) and DMAP (4-dimethylaminopyridine) and characterized by FT-IR, ¹H-NMR, ¹³C-NMR spectroscopies. The inclusion complexes of β -CD with AA or α -TO were synthesized in H₂O and characterized by FT-IR, UV-Vis spectroscopies, and DSC thermogram.

References:

1. Yu, J. et al. Materials 2015, 8, 6685.
2. Carole, F. et al. Carbohydrate Research 2000, 328, 585.

Poster44

Synthesis and Characterization of β -Cyclodextrin-L-Ascorbic Acid Conjugates

Mijin Jeong, Injun Song and Ildoo Chung

Department of Polymer Science and Engineering, Pusan National University
Busan 46241, Republic of Korea
E-mail: jmj2429@pusan.ac.kr

β -Cyclodextrin (β -CD) consists of cyclic oligosaccharides with seven D-glucose units linked by α -1,4-glucosidic linkage. The β -CD has the form of a truncated cone and torus with the primary hydroxyl functions oriented to the narrower end of the torus and the secondary hydroxyl functions oriented towards the wider end. The outer surface of β -CD has hydrophilic properties due to the assembly of hydroxyl groups, whereas the inner cavity of β -CD has hydrophobic properties. The hydrophobic inner cavity of β -CD is able to interact with a wide variety of guest molecules forming non-covalent inclusion complexes. Due to the rigidity and chirality of the hydrophobic cavity, β -CD can form inclusion complexes with some guest molecules through such intermolecular interactions by van der Waals forces and hydrogen bonding. The formation of inclusion complexes improves the physicochemical and biological properties of guest molecules such as increasing solubility and stability of drug, reducing toxicity of molecules and improving application performance of molecules.

Ascorbic acid (AA) is called vitamin C. AA is famous as a natural antioxidant, water-soluble vitamin and essential nutrient of the human, which is widely used as a food additive, pharmaceutical agent and cosmetic element. However, AA is highly sensitive to heat, alkali, oxygen, light and contact with traces of copper and iron. Consequently, AA is oxidized to dehydroascorbic acid. This destruction by oxidation is a serious problem in that a considerable quantity of the vitamin C contents of food is lost during processing, storage and preparation.

This study was aimed at the synthesis of β -cyclodextrin-ascorbic acid conjugates that have better stability than original ascorbic acid. Ascorbic acid was covalently bonded to oxidized β -cyclodextrin as a linkage. And it was characterized through FT-IR, NMR, MALDI-TOF, UV, respectively.

References:

1. Q. Jiang. et al. *Chinese Science Bulletin* 2010, **55**, 2835.
2. W. Buranaboripan. et al. *International Journal of Biological Macromolecules* , 2014, **69**, 27.

Poster45

Preparation and Characterization of Environmentally Sensitive Microcapsules

WeijinZhang^{1,2}, YushunJin¹, DanYu¹

¹Beijing Institute of Petrochemical Technology, No.19 Qingyuan North Road, Daxing District, Beijing, 102617, China;

²College of materials science and engineering, Beijing University of Chemical Technology, Chaoyang 100029, Beijing

Email : jinyushun@bipt.edu.cn

Poly(lactic acid) (PLA) macromonomer with double bond functional group were synthesized by lactide ring opening polymerization under the condition of hydroxyethyl methacrylate as initiator. In this study we reported a simple and convenient route to fabricate poly(lactic acid)-g-poly(acrylic acid)-co-poly(N-isopropylacrylamide) (PLA-g-P(NIPAm-co-AA)) nanocapsules by using Emulsion polymerization. (The drug loading nanocapsules with pH-response, temperature-responsive and biodegradable were designed by the N-isopropyl acrylamide (NIPAm) as temperature sensitive monomer, Acrylic acid (AA) is a pH response monomer and 5-fluorouracil (5-FU) as a model drug. The hollow structures and the multiple environmental stimuli-response properties were validated with transmission electron microscopy and dynamic light scattering techniques, respectively. Together with the convenient preparation, dual responsivity as well as the sustained release feature, it is implied that this polymeric nanocapsule might be a promising candidate for new drug carriers.

Preparation and Properties of Ethylene-Vinyl Acetate Copolymer Based Blend Foams

MinJi Kwon^{1,2}, *DaeHwi Lim*², *InChul Choi*², *Hae-Won Kwon*³,
and *Chang-Sik Ha*^{1,*}

¹Department of Polymer Science and Engineering, Pusan National University, Busan 46241, Korea

²Comtech Chemical CO. LTD., 8-48, Bunseong-Ro, 727 Rd, Gimhae, Gyeongnam 50827, Korea

³Hyundai Engineering CO. LTD., 75, Yulgok-Ro, Jongno-gu, Seoul 03058, Korea

E-mail: scarlett.kwon@ctc-bionics.com

In this study, ethylene-vinyl acetate copolymer (EVA) based blend foams with various polymers including polyolefin elastomer (POE) were prepared as a potential resilient material for reducing inter-floor noise. Various properties of EVA blend foams were measured, in particular, to reveal the effects of EVA contents and the kinds of a pair polymer for the EVA blend foams on the dynamic stiffness, which is one of key factors of resilient materials, in relation to hardness, specific gravity and resilience, which has yet not been introduced in the construction industry in the past.¹ When the EVA/POE ratio was 20/80 and the foaming ratio was 210 %, the dynamic stiffness was the lowest as 5.97 MN/m³. However, when the resilience is less than 20 %, the dynamic stiffness is high as 37.66 mN/m³ at the expansion ratio of 210%, even when the specific gravity is low.

Acknowledgements

This work was supported by the National Research Foundation of Korea (NRF) Grant funded by the Ministry of Science and ICT, Korea (NRF-2017R1A2B3012961; Brain Korea 21 Plus Program (21A2013800002)). The authors thank Comtech Chemical Co. Ltd. and Hyundai Engineering for their assistants in measurements.

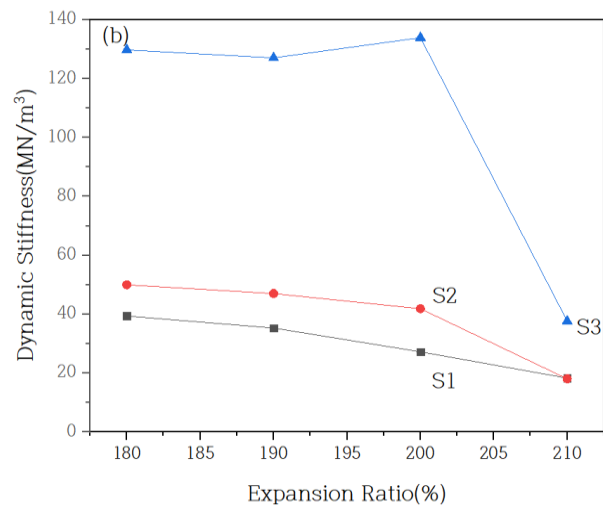


Fig. 1. Dynamic stiffness vs. expansion ratio of three typical EVA based blend foams S1, S2, and S3.

Reference:

1. K.-W. Kim, G.-C. Jeong, K.-S. Yang, and J.-T. Sohn, *Building and Environment*, 2009, **44**, 1595.

Poster47

Fabrication and Characterization of Cellulose / Montmorillonite Intercalated by Polyhedral Oligomeric Silsesquioxane Nanocomposites

Inho Shin^a, Yury Shchipunov^b, Chang-Sik Ha^{a}*

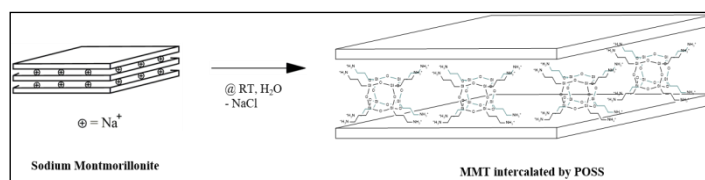
^aDepartment of Polymer Science and Engineering, Pusan National University,
Busan 46241, Korea

^bInstitute of Chemistry, Far East Department, Russian Academy of Sciences,
690022, Vladivostok, Russia.

E-mail : dlsgh9135@naver.com

Recently, biopolymers have received great attention due to their eco-friendly properties. Cellulose has been actively studied. It is most abundant biopolymer in the earth and can be renewable, biocompatible and biodegradable¹. Polymer-clay nanocomposites have attracted various applications such as packaging materials². Montmorillonite (MMT) is widely used reinforcing material. It can be treated with surfactants that help to exfoliate the layers of MMT in a polymer matrix. Polyhedral oligomeric silsesquioxane (POSS) has high thermal stability, flame retardation and good mechanical properties. POSS additive can assist in expanding interlayer space of sodium MMT³.

In this work, we report the cellulose nanocomposites using POSS-intercalated MMT as a nanofiller.



Scheme 1. Synthesis of montmorillonite intercalated by polyhedral oligomeric silsesquioxane

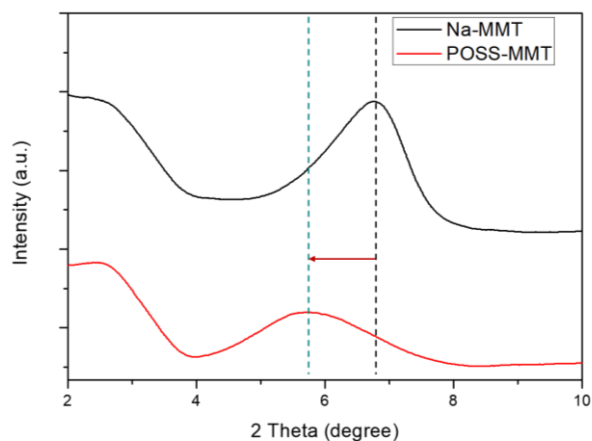


Figure 1. X-ray Diffraction of sodium-MMT and POSS-intercalated MMT

References:

1. S. Wang, A. Lu, L. Zhang, *Prog Polym Sci*, 2016, **53**, 169
2. S. Mahmoudian, M.U. Wahit, A.F. Ismail, A.A. Yussuf, *Carbohydr Polym*, 2012, **88**, 1251
3. R. Hojiyev, Y. Ulcay, M. Hojamberdiev, M.S. Çelik, W.M. Carty, *J Colloid Interf Sci*, 2017, **497**, 393

Flexible Solid-State Supercapacitors Printed on Textiles for Smart Garments

*Seong-Sun Lee, Keun-Ho Choi, Se-Hee Kim and Sang-Young Lee**

Department of Energy Engineering, School of Energy and Chemical Engineering, Ulsan National Institute of Science and Technology (UNIST), Ulsan, 689-798, Korea

*Email: syleek@unist.ac.kr

With the advent of Internet of Things (IoT), flexible/wearable electronics with portability and shape diversity including smart watch, roll-up displays, Google Glass, wearable/patchable sensors, soft robotics, and smart garments, draw considerable attention as one of disruptive technologies to bring unprecedented changes in our daily lives¹⁻³. Particularly, smart garments integrated with electronics require power sources in the form of textile to successfully realize devices. However, the key challenge to commercially available smart garments is conventional rigid and bulky batteries limiting design versatility and wearability. Here, we demonstrate a new class of flexible printed solid-state power sources that are fabricated directly on common cotton t-shirts via simple stencil printing. To demonstrate the feasibility and practical validity of the concept, electric double-layer supercapacitors (SCs) with activated carbon (AC) are chosen as a model of the electrochemical system. It is well known that printing is a facile and reliable technique conferring functionality to a wide diversity of substrates including textiles. In particular, stencil printing is one of mass-printing method that realized by pressing a rheologically tuned inks through stencil with desired pattern with a squeegee^{4, 5}. The key technology to realize flexible printed solid-state SCs with facile processibility and aesthetic versatility is to design electrode and electrolyte inks by fine-tuning of rheology based on the colloidal chemistry. To ultimately realize flexible power sources for smart garments, they should have tolerance to all kinds of stress applied for our daily lives, including thermal stress (ironing) and mechanical stress during dressing and undressing, laundering, wiring, and folding⁶. The uniqueness of materials and structure enables our flexible printed solid-state SCs to bear diverse stresses applied in our daily lives. As a result, flexible printed solid-state SCs featuring shape diversity are successfully fabricated on cotton t-shirts via a simple and facile

printing and aesthetically integrated with smart t-shirts. We envision that the flexible printed solid-state SCs hold great promise as a reliable and scalable platform technology to open a new concept of cell architecture and fabrication route toward flexible and wearable power sources with exceptional shape conformability, aesthetic versatility, and also thermal/mechanical stability.

References:

1. D. Rossi, D. Nat. Mater. 2007, 6, (5), 328-329
2. Gogotsi, Y. Nature 2014, 509, (7502), 568-570.
3. Nishide, H. O., K. Science 2008, 319, 737-738.
4. Kim, S. H.; Choi, K. H.; Cho, S. J.; Choi, S.; Park, S.; Lee, S. Y. Nano Lett. 2015, 15, (8), 5168-5177.
5. Hyun, W. J.; Secor, E. B.; Hersam, M. C.; Frisbie, C. D.; Francis, L. F. Adv. Mater. 2015, 27, (1), 109-115.
6. Sekiguchi, A.; Tanaka, F.; Saito, T.; Kuwahara, Y.; Sakurai, S.; Futaba, D. N.; Yamada, T.; Hata, K. Nano Lett. 2015, 15, (9), 5716-5723.

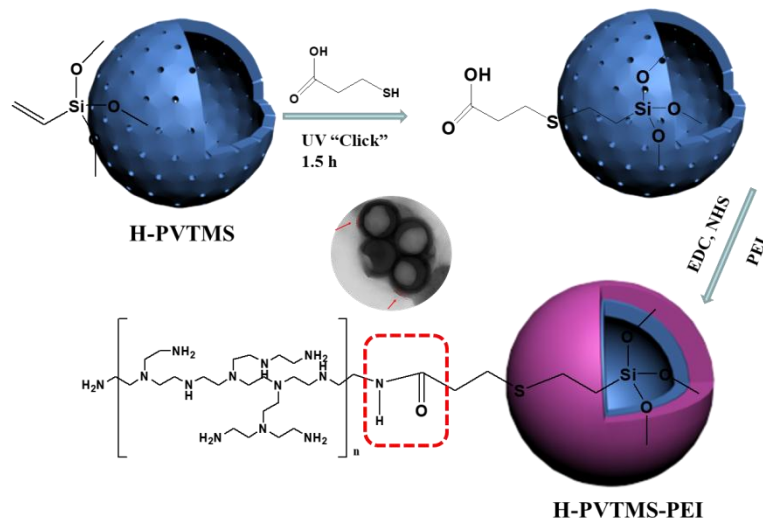
Poster49

Designed Synthesis of Monodisperse Hollow Polysilsesquioxane@PEI Spheres for Dye Removal

*Yong-Zhu Yan, Saravanan Nagappan, Sung Soo Park and Chang-Sik Ha**

Department of Polymer Science and Engineering, Pusan National University,
Busan- 46241, Republic of Korea
E-mail: zyancam@163.com

Efficient adsorption of pollutants from wastewater is of considerable importance for environmental protection; Thus, the construction of a new type of adsorbent materials with excellent adsorption capacity would be of significant interest. Herein, polysilsesquioxane@PEI hybrid hollow spheres were successfully synthesized in an aqueous medium by using vinyltrimethoxysilane (VTMS) as the precursor, followed by polyethylenimine (PEI) was assembled on the surface of hollow polysilsesquioxane to achieve high density active sites. Accordingly, the low density cavity and the reactive aminogroups on the surface of the hybrid polysilsesquioxane microspheres promise many potential applications. The novel spheres show a high adsorption capacity of 600.3 mg/g for Congo Red, which is higher than the adsorption capacity of single polysilsesquioxane hollow spheres. Adsorption mechanisms consisted of electrostatic interaction between the positively charged amino-groups and the negatively charged pollutant species in the aqueous solution. In the predicted application of polysilsesquioxane@PEI, other anionic dyes and metal ion, might be also effectively adsorbed from solution.



Scheme 1. Schematic Illustration of the Synthetic Procedure for Hollow polysilsesquioxane@PEI Composite

References:

1. F. Dong, W. Guo, S.S. Park, C.S. Ha, *J. Mater. Chem.*, 2011, 21, 10744-10749.
2. Z. Wang, F. Guo, C. Chen, L. Shi, S. Yuan, L. Sun, J. Zhu, *ACS Appl. Mater. Interfaces*, 2015, 7, 3314-3322.

Poster50

The Research of Low Temperature Curing Epoxy Resin for Winding Composites

Hao-YuanAn

College of Materials Science and Engineering, Beijing Institute of Petrochemical Technology, China
anhaoyuan@bipt.edu.cn

Resin is the base material of winding product, which determines the properties of winding product. Epoxy resin has lower cost and less shrinkage in curing reaction. Epoxy resin is often used as matrix resin in winding-molded composite products.

The curing temperature of commonly used epoxy resin is 160°C, and the curing time is too long. Too high curing temperature and too long curing time are unfavorable to product quality and production efficiency. In addition, the low viscosity of resin will reduce the resin content in the product. The high viscosity of resin is not conducive to fiber impregnation, which reducing the product properties. Therefore, the epoxy resin possessing low curing temperature and suitable viscosity is in need of development.

In this study, the curing temperature of epoxy resin was 100°C. The tensile strength of the resin casting was 39MPa, tensile modulus was 3.3GPa, elongation at break was 1.2%, bending strength was 135MPa and bending modulus was 3GPa. The interlaminar shear strength of carbon fiber/epoxy composite unidirectional plate was 74MPa. The epoxy resin has good comprehensive properties.

Poster 51

Modification of Titanium Dioxide by Doping with Zn for the Catalytic Ozonation of *p*-Chlorobenzoic Acid

Yifan Meng^{1,2}, *Shi Sun*^{1,3}, *Yingying Li*^{1,2}, *Yixin Yang*^{1*}, *Mingsheng Luo*^{1*}

1. Beijing Key Laboratory of Fuels Cleaning and Advanced Catalytic Emission Reduction Technology, College of Chemical Engineering, Beijing Institute of Petrochemical Technology, Beijing 102617, China
 2. College of Environmental and Energy Engineering, Beijing University of Technology, Beijing 100124, China
 3. China Institute of Atomic Energy, Beijing 102413, China
- E-mail: 18222511596@163.com

Titanium dioxide is one kind of stable, non-toxic, inexpensive and highly active catalyst, which is widely used in different types of catalytic processes. It is also competent to catalytic ozonation process for the degradation of refractory organic pollutants in industrial wastewater. In this study, commercial nanosized titanium dioxide P25 was chosen as the catalyst in the ozonation process of *p*-chlorobenzoic acid (*p*-CBA). And it was doped by transitional metals with the impregnation method to improve the catalytic activity, such as Fe³⁺, Zn²⁺ and Mn²⁺. Zn-doped titanium dioxide showed the best performance. Effect of the doping ratio and the calcination temperature was investigated and the modified titanium dioxide catalysts were characterized by SEM, BET, FTIR, XRD and pHzpc. It was shown that the surface hydroxyl groups and the pHzpc of titanium dioxide were increased by the doping process, which may be the reason of the enhancement of activity for the catalytic ozonation process.

Application of Graphene in the Catalytic Ozonation of *p*-Chlorobenzoic Acid in Aqueous Solution

Yingying Li^{1,2}, Yifan Meng^{1,2}, Dan Song¹, Jingchao Yang^{1,2}, Yixin Yang^{1*},
Mingsheng Luo^{1*}

1. Beijing Key Laboratory of Fuels Cleaning and Advanced Catalytic Emission Reduction Technology, College of Chemical Engineering, Beijing Institute of Petrochemical Technology, Beijing 102617, China

2. College of Environmental and Energy Engineering, Beijing University of Technology, Beijing 100124, China

In this study, graphene is used as catalyst in ozonation process of *p*-chlorobenzoic acid (*p*-CBA) in aqueous solution. Comparing with single ozonation process, graphene catalyzed ozonation showed the superiority in terms of the degradation of *p*-CBA. Screening experiments based on tert-butanol indicated that the catalytic ozonation reactions followed free radical mechanism. Characterization of graphene catalyst was carried out by means of BET, SEM, NH₃-TPD, Raman and pHzpc. The huge specific surface area of graphene caused the excellent adsorption capacity to *p*-CBA, which was conducive to the oxidation reactions taking place on the solid-liquid surface. NH₃-TPD analysis showed the strong acid groups on the surface of graphene, which were assumed to be the active sites to decompose ozone into free radicals. In addition, the effects of some experimental conditions such as graphene dosage, ozone amount, initial concentration of *p*-CBA, and pH value of solution were investigated.

Key words: graphene; catalytic ozonation; *p*-CBA; ozone

Hybrid Film Fabricated by Layer-by-Layer Assembly of Sacran and Imogolite Nanotubes

Linlin Li,¹ Wei Ma,² Akihiko Takada,³ Yuji Higaki,⁴ Maiko Okajima,⁵ Tatsuto Kaneko,⁵ Atsushi Takahara^{1,2,3}

1. Graduate School of Engineering, Kyushu University, 744 Motooka, Nishi-ku, Fukuoka 819-0395, Japan
2. International Institute for Carbon-Neutral Energy Research (WPI-I2CNER), Kyushu University, 744 Motooka, Nishi-ku, Fukuoka 819-0395, Japan
3. Institute for Materials Chemistry and Engineering, Kyushu University, 744 Motooka, Nishi-ku, Fukuoka 819-0395, Japan
4. Department of Integrated Science and Technology, Faculty of Science and Technology, Oita University, 700 Dannoharu, Oita 870-1192, Japan.
5. School of Materials Science, Japan Advanced Institute of Science and Technology (JAIST), 1-1 Asahidai, Nomi, Ishikawa, 923-1292, Japan
E-mail: linlin@ms.ifoc.kyushu-u.ac.jp

In this study, benefiting from the negatively charged surface of sacran, a natural polysaccharide extracted from the aphanothece sacrum¹, and the positively charged external surface of imogolite, a natural tubular aluminosilicate clay², a free-standing film was obtained by alternatively layer-by-layer (LBL) assembly of sacran and imogolite. The film thickness increased linearly with the increment of bilayers. UV-vis test indicated that this LBL film has better transparency than the sacran/imogolite blend film. Surface morphology of the sacran/imogolite LBL film showed that the thin film was uniform, and plenty of imogolite nanotubes were absorbed onto a sacran layer. The structure and the mechanical property of the films were also investigated. The mechanical performance of the sacran/imogolite LBL film is superior than that of neat sacran and sacran/imogolite blend film.

References:

1. Okajima, M. K.; Bamba, T.; Kaneko, Y.; Hirata, K.; Fukusaki, E.; Kajiyama, S. I.; Kaneko, T. *Macromolecules* 2008 41, 4061-4064.
2. Ma, W.; Higaki, Y.; Takahara, A. *Imogolite Polymer Nanocomposites*, Chapter 24, *Nanosized Tubular Clay Minerals Halloysite and Imogolite*, Elsevier 2016, Vol. 7, pp 628-671.

Poster54

Degradation of Ibuprofen by Nano-TiO₂ Catalyzed

Ozonation

Dan Song, Yingying Li, Yifan Meng, Yixin Yang, Mingsheng Luo**

Beijing Key Laboratory of Fuels Cleaning and Advanced Catalytic Emission Reduction Technology, College of Chemical Engineering, Beijing Institute of Petrochemical Technology, Beijing 102617, China

E-mail: song931108@163.com

Nano-TiO₂ catalyst was prepared by the sol-gel method and used in the catalytic ozonation process for the degradation of ibuprofen in aqueous solution. The TOC percentage removal increased markedly when nano-TiO₂ participated in the ozonation process. Characterization of nano-TiO₂ by means of BET and XRD indicated its high specific surface area and mixed crystal structures with anatase and rutile. Effect of catalyst dosage, ozone amount and initial concentration of ibuprofen on the TOC percentage removal was investigated. And the pH value of solution affected the adsorption and ozonation processes obviously, which suggested the significant influence of the surface charge of nano-TiO₂. The degradation products of ibuprofen by catalytic ozonation were analyzed by GC-MS. Undergoing the break of C-C bonds and the ring opening of benzene, ibuprofen was finally degraded into acetic acid. It is concluded that nano-TiO₂ catalyzed ozonation process is effective and safe for the removal of ibuprofen from wastewater.

Analysis of Modification Effect of Peroxide Masterbatch on Homo-polypropylene from Crystallization Behavior

Zengzeng Xue^b, Xu An^a, Mingshan Yang^{a,b**}

^aBeijing Institute of Petrochemical Technology, Beijing 102617, China;

^b Beijing University of Chemical Technology, Beijing 100029, China;

*Beijing University's high-level talents cross-cultivation "real training project" research (2019)

** Corresponding author.

E-mail: yangmingshan@bipt.edu.cn

Compared with the use of a novel catalyst to synthesize a high molecular weight polypropylene with controlled molecular weight in a polymerization reactor, a peroxide cooling master batch is added to a conventional polypropylene resin to control the degradation of the polypropylene to obtain a high-flow polypropylene. It is a preparation research program that is currently widely used. Studies have shown that the addition of peroxide masterbatch in PP can significantly reduce the molecular weight and distribution of PP resin, improve the flow properties of PP resin, and meet the application requirements of melt spinning¹.

This work was analyzed from the crystallization point of view, by studying the crystal morphology and crystallization behavior before and after modification of polypropylene², by means of differential scanning calorimeter (DSC), polarizing microscope (POM) and X-ray diffraction analyzer (XRD), the crystallization behavior difference of homo-polypropylene (the amount of peroxide masterbatch added was 0.35% and 0.61%) before and after the modification of the peroxide masterbatch was studied, thus providing a basis for the study of the modification effect of the peroxide masterbatch on homo-polypropylene from the perspective of molecular structure.

Keywords: homo-polypropylene, peroxide masterbatch, crystallization

References:

1. H. Azizi, I. Ghasemi and M. Karrabi, *Polymer Testing*, 2008, 27, 548-554.
2. W. Rungswang, C. Jarumaneeroj and S. Patthamasang, *Polymer*, 2019, 172, 41-51.

Curing Resin for 3D Printing

*Bao Zhu, Mingshan Yang **

College of Materials Science and Engineering, Beijing Institute of
Petrochemical Technology, Beijing 102617, P. R. China

*Correspond author.

E-mail: yangmingshan@bipt.edu.cn

As long-wave UV curing is more energy-saving and environmentally friendly than traditional 365-nm UV curing, most attention has been paid to it^{1,2}. In this work, a series of UV-curable resins were obtained by using cationic and free radical hybrid system and changing the types and dosages of prepolymer and initiator, and were cured by rheometer and FORM2 3D printer. The results showed that when the type of cationic photoinitiator was 261 and a small amount of PAS-50 was added, the resin could be cured under long-wave ultraviolet light; the optimum formulation was E44 20g, CY179 10g, SR454NS 40g, 261 4.0g, PAS-50 1.0g, 1173 2.0g, whose solid shrinkage rate was 6.2% (lower than that of imported and domestic products). The shrinkage rate of resin is 88.16%, the glass transition temperature is 56.2°C, and the gelation rate is 88.16%. Meanwhile, the curing period is 2s. After curing, the bending strength and bending modulus can reach 52.0MPa and 1476.7MPa.

Keywords: Ultraviolet curing, 3D Printing, Long-wave Curing

The Flame Retardant Properties of Black Phosphorene in Epoxy Resin

Ce Li, Xing Gao

^aBeijing Key Lab of Special Elastomer Composite Materials, College of Materials Science and Engineering, Beijing Institute of Petrochemical Technology, Beijing 102617, China.

^b College of Materials Science and Engineering, Beijing University of Chemical Technology, Beijing 100029, China.
E-mail: cuxiuguo@bipt.edu.cn

For the purpose of the study, epoxy (EP) composites added with black phosphorene (BP) were manufactured. The influence of BP on the fire behavior of EP-based composites was determined with a UL-94 HB test, supplemented by thermogravimetric analysis. The fire behavior study showed that BP may effectively decrease the flammability of EP in case of at only 1%wt% filler content while composites containing lower amounts of BP were characterized with significant improvement in tensile strength without reduction in flammability in reference to the unmodified EP. The results indicated that BP imparted flame retardance to EP, and that EP/1 wt % BP passed the V-0 rating. Moreover, TGA tests also show that the decomposition temperature of epoxy resin also increased of the filler used.¹⁻³

References:

1. Jian R K, Wang P, Duan W, et al. Synthesis of a novel P/N/S-containing flame retardant and its application in epoxy resin: thermal property, flame retardance and pyrolysis behavior[J]. *Industrial & Engineering Chemistry Research*, 2016:acs.iecr.6b03416.
2. Barczewski, Mateusz, et al. "Poly(vinyl chloride) powder as a low-cost flame retardant modifier for epoxy composites." *International Journal of Polymer Analysis and Characterization* (2019):1-10.

Poster58

Improved Dielectric and Mechanical Properties of Thermoplastic Polyurethanes Elastomer Achieved by Blending with Small Molecules

*Jingjing He, and Yongri Liang**

Beijing Key Lab of Special Elastomer Composite Materials, College of
Materials Science and Engineering, Beijing Institute of Petrochemical
Technology, Beijing 102617
E-mail: 416269894@qq.com

Dielectric elastomer (DE) which is one kinds of electroactive polymers (EAP) has been attracted more attention due to its wide applications in the actuators and sensors. In this work, we investigated the effect of small molecules induced hydrogen bonding (H-bonding) on microphase separation, dielectric properties and mechanical properties of thermoplastic polyurethane (TPU). We found that the amino-terminated small molecules can form H-bonding with HSs result in somewhat destroying the H-bonding between HSs. Accordingly, the dielectric and mechanical properties can be adjusted by the amount and types of amino-terminated small molecules. Our results showed that the dielectric constant was increased at least 1.5 times when adding 15 wt% of 4,5-dichloro-o-phenylenediamine. The tensile strength decrease with the increase in the content of 4,5-dichloro-o-phenylenediamine, but it still have good mechanical properties. Our results can provide a new insight into fabrication high performance of TPU based DE.

Keywords: dielectric elastomer, hydrogen bond, dielectric constant

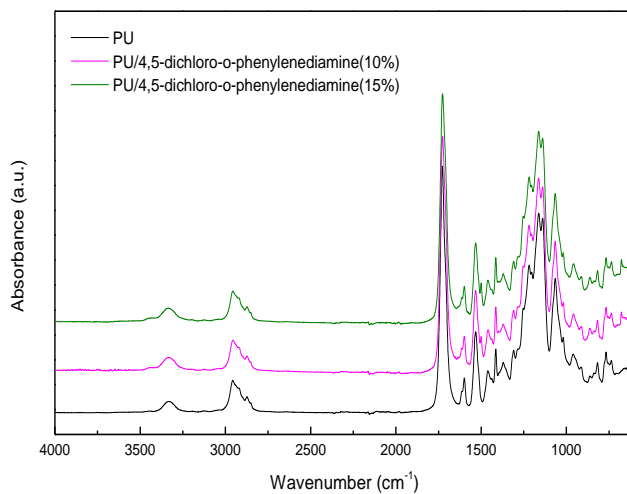


Fig. 1. FTIR spectrum of PU and mixture

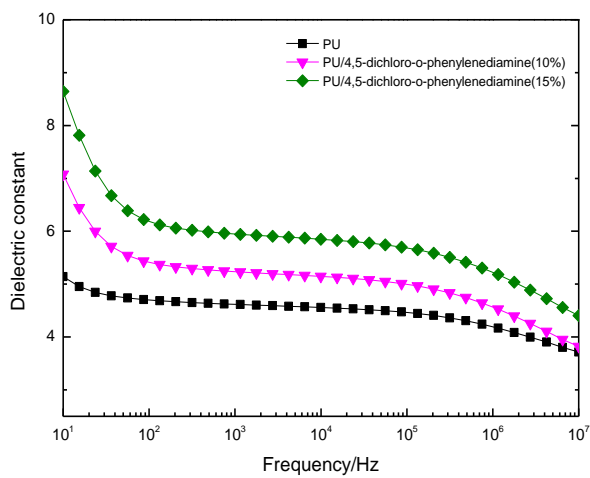


Fig. 2. Dielectric constant of PU and mixture

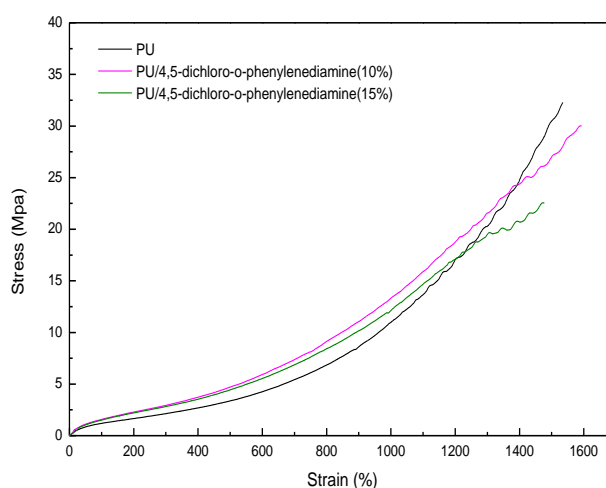


Fig. 3. Stress-strain curves of PU and mixture

Acknowledgements

This research work was supported by Project of High-level Teachers in Beijing Municipal Universities in the Period of 13th Five-year Plan (CIT&TCD20190315).

Simulation of Liquid Seepage in Medical Dry Chemical Diagnostic Reagent Materials

Ou Shen, Guang-Xiang He

Beijing Institute of Petrochemical Technology, No. 19 Qingyuan North Road,
Daxing District, Beijing, China.
E-mail: Snowwyte@163.com

With people's attention to health, the requirements of convenience, rapidity and accuracy of medical materials are becoming increasingly stringent. One of the quicker detection methods in medical materials is medical dry chemical diagnostic reagent material. Due to the seepage effect of the diffusion layer of medical dry chemical diagnostic reagent determines the accuracy of detection results, in order to investigate the seepage law of the diffusion layer, the lattice Boltzmann method was used to simulate the serum seepage in polystyrene dry chemical diagnostic reagent material instead of the expensive experimental method. The numerical simulation results are in good agreement with the experimental results. Moreover, we were also studied the influence of different particle sizes of micro-spheres on seepage, and it was concluded that larger particle sizes were more conducive to seepage. The results show that the larger the particle size of the micro-spheres, the faster the seepage speed it was, and the case of particle size larger than 2 μ m is more suitable for the occasion of higher seepage capacity requirements.

Poster60

Hydrodynamic Characteristics of p-Xylene Oxidation

Reactors with an Acetic Acid System

Shanglei Ning, Haibo Jin , Suohe Yang , Gaungxiang He , Xiaoyan Guo

Beijing Key Laboratory of Fuels Cleaning and Advanced Catalytic Emission Reduction Technology, School of Chemical Engineering, Beijing Institute of Petrochemical Technology, Beijing 102617, China

E-mail: 2017520021@bipt.edu.cn

As a common multi-phase reactor, the bubble column reactor has been widely used in chemical and biochemical due to its lack of any mechanically operated parts, large phase-contacting area, easy operation, high mass transfer and heat transfer efficiency^[1,2]. The middle of some polymers is often done in the bubble column reactor. Different reaction conditions have different effects on the hydrodynamic behavior in the bubble column. It is significant to improve the acid reaction rate by studying the hydrodynamic behavior of the acid reaction system.

In this study, the experiment was carried out in a glass bubble column with a diameter of 150 mm and a height of 2200 mm. The fiber probe and differential pressure method^[3] were installed in the height range of 650-700 mm on both sides of the bubble column to get the gas holdup. The experimental system was an air-acetic acid system under atmospheric pressure and superficial velocity (0.01–0.10 m/s). The gas holdup, bubble rise rate and bubble size distribution in the bubble column were collected by differential pressure transmitters and fiber probe. The results show that different concentrations of acetic acid have a great influence on the surface tension of the liquid in the bubble column, which will increase the gas holdup in the column. With the superficial gas velocity increases, the gas holdup increases gradually and the bubble size is uniform, it will improve the mass transfer between liquids and air.

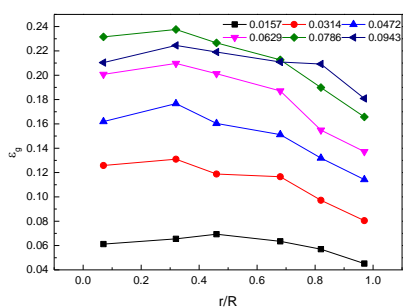


Fig. 1 Effect of the acetic acid concentration of 1% on the gas holdup

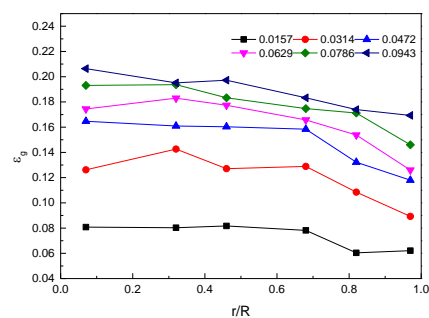


Fig. 2 Effect of the acetic acid concentration of 20% on the gas holdup

References:

1. Parisien, V.; Farrell, A.; Pjontek, D.; McKnight, C.; Wiens, J.; Macchi, A. Bubble swarm characteristics in a bubble column under high gas holdup conditions. *Chem. Eng. Sci.* 2017, 157, 88–98, doi:10.1016/j.ces.2016.04.051.
2. Hur, Y.; Yang, J.; Jung, H.; Lee, K. Continuous alcohol addition in vaporized form and its effect on bubble behavior in a bubble column. *Chem. Eng. Res. Des.* 2014, 92, 804–811, doi:10.1016/j.cherd.2013.08.006.
3. Zhang, T.; Jin, H.; He, G.; Yang, S.; Tong, Z. Application of Pressure Transducing Technology to Measurement of Hydrodynamics in Bubble Column. *Chin. J. Chem. Eng.* 2004, 55, 476–480, doi:10.3321/j.issn:0438-1157.2004.03.008.

Poster61

Synthesis of ϵ -Caprolactone by Cyclohexanone Baeyer-Villiger Green Oxidation

Qianqian Zhu, Haibo Jin , Gaungxiang He , Xiaoyan Guo

Beijing Key Laboratory of Fuels Cleaning and Advanced Catalytic Emission Reduction Technology, School of Chemical Engineering, Beijing Institute of Petrochemical Technology, Beijing 102617, China
E-mail: 2505348448@qq.com

ϵ -Caprolactone is an important organic synthesis intermediate and a novel polyester monomer. The polycaprolactone obtained by ring-opening has a wide range of uses in biomedical materials, environmentally friendly plastics and other fields. Oxidation of ϵ -caprolactone by Baeyer-Villiger with H_2O_2 as oxidant is environmentally friendly, safe and economical, and therefore has received extensive attention. Due to the weak oxidation ability of H_2O_2 , a certain amount of high-efficiency catalyst needs to be added in the reaction process to improve the reaction efficiency. In this work, a series of composite metal oxides of magnesium, aluminum and other metals were prepared by co-precipitation method. The physicochemical properties were characterized by XRD, BET and CO_2 -TPD. This work also studied metal ion ratio, calcination time and calcination temperature during catalyst preparation, oxidant, solvent usage, reaction temperature and reaction time during the reaction. The possible reaction mechanism during the reaction is further discussed.^[1-4]

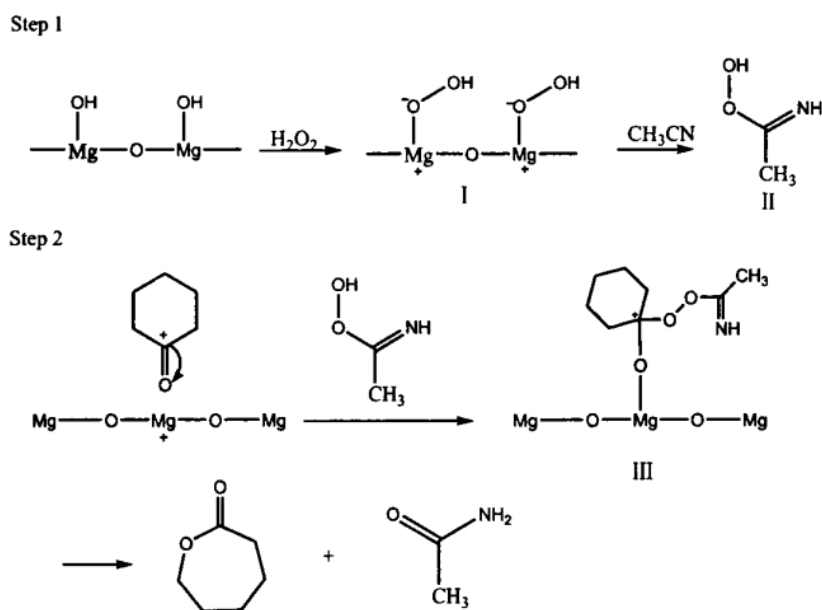


Fig. 1 Reaction mechanism of cyclohexanone catalyzed by MgO

References:

1. Joanna Olszówka, Robert Karcz, et al. Catalysis Communications, 2017, **196-201**
2. Ce'sar Jimenez-Sanchidria'n , Julia Mari'a Hidalgo, et al. Applied Catalysis A: General 2006, **86-94**
3. Qingguo Ma, Wanzhen Xing et al. Catalysis Communications, 2014, **5-8**
4. Ce'sar Jimenez-Sanchidria'n, Jose' Rafael Ruiz. Tetrahedron, 2008, **2011-2026**

Poster62

Preparation and Application of Barium Sulfate Multifunctional Layer

JiaqiLiu , XiaoyanGuo , HaiboJin , GuangxiangHe

Beijing Key Laboratory of Fuel Cleanliness and Efficient Catalytic Reduction
Technology, College of Chemical Engineering, Beijing Institute of
Petrochemical Technology, Beijing 102617, China
E-mail: 1275077101@qq.com

Barium sulfate has excellent characteristics such as non-toxicity, chemical stability, high reflectivity and high whiteness, so is widely used as a raw material and filler for rubber, plastics, pigments, an indicator of X-ray image, a filler for papermaking, and so on. The gap formed between the barium sulfate microsphere particles can uniformly permeate and disperse the serum, and at the same time achieve the purpose of filtration separation. Because the uniform barium sulfate microspheres have a high light reflectivity, the barium sulfate microspheres can be used as a medical dry diagnostic multifunctional layer. The raw material for preparing the multifunctional layer is a barium sulfate microsphere prepared by complex precipitation method, which is mixed with cellulose acetate, acetone is used as a solvent, Tween 80 is used as a surfactant, stirred and then coated by a coater. Barium sulfate multifunctional layer. The factors influencing the preparation of the multifunctional layer and its application are described below.

References:

- [1] Hafkenscheid J C, Van d V J. Two dry-reagent systems evaluated for determinations of enzyme activities[J]. *Clinical Chemistry*, 1988, 34(1):155-157
- [2] Valkirs G E, Barton R. ImmunoConcentration--a new format for solid-phase immunoassays[J]. *Clinical Chemistry*, 1985, 31(9):1427-1431
- [3] Hagren V, Connolly L, Elliott C T, et al. Rapid screening method for halofuginone residues in poultry eggs and liver using time-resolved fluorometry combined with the all-in-one dry chemistry assay concept[J]. *Analytica Chimica Acta*, 2005, 529(1):21-25
- [4] Liu Dan. The establishment of dry biochemical analysis methods and its methodological evaluation [d]. Changchun City: Changchun University of Science and Technology, 2014
- [5] Zhao Y H, Liu J R. Effect of EDTA and Phosphate on Particle Size during Precipitation of Nanosized BaSO₄ Particles[J]. *Chemistry Letters*, 2006, 35(9): 1040-1041
- [6] Chen Q, Shen X. Formation of Mesoporous BaSO₄ Microspheres with a Larger Pore Size via Ostwald Ripening at Room Temperature[J]. *Crystal Growth & Design*, 2010, 10(9): 3838-3842

Gas-Liquid Two-Phase Flow Characteristics in Microchannels Based on Electrical Resistance Tomograph

*Fangfang Tao, Haibo Jin**

Beijing Key Laboratory of Fuels Cleaning and Advanced Catalytic Emission Reduction Technology, School of Chemical Engineering, Beijing Institute of Petrochemical Technology, Beijing 102617, China
E-mail: 5120130056@bipt.edu.cn

Microchannels have advantages of large specific surface area, high mass transfer and heat transfer efficiency, easy amplification and no amplification effect. With the recent development of microchannels technology, microchannel reactors have gradually been introduced into the preparation technology of micro/nanoparticles. Therefore, it is urgent to understand the changes in the internal flow pattern and gas holdup of the microchannels^{1,2}. At present, some optical measuring methods have been used to visualize the two-phase flow characteristics in microchannels. But their inherent optical scattering problem will become even more severe within the micro dimension. The application of promising Electrical Resistance Tomography (ERT) to detect two-phase flow in microchannels was discussed in this paper. The microchannels with a hydraulic diameter of 1.1 mm were used as the most containers, and the superficial liquid velocity (UL: 0.438-1.491 m/s) and the superficial gas velocity (UG: 0.088-1.666 m/s) were respectively investigated for air and liquid (Water, glycerol solution of wt.5%-wt.25%, ethanol solution of wt.5%-wt.25%). The influence of flow parameters (friction pressure drop, flow pattern, gas holdup, etc.) in the system. The experimental results show that the air-ethanol solution has a great influence on the gas holdup. And with the increase of the concentration of ethanol solution, the gas holdup showed a small trend, but the flow pattern did not change significantly. The air-glycerin solution has little effect on the gas holdup, but has a large influence on the convection and flow transition lines. As the concentration of glycerol increases, the bullet flows to the transition line of the turbulent flow and moves to the left. This also indirectly shows that the surface tension is more sensitive to the change in gas holdup. Viscosity is more dependent on the change in flow pattern and flow pattern transition line in terms of surface tension.

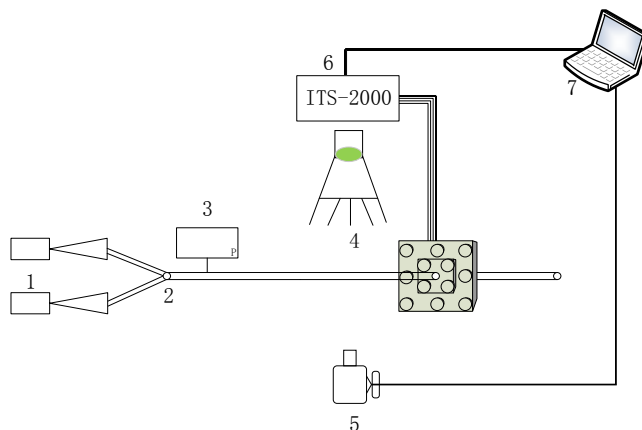


Fig. 1 Experimental equipment diagram (1-injection pump; 2-Y microchannel; 3-differential pressure sensor; 4-LED lamp; 5-high speed camera; 6-ITS-2000; 7-computer)

References:

1. B. Zhang, B. Yang, S. Yang, et al. *Journal of Chemical Industry and Engineering(China)*, 2018, **69(4)**: 1461-1468.

The CWPO Degradation of m-Cresol on Activated Carbon-Based Catalysts: Surface Chemical Characteristics

*Yunlong Zhang, Haibo Jin**

Beijing Key Laboratory of Fuel Cleanliness and Efficient Catalytic Reduction Technology, College of Chemical Engineering, Beijing Institute of Petrochemical Technology, Beijing 102617, China
E-mail: 501976826@qq.com

Activated carbon (AC) is commonly used as an adsorbent for purifying wastewater due to its remarkable surface area, microporous structure and excellent hydrothermal and chemical stability. In addition, AC is an attractive support for transition metal species (i.e., Fe), which are active in CWPO¹⁻³. Furthermore, AC itself can exhibit catalytic activity, which is considered to not only benefit from the above physical properties but can also be influenced by the surface oxygen groups and structural defect features of activated carbon⁴⁻⁵. In addition, the catalytic activity of AC primarily relies on the ability of some metal species to promote the decomposition of hydrogen peroxide (H₂O₂) via hydroxyl radical (\cdot OH) formation. Nevertheless, in the heterogeneous catalytic system, the CWPO application has been primarily limited due to leaching of the active metallic species on the catalysts, which results in deactivation of the catalysts. Therefore, the mechanism of the intrinsic catalytic activity of SAC was investigated in this study with aqueous pretreatment on carbon, and the performance of the modified ACs on m-cresol adsorption and catalytic degradation by CWPO was evaluated in a batch reactor. Furthermore, based on the use of iron oxides supported on SAC, long-term experiments for degradation of m-cresol were performed along with monitoring the valence of iron species and surface oxygen groups (SOGs) on the activated carbon catalysts by Mössbauer spectroscopy and temperature-programmed desorption (TPD).

References:

1. Dominguez CM, A.; Ocon P, B.; Quintanilla A, C. ; Casas JA, D.; Rodriguez JJ, E. Highly efficient application of activated carbon as catalyst for wet peroxide oxidation. Applied Catalysis B-Environmental 2013, 140, 663-670, 10.1016/j.apcatb.2013.04.068.

2. Ribeiro RS, A. Activated carbon xerogels for the removal of the anionic azo dyes Orange II and Chromotrope 2R by adsorption and catalytic wet peroxide oxidation. *Chemical Engineering Journal* 2012, 195, 112-121, 10.1016/j.cej.2012.04.065.
3. Messele SA, A. Effect of activated carbon surface chemistry on the activity of ZVI/AC catalysts for Fenton-like oxidation of phenol. *Catalysis Today* 2015, 240, 73-79, 10.1016/j.cattod.2014.03.063.
4. Shimodaira N, A.; Masui A, B. Raman spectroscopic investigations of activated carbon materials. *Journal of Applied Physics* 2002, 92(2), 902-909, 10.1063/1.1487434.
5. Figueiredo JL, A.; Pereira MFR, B. ; Freitas MMA, C.; Orfao JJM, D. Modification of the surface chemistry of activated carbons. *Carbon* 1999, 37(9), 1379-1389. 10.1063/1.4736568.
6. Lin HJ, A.; Li HJ, B.; Shen QL, C.; Shi XH, D.; Feng T, E.; Guo LJ, F. 3C-SiC Nanowires In-Situ Modified Carbon/Carbon Composites and Their Effect on Mechanical and Thermal Properties. *Nanomaterials* 2018, 8(11). 10.3390/nano8110894.

Simulation Study on Fluid Dynamics Behavior in a Bubble Column by CFD-PBM Coupled Model

Wenlong Zhang, Haibo Jin

Beijing Key Laboratory of Fuels Cleaning and Advanced Catalytic Emission
Reduction Technology, School of Chemical Engineering, Beijing Institute of
Petrochemical Technology, Beijing 102617, China

E-mail: zhangwl199501@163.com

Bubble column reactors are widely used in biodiesel production, Fischer-Tropsch synthesis, hydrocracking of petroleum residue, wastewater treatment and many other important processes because of its unique advantages. They have the advantages of low cost, simple construction, high-energy efficiency and good mass transfer performance^[1,2]. Gas holdup, bubble size and mass transfer rate are important parameters for reactor design and amplification^[1,3]. Therefore, accurately predicting the change of hydrodynamic parameters in the bubble column has significance for the design and amplification of the bubble column.

The computational fluid dynamics (CFD) is an important tool to quantitatively study the multiphase behaviors in a bubble column^[4]. It can simulate the gas content distribution, phase velocity and direction of motion, turbulence intensity distribution in the tower, etc. However, CFD simulations of bubble columns using organic liquids are still limited, and CFD and population equilibrium models (CFD - PBM) have been developed to predict hydrodynamic behavior and local bubble size distribution. In this paper, the ability of CFD - PBM coupling model to simulate complex multiphase behavior in bubble column is studied. Combined with bubble coalescence and break model, parameters such as gas holdup, liquid velocity distribution and bubble size distribution in bubble column are studied. And the predicted simulation results agree well with the experimental data.

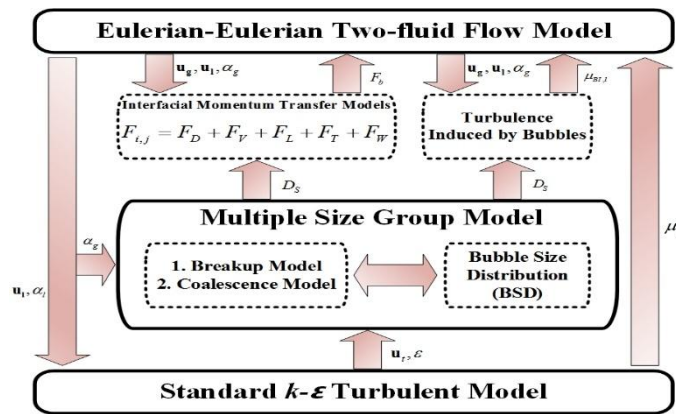


Fig.3-1 CFD-PBM coupling mechanism diagram

References:

1. A. Anastasiou, A. Passos, A. Mouza, Bubble columns with fine pore sparger and non-Newtonian liquid phase: prediction of gas holdup, Chem. Eng. Sci. 2013, 98, 331–338.
2. T.F. Wang, J.F. Wang, Y. Jin, Slurry reactors for gas-to-liquid processes: a review, Ind. Eng. Chem. Res. 2007, 46, 5824–5847.
3. P. Rollbusch, M. Bothe, M. Becker, M. Ludwig, M. Grünewald, M. Schlüter, R. Franke, Bubble columns operated under industrially relevant conditions current understanding of design parameters, Chem. Eng. Sci. 2015, 126, 660–678.
4. Y. Liu, O. Hinrichsen, Study on CFD-PBM turbulence closures based on $k-\epsilon$ and Reynolds stress models for heterogeneous bubble column flows, Comput. Fluids 2014, 105, 91–100.

Poster66

A Hierarchical Graphene Oxide Hydrophobic Coating for Improved Wear Resistance and Corrosion Resistance

Li Li^a, Jia Qi,^a Tianlu Li^a, Tengyan Zhang,^a Kang Wang,^a Fei Chen^{a,c}

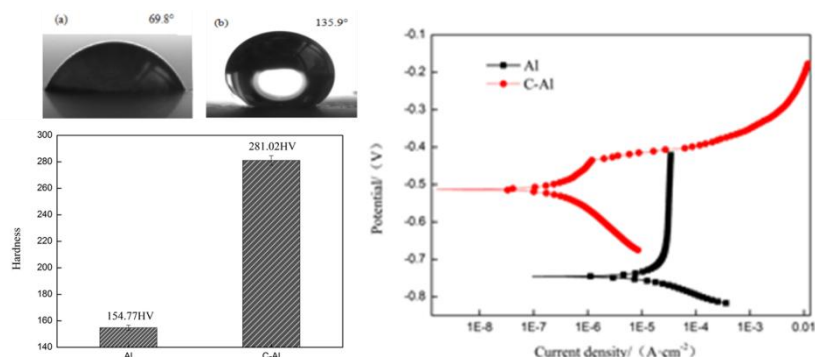
^a College of Materials Science & Engineering, Beijing Institute of Petrochemical Technology, Beijing 102617, People's Republic of China

^b Department of Materials Science and Engineering, Beijing University of Chemical Technology, Beijing 100029, China

^c Beijing Key Lab of Special Elastomer Composite Materials, Department of Material Science and Engineering, Beijing Institute of Petroleum Technology, Beijing 102617, China

E-mail: lili_7116@126.com

The poor stability and wear-resistance of superhydrophobic materials are still major problems that restrict their practical application. In this work, with the attractive mechanical and barrier properties of graphene oxide (GO), Polyvinyl alcohol (PVA) and PVA-GO are deposited on aluminium alloy by layer-by-layer method separately, and after deposition of perfluorosilane by solution method, leading to a hydrophobic hierarchical coating. PVA-GO plays as a protective hard layer. The friction coefficient of the hybrid multilayer coating was investigated, and obtained improved wear resistance. Moreover, the electrochemical corrosion property of the hierarchical coating also improved.



Simultaneous Removal of NO and Soot Catalytic Performance of La_{1-x}Na_xMnO₃ Perovskite Catalysts

Xiaogang Liu^a, Yu Zhao^a, Jinru Sun^{a,b}, Yu Tian^{a,b}, Cuiqing Li^a, Yongji Song^a, Hong Wang^{a,*}

^a College of Chemical Engineering, Beijing Institute of Petrochemical Technology/ Beijing Key Laboratory of Fuels Cleaning and Advanced Catalytic Emission Reduction Technology, Beijing, China; ^b College of Environment and Energy Engineering, Beijing University of Technology, Beijing, China
E-mail: wanghong@bipt.edu.cn

Perovskite-type complex oxide are regarded as potential catalysts for the simultaneous removal NO and soot owing to their low price, thermal stability and more oxygen vacancies^[1]. The catalysts of La_{1-x}Na_xMnO₃ (x=0.05, 0.10, 0.15, 0.20) perovskite oxide were prepared by solvothermal method, which were characterized by means of XRD, FT-IR and NO-TPD, and their catalytic performance for the simultaneous removal NO and soot was evaluated in a fixed micro-reactor.

XRD results showed that all catalysts presented the peaks corresponding to the perovskite structure (LaMnO₃, PDF#89-0680), when $x \geq 0.10$, four peaks attributing to La(OH)₃ appeared at 2θ about 15.67°, 27.97°, 39.48° and 48.64°, indicating that Na⁺ ions can't fully enter the perovskite frame. FT-IR results revealed that a stretching vibration of the Mn-O bond in the MnO₆ octahedron was observed at about 620 cm⁻¹, indicating that the catalysts had formed perovskite structure^[1] (see Fig.1(a)). NO-TPD results showed that the detected NO between 250~550 °C was the production of decomposed nitrites or nitrates on the perovskite surface^[2] (see Fig.1(b)). With Na⁺ substitution amount increased, the desorption peak shifted to higher temperature and the amount desorbed NO decreased. This indicated the decomposition temperature of nitrites or nitrates increased, which made it difficult to migrate to solid-solid boundary and oxidize the soot. Activity results showed that with the increase in the Na⁺ substitution amount, the maximum conversion (X_{NO}) decreased, reaction temperature (T_{NO}) increased, the combustion temperature of soot (T_{max}) increased and the selectivity of CO₂ (S_{CO_2}) decreased. When $x=0.05$, namely, La_{0.95}Na_{0.05}MnO₃ had good catalytic activity, X_{NO} is 33.9%, T_{NO} is 463 °C, T_{max} is 461 °C and S_{CO_2} is 98.6%. The reason for the catalytic activity

of $\text{La}_{1-x}\text{Na}_x\text{MnO}_3$ catalysts ($x \geq 0.10$) decreased may be related to the presence of $\text{La}(\text{OH})_3$ and the poor adsorption and desorption performance of NO.

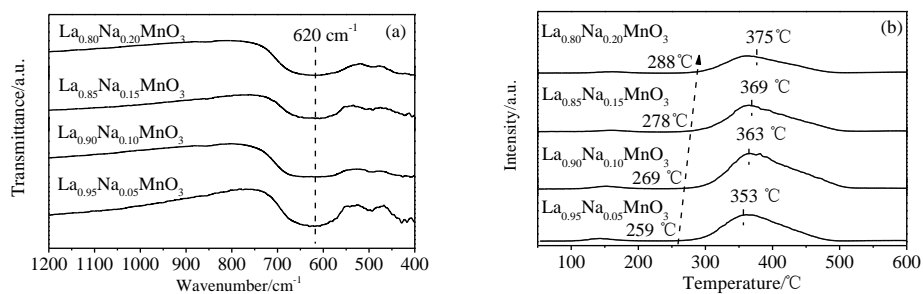


Fig.1 FT-IR spectra (a) and NO-TPD (b) of $\text{La}_{1-x}\text{Na}_x\text{MnO}_3$ catalysts

References:

1. H. WANG, J. LIU, Z. ZHAO, Y. C. WEI, C. M. XU. *Catal Today*, 2012, 184(1):288-300.
2. Z. Q. LI, M. MENG, Y. Q. ZHA, F. F. DAI, T. D. HU, Y. N. XIE, J. ZHANG. *Appl Catal B: Environ*, 2012, 121-122:65-74.

Effect of Crystallization Temperature on the Performance of Catalytic Decomposition of N₂O over Co₃O₄ Catalysts

Jinru Sun^{1,2}, Xiaogang Liu¹, Yu Zhao¹, Yu Tian^{1,2}, Hong Wang^{1}, Cuiqing Li¹, Yongji Song¹*

1 College of Chemical Engineering, Beijing Institute of Petrochemical Technology/Beijing Key Laboratory of Fuels Cleaning and Advanced Catalytic Emission Reduction Technology, Beijing 102617, China; 2 College of Environmental and Energy Engineering, Beijing University of Technology, Beijing 100124, China

E-mail: wanghong@bipt.edu.cn

Nitrous oxide (N₂O) is the third largest greenhouse gas, which destroys the ozone layer seriously. Reducing N₂O emissions has become one of the urgent problems in the field of environmental protection¹. Co₃O₄ catalysts were prepared by hydrothermal method. The effects of different crystallization temperatures (150, 160, 170 and 180 °C) on the morphology and activity of the catalysts were investigated. The catalysts were characterized by XRD, SEM and H₂-TPR. The catalytic performance of Co₃O₄ catalyst for N₂O decomposition was evaluated in a micro fixed-bed reactor.

XRD characterization showed that all the catalysts had spinel structure (PDF#42-1467). SEM results (see Fig. 1) show that the Co₃O₄ catalysts are all spheres assembled by nanoparticles, and the sphere size decreases with the increase of crystallization temperature. The results of H₂-TPR show that there are two reduction peaks in Co₃O₄ catalyst, one is the reduction process from Co³⁺ to Co²⁺ and the other is the reduction process from Co²⁺ to Co. There is no significant difference in the reduction temperature between the catalysts, but the hydrogen consumption of the catalyst at Co₃O₄-180 °C is significantly higher than that of other catalysts.

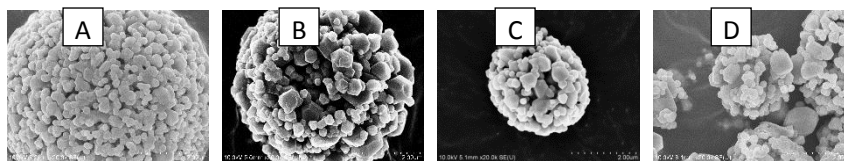


Fig. 1 SEM Photographs of Co_3O_4 Catalyst (A. 150°C B. 160°C C. 170°C D. 180°C)

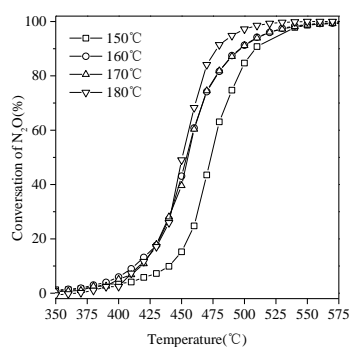


Fig. 2 Co_3O_4 catalyst activity evaluation result

From Fig. 2, it can be seen that the crystallization temperature has an effect on the activity of Co_3O_4 catalysts for N_2O , but it is not significant. Among them, Co_3O_4 -180°C catalyst has better catalytic activity, T_{95} is 492°C, which is 38°C lower than T_{95} of Co_3O_4 -150°C catalyst.

References:

1. Y.Z. Wang, K. Zheng, X.B. Hu, W. Zhou, X.H. Wei, Y.X. Zhao, *Molecular Catalysis*, 2019, **470**, 104-111.

Extraction and Characterization of Humic Acid from Lignite

*Piyue Gong, Jintong Du, Haiying Huang**

State Key Laboratory of Polymer Physics and Chemistry, Changchun Institute of Applied Chemistry, Chinese Academy of Sciences, Changchun, 130022, P. R. China

E-mail: pygong@ciac.ac.cn

Humic Acid (HA) is a kind of natural organic polymers, which existed in variety form in soil, peats and brown coals. Due to the diversity of functional groups and surface activities, humic acid plays an indispensable roles in the soil improvement as fertilizer, absorbent, adhesion, heat preservation and water-retaining agent etc.¹⁻³ In general, the surface functional groups of HA need to be activated for effective utilizing, and its composition and properties largely depend on both the origin of material and extraction procedure. Therefore, choosing the proper separation method based on different source and characterization of the HA is essential to determine the biochemical properties of HA before further application.

In this work, HA isolated from lignite, which containing large amount of humic acid. Through modifying the traditional alkaline extraction-acidic separation method, the influence of different alkaline concentration, pH in solution, acidification time, temperature on the extraction efficiency of HA were examined to achieve the optimum extracting condition with highest yield. The extractives were further characterized by Fourier transform infrared spectroscopy (FTIR), UV-vis spectrometer and Elemental analyses. Our results indicated that the humic acid isolated from lignite have similar structural and functional features with commercial humic acid. Most importantly, it can serve as adhesion agent applying in biodegradable liquid film mulching field, hence effectively replace the plastic film reducing the white pollution.

References:

1. K. H. Tan, *Humic Matter in Soil and the Environment: Principles and Controversies*, 2014, 2nd Edn. Boca Raton, FL, CRC Press.
2. H. Tiessen, E. Cuevas, P. Chacon, *Nature* 1994, 371, 783-785.
3. M. Klučáková, M. Pavlíková, *Journal of Chemistry*, 2017, 2017, 1-5.

Poster70

Preparation of polystyrene microspheres and its application in the diffusion of dry chemical reagent slides

He Nan Yuan^{1,2}, Bin Zhang^{1,2}, Guang Xiang He^{*1,2}

(1. College of Chemical Engineering, Beijing Institute of Petrochemical Technology, Beijing 102617, China;

2. Beijing Key Laboratory of Fuels Cleaning and Advanced Catalytic Emission Reduction Technology, Beijing 102617, China)

Abstract. In order to improve the efficiency and accuracy of dry chemical reagent slides detection, CRP dry chemical reagent was investigated, it was made of polystyrene microspheres, which was prepared in the laboratory. A research about the effect of surfactant (TX100) and stirring time on diffusion was proposed. The prepared diffusion layer has the best effect on serum diffusion when the stirring time is 50min. By changing the reaction temperature, monomer concentration, we can control the particle size of polystyrene microspheres, we did a research on the reason why it is feasible.

Keywords: polystyrene microspheres; diffusion; dry chemical reagent slides

1. Introduction

With the rapid development of economy and technology, as well as the prevalence of "Internet plus" artificial intelligence, people's pursuit of their life quality has also been improved in this emerging era of big data. Due to the great pressure in work and life, irregular work and rest, the sudden death of staying up late, overeating and other phenomena will occur, which will lead to a series of health problems. Therefore, timely, efficient and rapid detection methods are needed, which puts forward higher requirements for the rapidity, accuracy, and convenience of testing methods. Compared with wet chemical in vitro diagnostic reagents, the dry chemical in vitro diagnostic reagents are convenient, accurate, pollution-free and easy to operate (Lapekas P. 1994, Ng R H et al. 1992, Li et al. 2003, Zipp, A. et al. 1981). Therefore, in recent years, the dry chemical in vitro diagnostic reagents have attracted more and more scholars' attention and shown a rapid development trend. Dry chemistry is an analytical method for the color reaction of the liquid in the sample to be tested with the dry reagent solidified on the carrier (Mao et al. 2009). The dry chemical in vitro diagnostic reagent, commonly known as "dry chemical reagent slides", is divided into three parts: the diffusion layer, the reagent layer, and the substrate layer. If the serum diffused through the diffusion layer, it reacts with the reagent layer to obtain the component concentration. Most scholars at home and abroad have focused on the formulation of the dry tablet reagent layer but neglect

the research on the diffusion layer. Lack of detailed reports on the diffusion law in the diffusion layer, which is not conducive to the research the effect of diffusion effect on the test results and the development of dry chemical reagent slides detection technology

At the present stage, the diffusion layer materials of dry chemical reagent slides are mostly prepared by polysulfone (Tian et al. 2012), polysulfone acid (Cai. 2015), titanium dioxide (Guo et al. 2017) and so on. Polystyrene microspheres are characterized by uniform particle size concentration and strong surface reaction ability, and have been widely used in biomedicine, microelectronics and other fields in recent years (Lee S G and Ha J W. 2016, Song J S et al. 2006, Steff A M et al. 2015). He et al. (2007) prepared sulfonated polystyrene microspheres for protein adsorption, indicating that the polystyrene microspheres have good reaction performance and provide good theoretical support for the application of the polystyrene microspheres to dry chemical reagent slides. Meyer et al. (2007) used a magnetic sensor to determine the concentration of C-reactive protein (CRP), which was characterized by high sensitivity and good accuracy. However, the sample needed pretreatment and the operation was complicated.

In this study, we can determine the concentration of CRP in the serum by the dry chemical reagent slides. We researched the diffusion law of the diffusion layer prepared by microspheres with different particle sizes. By changing by changing the reaction temperature, monomer concentration, we can control the particle size of polystyrene microspheres.

2. Experimental

2.1. Materials

Styrene (St) was purchased from Sinopharm. Ethanol and polyethylene glycol (PEG600) were purchased from Beijing Chemical Corporation. Polyvinylpyrrolidone (PVP, Mw ~55000), Triton (TX-100), 2,2'-azobis-(2-methylbutyronitrile) (AMBN), acrylic acid (AA) and phosphate buffer (pH=7.4) were purchased from J&K Scientific Ltd. The deionized water used in the experiment was self-made.

A Zeiss-Supra 55 field emission scanning electron microscope (SEM) made in Carl Zeiss (Germany) was utilized at operating voltages from 2 to 5kV to observe particle morphology. The particle size of microspheres was measured by a Rise-2008 Laser granulometer made in Jinan runzhike co. Ltd at a rate of 2000 rpm.

2.2. Processing

2.2.1 Preparation of diffusion layer materials

The dispersant (PVP55, 3.6g), co-dispersant (Triton, TX-100, 760 μ L), initiator (AMBN, 0.5g), monomer (St, 14g), and the solvent (ethanol, 14mL) were added to a 250mL four-necked reaction flask equipped with a nitrogen inlet, a thermometer, and a condenser. After a homogeneous solution was formed at indoor temperature, the solution was deoxygenated by bubbling nitrogen 30min. The flask was then placed in an oil bath at 70 $^{\circ}$ C and subjected to mechanical stirring for 1 hour at a rate of 200 rpm. After 1 hour, add ethanol (14mL), St (14g) and AA(1mL) mixture, keep stirring and continue to react with nitrogen for 23h, and cool down to obtain the emulsion product.

2.2.2 Preparation of diffusion layer

Phosphate choline, dye agent, enzyme standard antibody and adhesive (PEG) are dissolved in buffer solution in a certain proportion, mixed with polystyrene microspheres dispersed in ethanol and used coating machine to coat the mixture on the base layer, and dried.

2.3. Characterization

The particle size of the microspheres was measured by a laser granulometry. A small amount of microsphere emulsion was diluted with water to a nearly transparent shape, and then ultrasonic oscillation was performed for 20min. After that, evenly dispersed microspheres were added to the laser granulator and tested under the condition of pump speed of 2000 r/min. In the Eq. (1), d_n is the average particle size, n represents the number of microspheres involved in the calculation, and d_i represents the particle size of the microsphere.

$$d_n = \frac{\sum d_i}{n} \quad (1)$$

The morphology and arrangement of microspheres were observed by SUPRA55 field emission scanning electron microscope (SEM). The surface adhered to the sample table for gold spraying, and the morphology of the microspheres was observed. The microspheres were made into dry chemical reagent slides, a small part of which was cut and glued to the surface of conductive adhesive for gold spraying, and the arrangement of the microspheres was observed.

The diffusion time of serum on dry chemical reagent slides was measured by a stopwatch. Time starts when a drop of serum is dripped onto it. Stop timing after spreading and take the measured time as the diffusion time of serum on the dry chemical reagent slides.

The diffusion layer with the surfactant was characterized by a DSA30 optical contact angle measuring instrument manufactured by KRUSS, Germany. The measurement uses the droplet method, the droplet volume is 2 μ L, and the dropping speed is 0.2mL/min

3. Results and discussion

3.1. Preparation of microspheres with different particle sizes

3.1.1 Effect of reaction temperature on particle size

Polystyrene microspheres were prepared according to the method described in 2.2.1. The effects of temperature on particle size were investigated under the condition at a stirring rate of 300r/min. Experiments were conducted at temperatures of 55 $^{\circ}$ C, 60 $^{\circ}$ C, 65 $^{\circ}$ C, 70 $^{\circ}$ C and 75 $^{\circ}$ C respectively. According to the SEM microscope, Fig.1, the particle size of the microspheres gradually increased with the increase of temperature. The results indicate when the reaction temperature was 55 $^{\circ}$ C, 60 $^{\circ}$ C, 65 $^{\circ}$ C, 70 $^{\circ}$ C, and 75 $^{\circ}$ C, the particle sizes of the prepared polystyrene microspheres were 1.3 μ m, 1.9 μ m, 2.6 μ m, 3.0 μ m, and 3.5 μ m, respectively. When the reaction temperature was below 60 $^{\circ}$ C, the microspheres showed some adhesion. As the

reaction temperature increased, the microspheres showed a dispersive state. With the increase of temperature, the homogeneity of microspheres becomes better, but the homogeneity of microspheres becomes worse when the temperature reaches 75 °C.

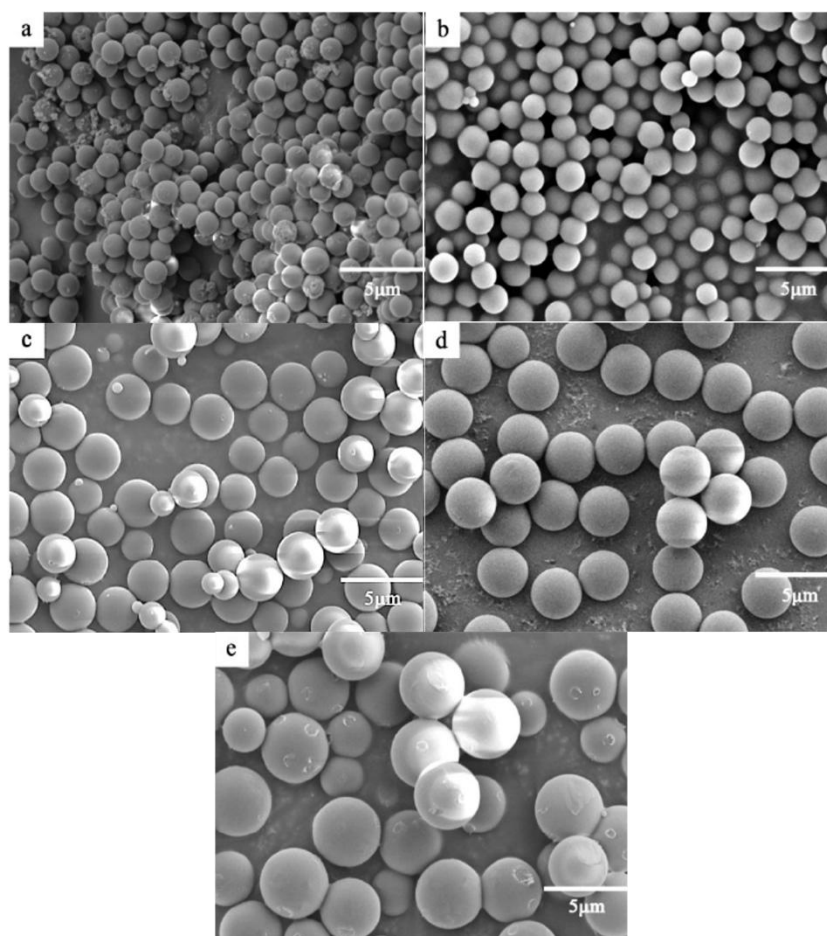


Fig.1 SEM micrographs of polystyrene microspheres in different temperature (a. 55 °C; b. 60 °C; c. 65 °C; d.70 °C; e. 75 °C)

There may be two reasons for this phenomenon. On the one hand, temperature affects the solubility of polymer long chains in polymerization systems. As the temperature increases, the solubility of the system to the long-chain increases, and the critical length of the long-chain becomes longer. During precipitation, the long chains are longer, and the particle size of the microspheres formed after winding and folding becomes larger. On the other hand, temperature affects the reaction rate of the whole reaction system. Increasing the temperature will accelerate the decomposition rate of the initiator, which is the control step of the whole reaction. As the temperature increases, the concentration of free radicals produced by the decomposition of the initiator is high, the polymerization reaction is accelerated, and more winding of polymer chains makes the particle size of the microspheres larger. To sum up, 70 °C was finally selected as the reaction temperature.

3.1.2 Effect of monomer concentration on particle size

The effects of monomer concentration on particle size and morphology were investigated at a temperature of 70 °C and at a stirring rate of 300r/min with ethanol as the solvent. The five experimental conditions of monomer concentration of 15wt%, 20wt%, 25wt%, 30wt% and 35wt% were investigated respectively. The SEM microscope Fig.2 indicates, that the particle size of the microspheres increases with the increase of monomer concentration. When the monomer concentration was 15wt%, the particle size of the microspheres was only 2.5 μm, and as the monomer concentration increased to 35wt%, the particle size of the microspheres reached 6.7 μm. (when the monomer concentration was 20wt%, 25wt%, and 30wt%, the particle size was 3.0 μm, 3.6 μm, 6.2 μm, respectively) However, with the increase of monomer concentration, the homogeneity of microspheres gradually decreased.

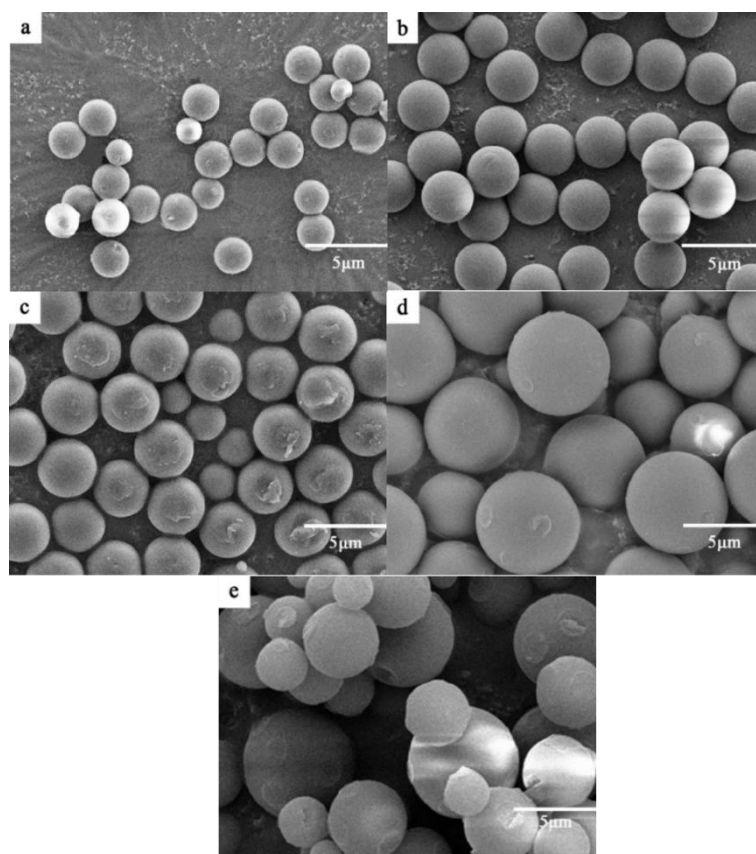


Fig.2 SEM micrographs of polystyrene microspheres monomer concentrations (a. 15wt%; b. 20wt%; c. 25wt%; d. 30wt%; e. 35wt%; f. 40wt%)

The reason for this is that the number of nucleation in the polymerization system is the same under the same concentration of the initiator and stabilizer. If the monomer concentration is low, that is, the total amount of monomer is low, the reaction cannot get enough raw materials for the polymer long-chain growth, so the particle size of polystyrene microspheres is small. With the increase of monomer quantity, sufficient raw materials can be obtained for the chain growth reaction, thus the particle size of the microspheres becomes larger.

3.2. The factors affecting the diffusion rate of diffusion layer

3.2.1 Effects of and stirring time on diffusion rate

As shown in Fig.3, Fig.3 (a-e) represents the multifunctional layer prepared by the emulsion with stirring time of 10min~50min respectively. The surface of diffusion layer becomes smooth with the increasing of stirring time of the emulsion. When the stirring time was 10min, there were many obvious particle bulges on the surface which indicated that the stirring process was too short and the microspheres were not well dispersed in ethanol. Until the stirring time reaches 50min, the raised particles can hardly be seen on the surface.

In order to investigate the diffusion effect of the diffusion layers prepared with different stirring times on serum, the diffusion layers prepared with stirring times of 10min, 30min and 50min were respectively taken and 10 μ L serum was added. The phenomena after diffusion were shown in Fig.6. The surface diffusion rate of the diffusion layer prepared by the serum after stirring for 10 min is slow, most of the serum is difficult to diffuse and permeate into the diffusion layer, and only accumulate on the surface. When the stirring time was 30min, the diffusion effect of the diffusion layer prepared was slightly improved, and the residual serum on the surface was reduced, but the diffusion effect was still not ideal, and the diffusion rate was still relatively slow. The diffusion layer obtained after stirring for 50min has the best diffusion effect on serum, with almost no residual serum on the surface. Most of the serum diffuses into the diffusion layer, and the diffusion speed is extremely fast. Therefore, the surface smoothness of diffusion layer has an important influence on the diffusion effect and diffusion rate of serum.

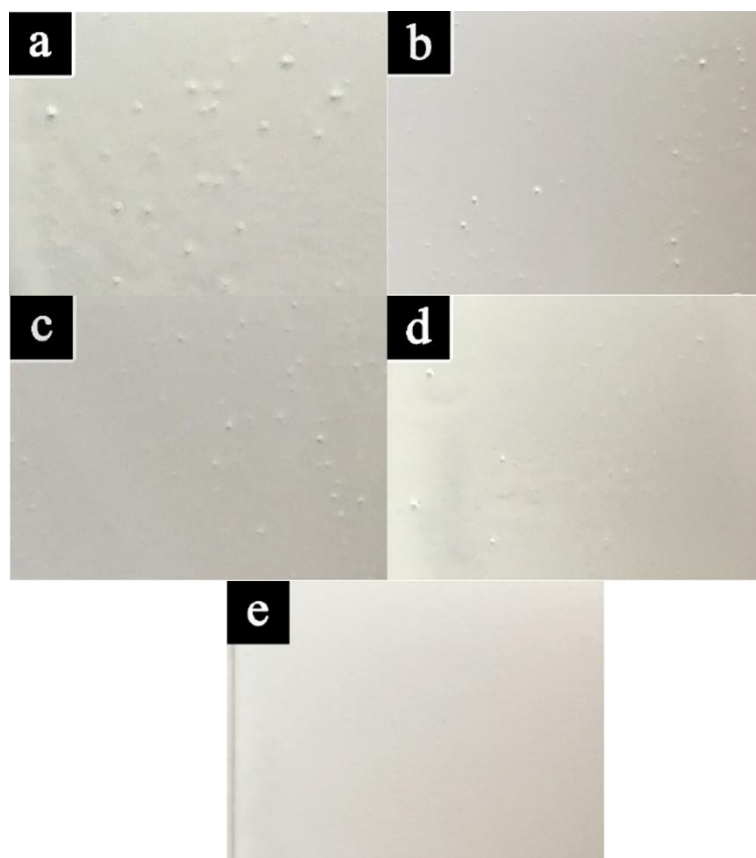


Fig.3 Effect of stirring time on diffusion layer (a. 10min; b. 20min; c. 30min; d. 40min; e. 50min)

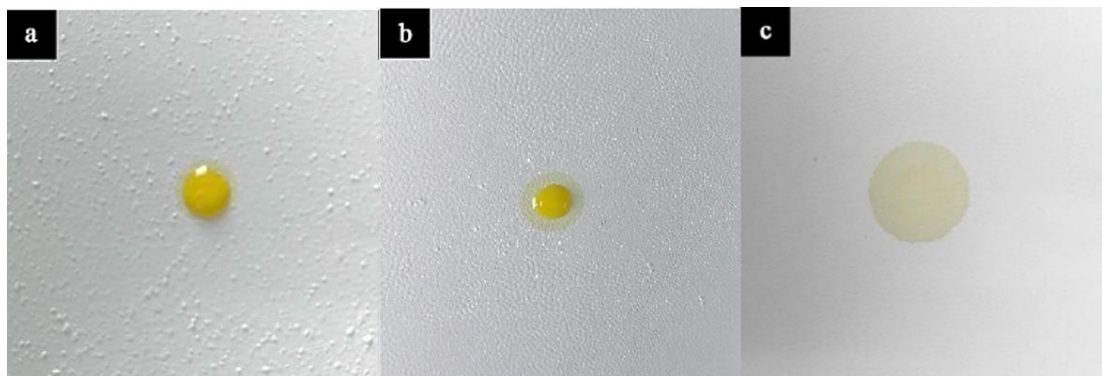


Fig.4 The effect of stirring time on the diffusion of serum by diffusion layers (a. 10min; b. 30min; c. 50min)

3.2.2 Effect of surfactant on diffusion rate

The molecule of surfactant has a hydrophilic group on one end and a hydrophobic group on the other. Polystyrene microspheres are organic pellets. Although the carboxyl group is modified on the surface to reduce the surface tension of serum diffusion, the content of the carboxyl group is low, but the surface tension of serum is still high when it diffuses.

According to the method described in 2.2.2, two identical carboxylated polystyrene microsphere emulsions were prepared for the particle size of 3 μm and a mass fraction of microspheres of 35%. One part was added with a trace amount of surfactant (TX100), the other without surfactant, stirred for 50mins, and then made into a diffusion layer. After drying naturally, added 10 μL serum to the diffusion layer and determined when the serum is completely diffused.

Fig. 5 and Fig. 6 indicate that, if the serum is added for a duration of 5s, the contact angle of the serum and the surface of the diffusion layer will not be much different when the surfactant is not added, so the diffusion layer has a strong hydrophobicity. When the serum is added to the diffusion layer without TX100, the contact angle on the diffusion layer was significantly smaller than serum diffused for a duration of 1s. It means the addition of surfactant reduces the influence of surface tension between serum and microspheres in the diffusion process, greatly accelerates the diffusion rate of serum and improves the hydrophobicity of the diffusion layer.

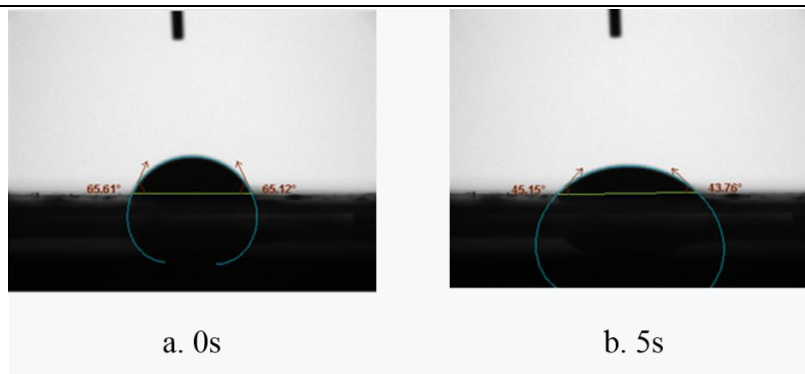


Fig.5 Contact angle of serum on diffusion layer without surfactant

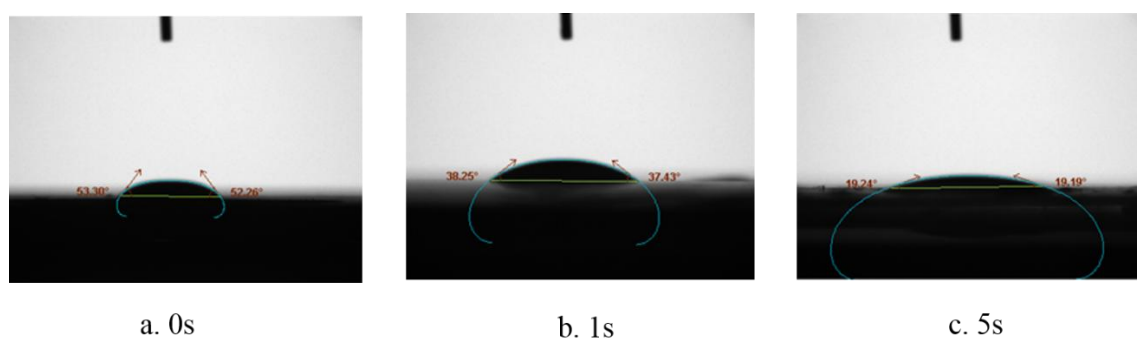


Fig.6 Contact angle of serum on diffusion layer with TX100

4. Conclusions

- To control the particle size of polystyrene microspheres, the effects of temperature and monomer concentration on the particle sizes were investigated. Polystyrene microspheres with uniform particle size were prepared with ethanol at the reaction temperature of 70 °C and monomer concentration of 20wt%.
- The optimum conditions for preparation of diffusion layer using polystyrene microspheres were determined as follows: Triton was selected as surfactant to improve the hydrophobicity of diffusion layer, and the stirring time was controlled to be 50min.

Acknowledgments

This research is supported by the National Natural Science Foundation of China (91634101, 21601016), the Beijing Municipal Natural Science Foundation (2174073), and the Project of Construction of Innovative Teams and Teacher Career Development for Universities and Colleges under Beijing Municipality (IDHT20180508)

References

- LAPEKAS P. (2003), “New technologies for laboratory productivity”, *J. Journal of Healthcare Material Management*, **12**(3), 30-34.

- Ng R H, Sparks K M, and Statland B E. (1992), "Colorimetric determination of potassium in plasma and serum by reflectance photometry with a dry-chemistry reagent", *J. Clinical Chemistry*, **38**(7), 1371-1372.
- Li G X, Lu X, J, Gao B X, et al. (2003). "Comparison of dry chemistry and liquid chemistry in clinical biochemistry", *J. West China Medical Journal*, **18**(1), 69-70.
- Zipp, A. (1981). "Development of dry reagent chemistry for the clinical laboratory", *J. The Journal of Automatic Chemistry*, **3**(2), 71-75.
- Mao X, Xu H, Zeng Q, Zeng L, Liu G, et al. (2009). "Molecular beacon-functionalized gold nanoparticles as probes in dry-reagent strip biosensor for DNA analysis", *J. Chem Commun* **4**(21), 3065-3067. doi:10.1039/b822582f.
- Lee, S. G., & Ha, J.-W. (2016). "Synthesis of highly carboxylated monodisperse polystyrene microspheres by dispersion polymerization in fluorinated alcohol", *J. Macromolecular Research*, **24**(8), 675-683. doi:10.1007/s13233-016-4093-6
- Tian Y, Chen H Y, Wang M. (2012). "Development of dry chemistry method for alanine aminotransferase", *J. Chinese Journal of Biologicals*, **25**(7), 881-883. doi:10.13200/j.cjb.2012.07.90.tiany.021
- Cai H P. (2015). "Two High-density Lipoprotein Cholesterol Directly Performance Evaluation of Assay Reagents", *J. Guide of China Medicine*, **13**(2), 47-48. doi:10.15912/j.cnki.gocm.2015.02.031
- Guo X Y, Li Y, Zheng Y, et al. (2017). "Synthesis and characteristics of homogeneous titania microspheres", *J. Fine Chemicals*, **34**(12), 1404-1411.
- Jing-She Song, L. C, and Mitchell A. Winnik (2006). "Monodisperse micrometer-size carboxyl-functionalized polystyrene particles obtained by two-stage dispersion polymerization", *J. Macromolecules*, **39**(17), 5729-5737.
- Ann-Muriel Steff, M. n. F., Chantal Arguin, and Patrice Hugo (2015). "Detection of a Decrease in Green Fluorescent Protein Fluorescence for the Monitoring of Cell Death: An Assay Amenable to High-Throughput Screening Technologies", *J. Cytometry*, **45**(4), 991-994. doi:10.1002/cyto.10024
- He R, Cao G C, Chen M Q, et al. (2007). "Preparation of polystyrene microspheres with sulfonic acid group on the surface and adsorption of bovine serum albumin", *J. Chemical Industry and Engineering Progress*, **26**(7), 973-979. doi:10.16085/j.issn.1000-6613.2007.07.015
- Meyer, M. H., Hartmann, M., Krause, H. J., Blankenstein, G., Mueller-Chorus, B., Oster, J. Keusgen, M. (2007). "CRP determination based on a novel magnetic biosensor", *J. Biosens Bioelectron*, **22**(6), 973-979. doi:10.1016/j.bios.2006.04.001.

Note

Note

Note

Note